The Late Triassic Metallogenic Setting of the Greens Creek Massive Sulfide Deposit in Southeastern Alaska

By Cliff D. Taylor, John Philpotts, Wayne R. Premo, Alan L. Meier, and Joseph E. Taggart, Jr.

Chapter 2 of
Geology, Geochemistry, and Genesis of the Greens Creek Massive Sulfide Deposit, Admiralty Island, Southeastern Alaska
Edited by Cliff D. Taylor and Craig A. Johnson

Professional Paper 1763

U.S. Department of the Interior
U.S. Geological Survey

Contents

Figures

Tables

The Late Triassic Metallogenic Setting of the Greens Creek Massive Sulfide Deposit in Southeastern Alaska

By Cliff D. Taylor, John Philpotts, Wayne R. Premo, Alan L. Meier, and Joseph E. Taggart, Jr.

Abstract

The Alexander terrane of southeastern Alaska contains a belt of unusual volcanogenic massive sulfide (VMS) deposits along its eastern margin. The deposits occur within a lithologic sequence that is exposed discontinuously along its 600-kilometer strike length and consists of a 200–800-meter thickness of conglomerate, limestone, marine clastic sediment, and tuff with intercalated and overlying mafic pyroclastic rocks and pillowed flows. The rocks range in age from Anisian (Middle Triassic) to late Norian (middle Late Triassic). Major deposits within the belt, which is referred to herein as the Alexander Triassic Metallogenic Belt (ATMB), are Greens Creek, the most economically significant VMS deposit in Alaska, and Windy Craggy, the largest VMS deposit known in North America.

The VMS deposits vary in structural appearance, chemistry, and stratigraphic setting along strike within the ATMB, which suggests spatial or temporal changes in the tectonic environment. In the southern portion of the belt, the deposit host rocks are felsic volcanics and overlying shallow-water limestones. In the central portion of the belt, a pebble conglomerate appears at the base of the section, suggesting higher energy deposition in a near-slope or basin-margin setting. In the north, the felsic volcanics, limestones, and conglomerates give way to deeper water sediments and mafic volcanic rocks. There is an accompanying change in the sulfide deposits from dominantly structurally controlled Pb-Zn-Ag-Ba±Cu deposits in the south (for example, west of Ketchikan), to sulfosalt-bearing VMS deposits (for example, Greens Creek on Admiralty Island), to larger Cu-Zn±Co±Au VMS deposits in the north (for example, Windy Craggy in northeastern British Columbia).

Igneous activity in the ATMB was characterized by bimodal volcanism and hypabyssal emplacement of mafic-ultramafic magmas. Analyses of immobile trace elements and rare earth elements suggest that the felsic rocks change from calc-alkaline rhyolites in the southern ATMB to peralkaline rhyolites in the middle part of the belt. The capping basaltic rocks have compositions consistent with variable assimilation of mature island arc crust by more primitive, midocean ridge-type or intraplate-type basaltic melts. Radiogenic isotope data for the capping basalts and associated gabbros support the variable assimilation hypothesis (epsilon-Nd=+4–+9, initial $^{206}Pb/^{204}Pb$=18.42–18.92, initial $^{87}Sr/^{86}Sr$=0.7037–0.7074).

Overall, the regional geology and geochemistry are consistent with sulfide deposition in the south having occurred in shallow, subaqueous environments on the flanks of the Alexander terrane, and sulfide deposition farther north having occurred in progressively deeper environments in an evolving back-arc or intra-arc rift. In their ore and host-rock geochemistry and sulfide mineralogy, the ATMB deposits resemble deposits that have been found at active sea-floor hydrothermal vents (white smokers) associated with back arcs of the southwest Pacific Ocean. A modern analog for the ATMB may be the southward projection of the Lau basin, from the active sea-floor hydrothermal vents of the Valu Fa Ridge to the Taupo Volcanic Zone of the North Island, New Zealand.

Introduction

Numerous papers (compilations by Cobb, 1972, 1978; Berg and Grybeck, 1980; Goldfarb and others, 1987; Taylor and others, 1992; Newberry and Brew, 1997, 1999; Newberry and others, 1997; Taylor and others, 2008) over the last few decades have identified a series of unusual polymetallic volcanogenic massive sulfide (VMS; see reviews by Franklin and others, 1981, and Large, 1992) deposits hosted in an Upper Triassic sequence of volcano-sedimentary rocks that stretch the length of southeastern Alaska (fig. 1). Assuming that correlations among host rocks are correct, these deposits constitute a metallogenically important belt that comprises the easternmost and youngest portion of the Alexander terrane (fig. 2). With the notable exception of the world-class Greens Creek mine having estimated reserves of 21.9 million metric tonnes of ore at 13.9 percent zinc, 5.1 percent lead, 4.8 grams per metric tonne gold, and 599 grams per metric tonne silver at zero cutoff, these are generally small deposits (less than 1 million metric tonnes) dominated by Ba-Zn-Pb-Ag ± Cu-Au, or Cu-Zn ± Au. From south to north, they occur on Annette and Gravina Islands near Ketchikan (fig. 1, inset a), through Keku Strait (fig. 1, inset c) and Duncan Canal–Zarembo Island area west of Petersburg (fig. 1, inset b), through Admiralty Island south of Juneau (fig. 1, inset d), and on and near Mt. Henry Clay west of Haines (fig. 1, inset f). If correlation to

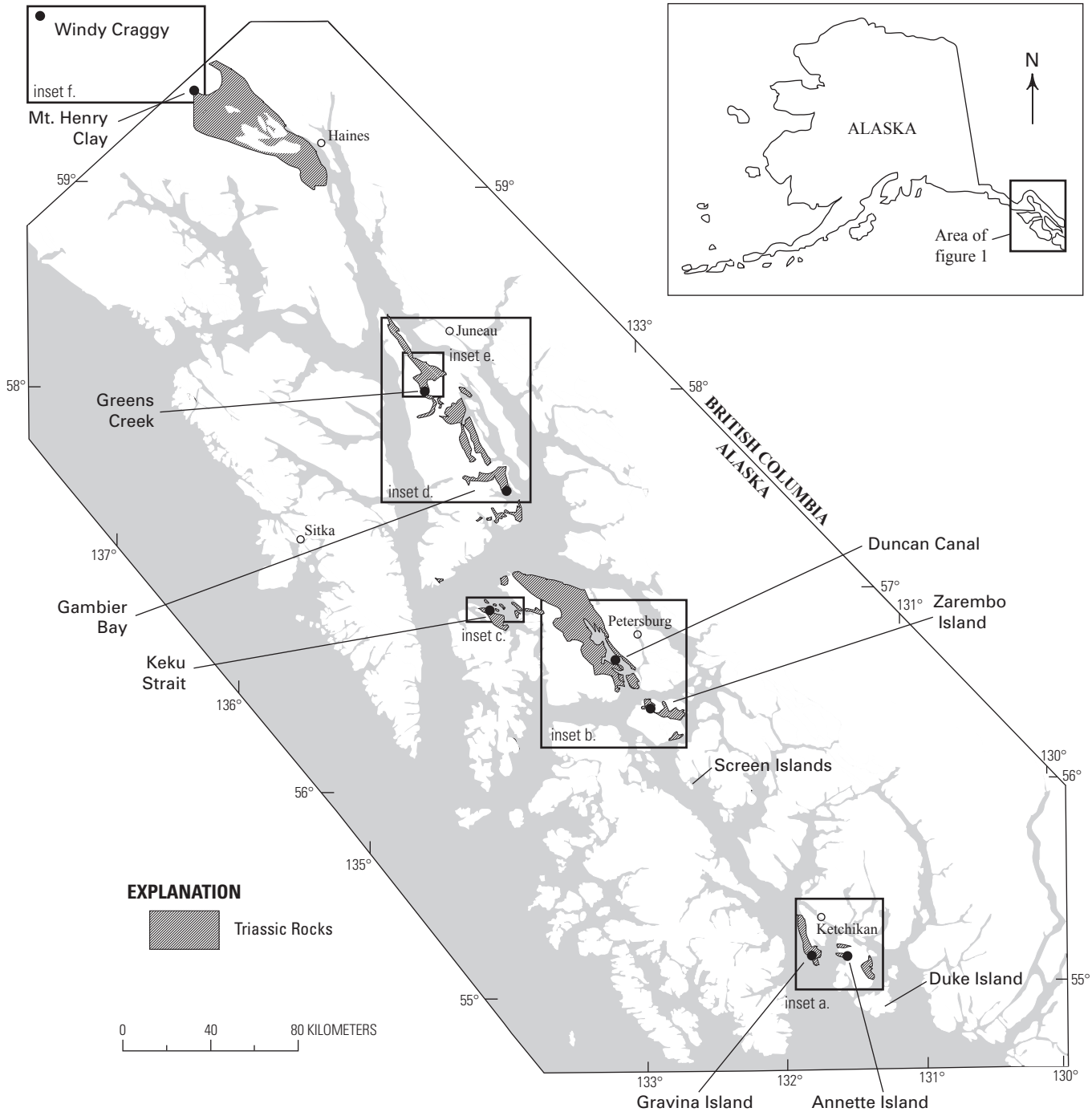

Figure 1. Generalized map of southeastern Alaska (modified from Gehrels and Berg, 1992) showing the locations of mines, mineral deposits, and mineral occurrences (all shown as solid circles) and other features discussed in the text, in relation to the Alexander Triassic Mineral Belt (ATMB). (Inset a) Detailed map of the southern ATMB showing the locations of mines, mineral deposits, and mineral occurrences and other features discussed in the text on Annette and Gravina Islands. (Inset b) Detailed map of the central ATMB showing the locations of mines, mineral deposits, and mineral occurrences and other features discussed in the text in the Duncan Canal area and on Woewodski and Zarembo Islands. (Inset c) Detailed map of the central ATMB showing showing the locations of mines, mineral deposits, and mineral occurrences and other features discussed in the text in the Keku Strait area. (Inset d) Detailed map of the central ATMB showing the locations of mines, mineral deposits, and mineral occurrences and other features discussed in the text on Admiralty Island. (Inset e) Detailed map of the Greens Creek mine area on northern Admiralty Island showing the locations of mines, mineral deposits, and mineral occurrences and other features discussed in the text. (Inset f) Detailed map of the northern ATMB showing the locations of mines, mineral deposits, and mineral occurrences and other features discussed in the text between the Mt. Henry Clay area and Windy Craggy.

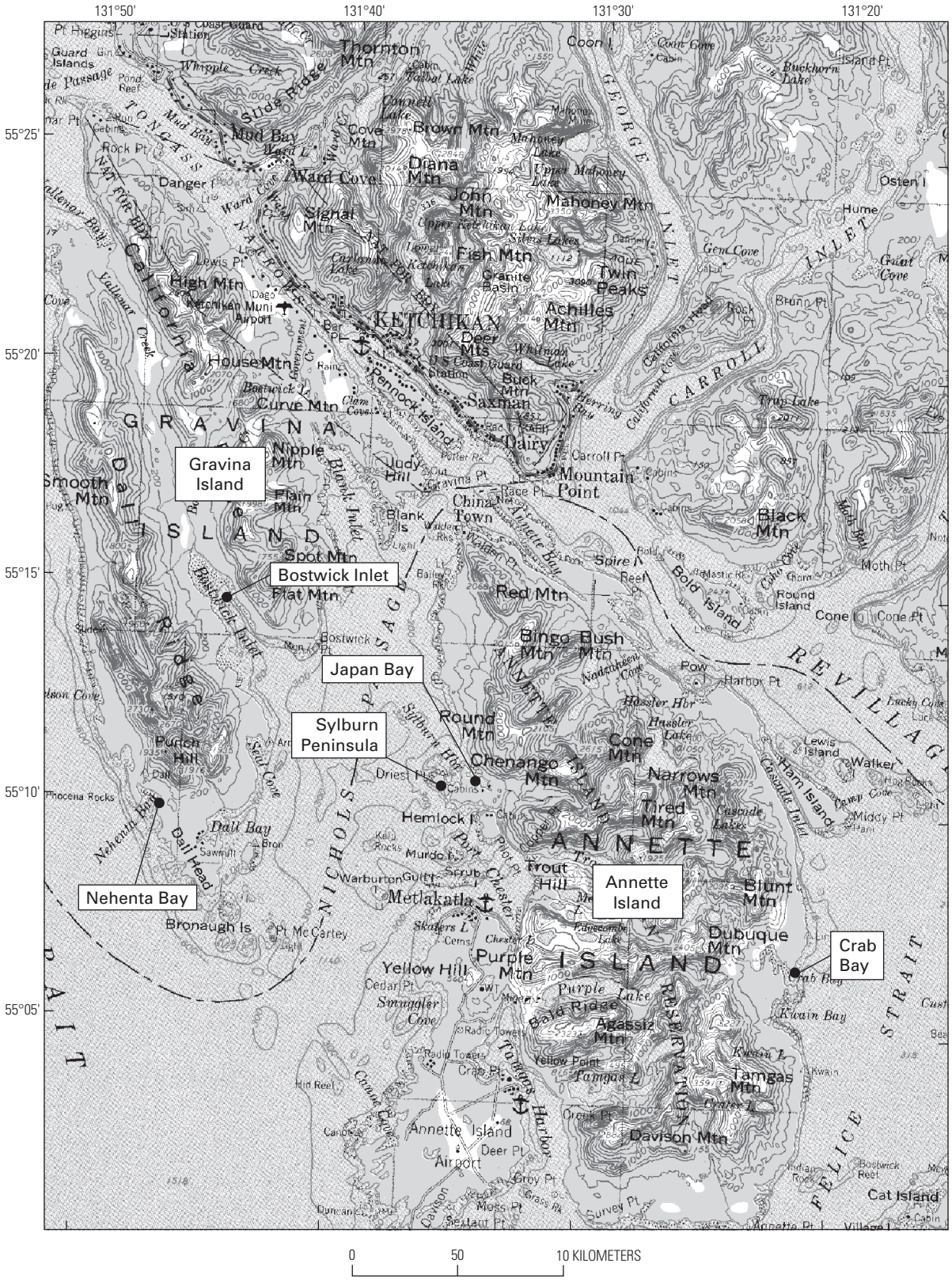

Figure 1, inset a. Detailed map of the southern ATMB showing the locations of mines, mineral deposits, and mineral occurrences and other features discussed in the text on Annette and Gravina Islands.

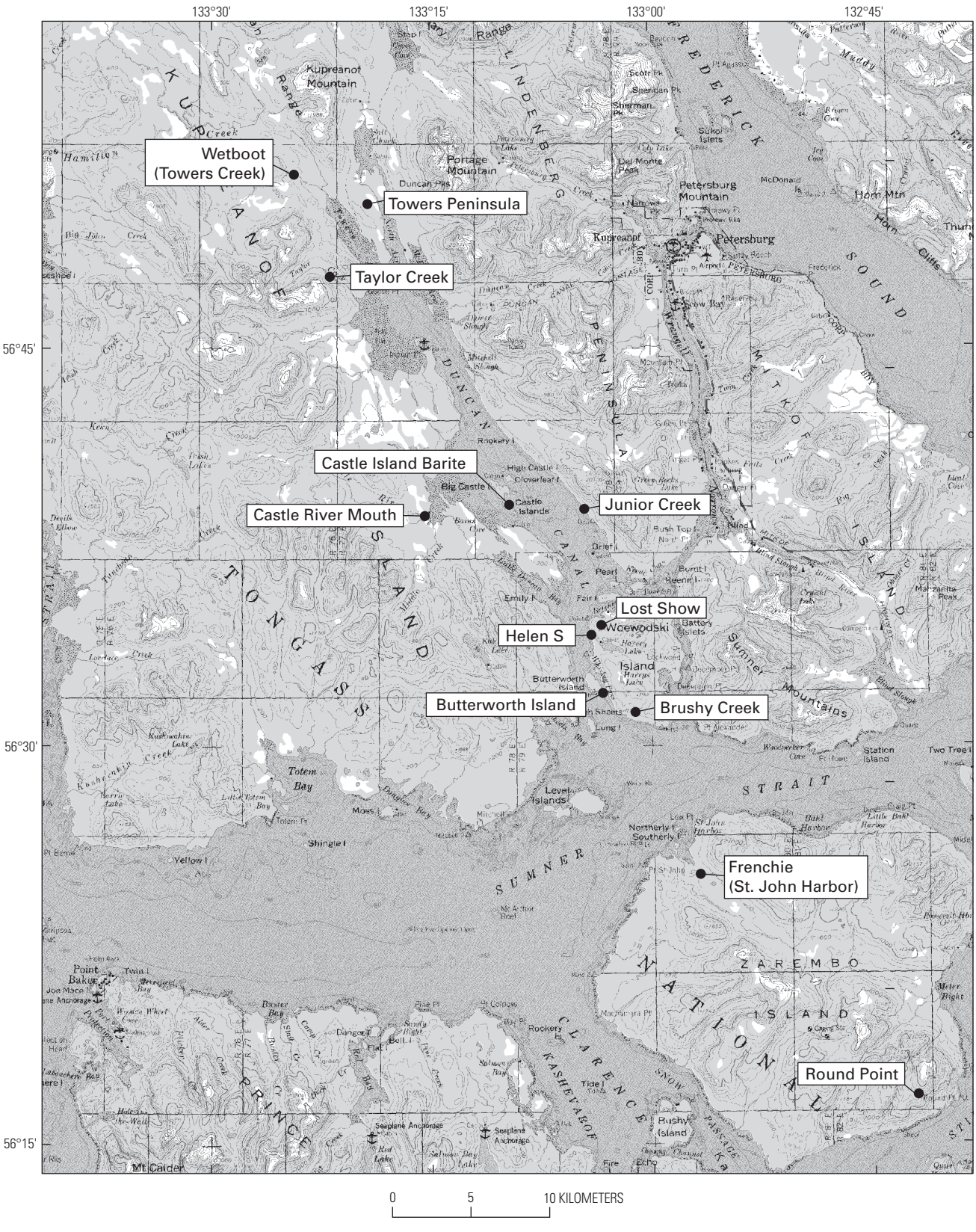

Figure 1, inset b. Detailed map of the central ATMB showing the locations of mines, mineral deposits, and mineral occurrences and other features discussed in the text in the Duncan Canal area and on Woewodski and Zarembo Islands.

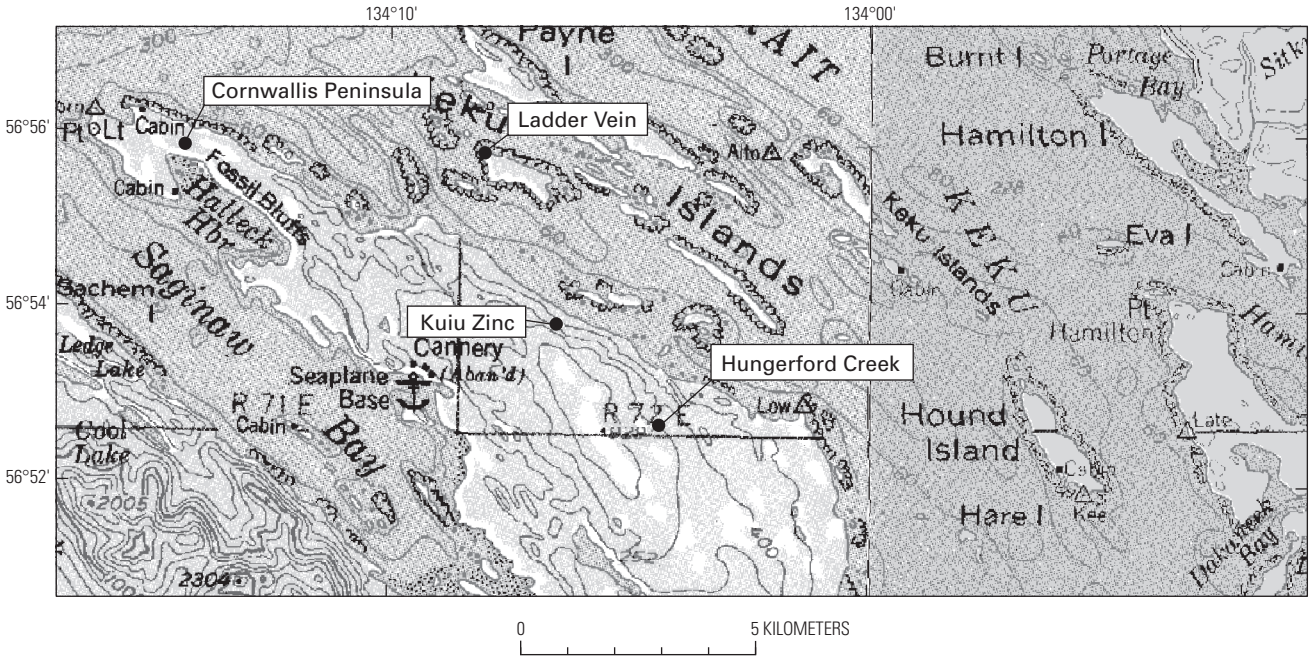

Figure 1, inset c. Detailed map of the central ATMB showing showing the locations of mines, mineral deposits, and mineral occurrences and other features discussed in the text in the Keku Strait area.

the Windy Craggy deposit (reserves estimated at 297.4 million metric tonnes at 1.38 percent copper, 0.07 percent cobalt, 0.2 gram per metric tonne gold, and 3.8 grams per metric tonne silver; Peter and Scott, 1999) to the north is correct, then a belt approximately 600 kilometers in length is defined that contains the largest Besshi-type VMS deposit (see review by Slack, 1993) in the world and the leading producer of silver in the United States. This metallogenic belt is herein referred to as the Alexander Triassic Metallogenic Belt (ATMB).

Host lithologies identify a distinctive geologic setting. The VMS deposits are nearly uniformly hosted within a thin package of structurally dismembered Upper Triassic (Norian) rocks characterized by bimodal volcanics and abundant flysch-type sediments. Mafic volcanic rocks predominate and commonly are volcaniclastics or flow breccias with lesser pillowed and massive flows. At larger, more obviously stratiform occurrences, sediments tend to be basinal in appearance, with high proportions of graphitic argillite and thin lenses of pyrite. Metamorphic grade varies from prehnite-pumpellyite to mid-greenschist. The base of the package is typically marked by the presence of angular to rounded polymictic conglomerate with clasts composed of the immediately underlying unit. In places, discrete packages of conglomerate occupy flow channels that migrate laterally and vertically within a short distance. High-angle faults of probable normal displacement are common and tend to mark changes in lithology, such as from sedimentary to volcanic rocks. Thin carbonate units are common as well and are generally dolomitic. Small outcrops of serpentinized mafic/ultramafic rock also tend to be spatially associated with deposits throughout the ATMB.

From south to north, a distinct variation in both the nature of the deposits and the host rocks is evident. At the southern end of the ATMB, the felsic component of the bimodal volcanic rocks is significant and becomes more rare or even absent northwards. The volcanic stratigraphy on both Annette and Gravina Islands is characterized by a thick sequence of rhyolitic volcaniclastics and tuffs low in the Upper Triassic section, which give way to voluminous mafic volcaniclastics and flows in the upper portion of the section. On the Cornwallis Peninsula in the Keku Strait area, minor mafic volcanic rocks constitute the base of the package and are overlain by a thick sequence of rhyolitic volcaniclastics and flows. Felsic volcanic rocks are rare north of Keku Strait. The northernmost occurrence of felsic volcanic rocks is on Mt. Henry Clay where thin flows of trachyandesite and quartz-sericite-pyrite altered rhyolite and rhyolitic tuffs are associated with the occurrences (Green and others, 2003). Additional but perhaps less obvious regional changes in the host rocks are an increase in the percentage of volcanic to sedimentary rocks to the north, and possibly an increase in metamorphic grade.

A noticeable change in the nature of the deposits parallels the change in host rock lithology. The deposits in the south are predominantly zinc-lead-silver bearing with large amounts of barite. In fact, some of the deposits such as on the Sylburn Peninsula on Annette Island and the Castle Island barite deposit in the Duncan Canal area are composed primarily of barite with minor sphalerite, galena, and tetrahedrite. These deposits share many similarities with Kuroko-type ores (for example, Franklin, 1986, 1993). From the latitude of about Petersburg to the north, deposits appear that contain

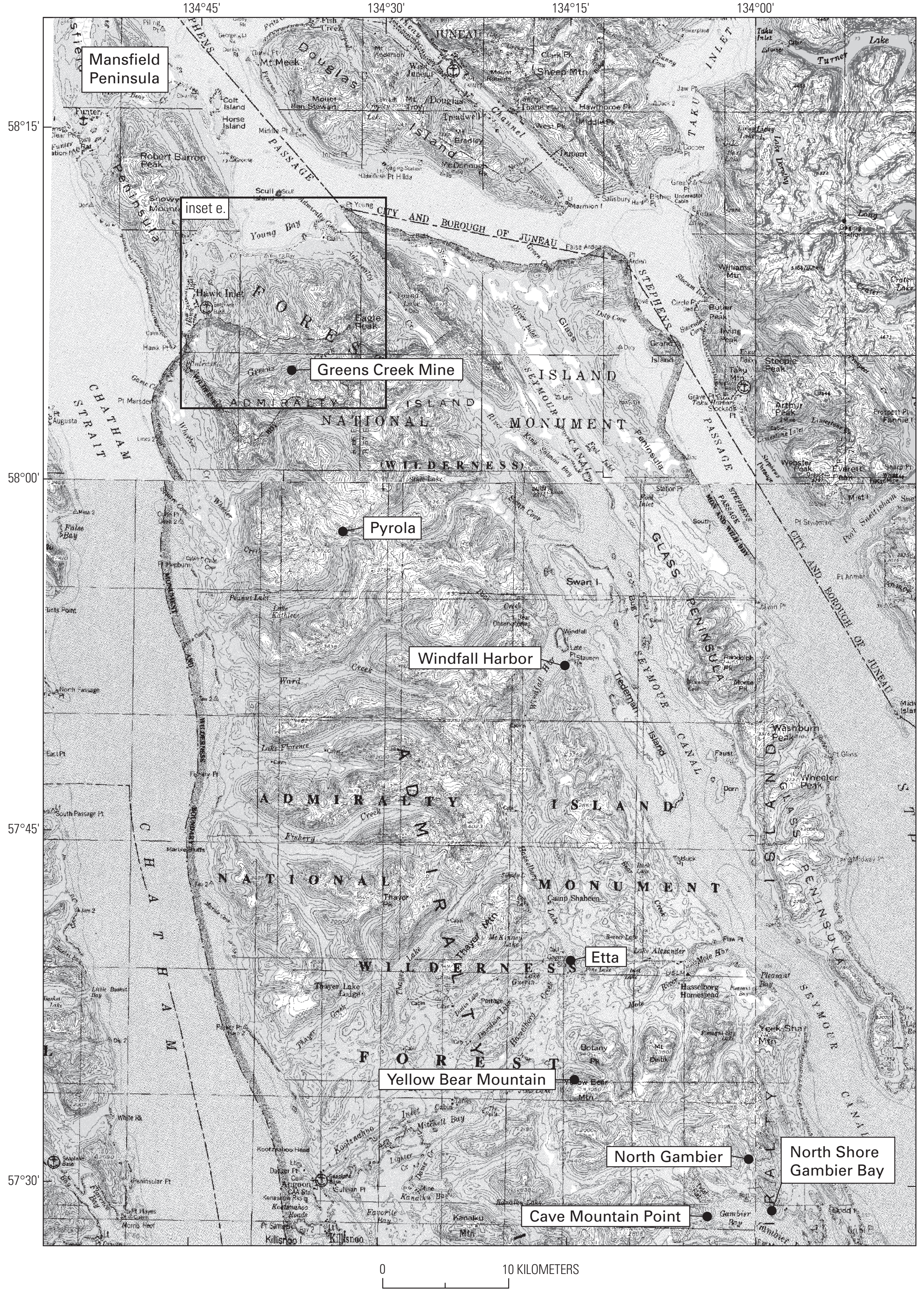
134°45'
134°30'
134°15'
134°00'
58°15'
58°00'
57°45'
57°30'
Mansfield Peninsula
inset e.
Greens Creek Mine
Pyrola
Windfall Harbor
Etta
Yellow Bear Mountain
North Gambier
North Shore Gambier Bay
Cave Mountain Point
0
10 KILOMETERS

Figure 1, inset d (facing page). Detailed map of the central ATMB showing the locations of mines, mineral deposits, and mineral occurrences and other features discussed in the text on Admiralty Island.

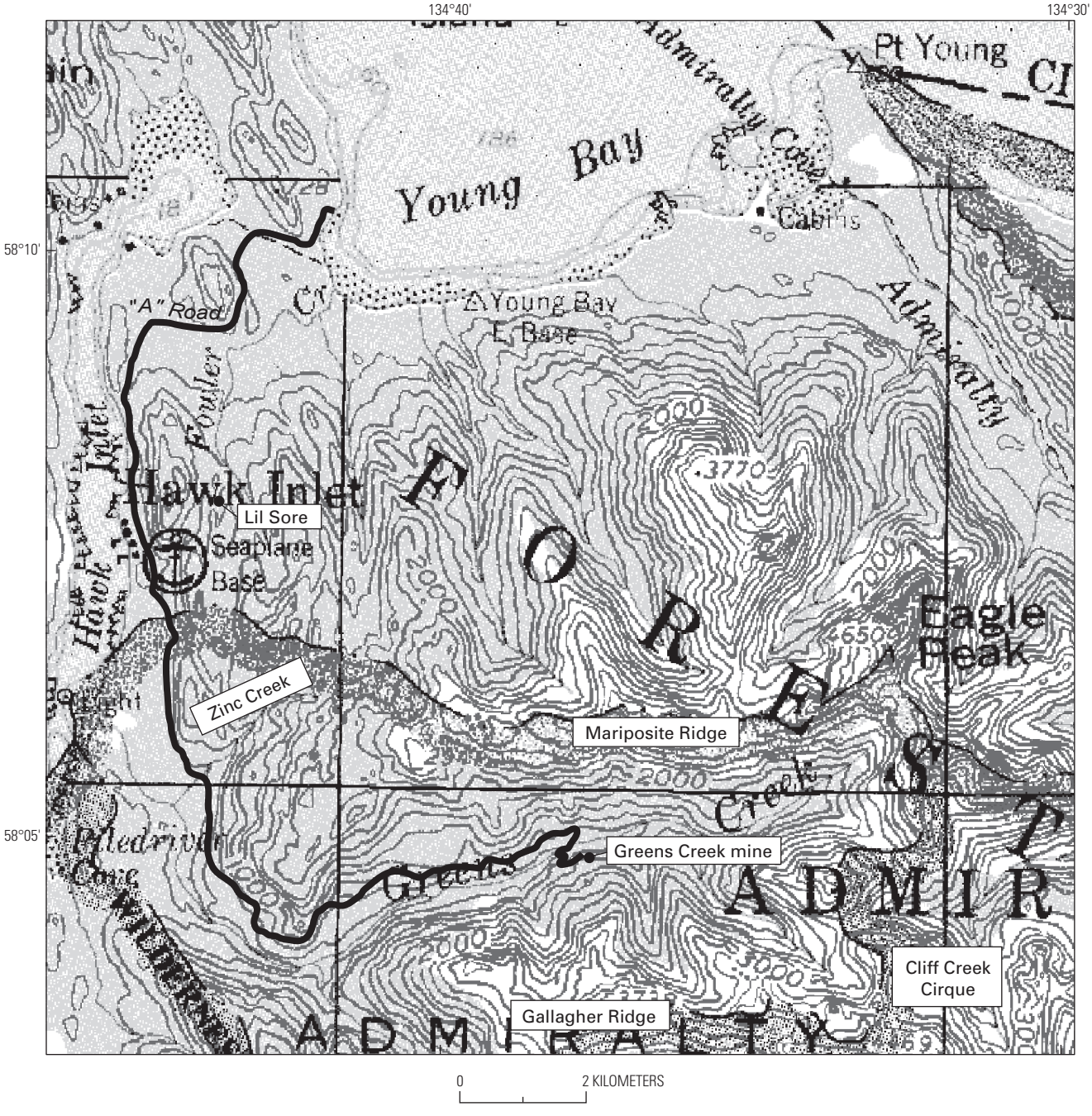

Figure 1, inset e. Detailed map of the Greens Creek mine area on northern Admiralty Island showing the locations of mines, mineral deposits, and mineral occurrences and other features discussed in the text. (Inset f) Detailed map of the northern ATMB showing the locations of mines, mineral deposits, and mineral occurrences and other features discussed in the text between the Mt. Henry Clay area and Windy Craggy.

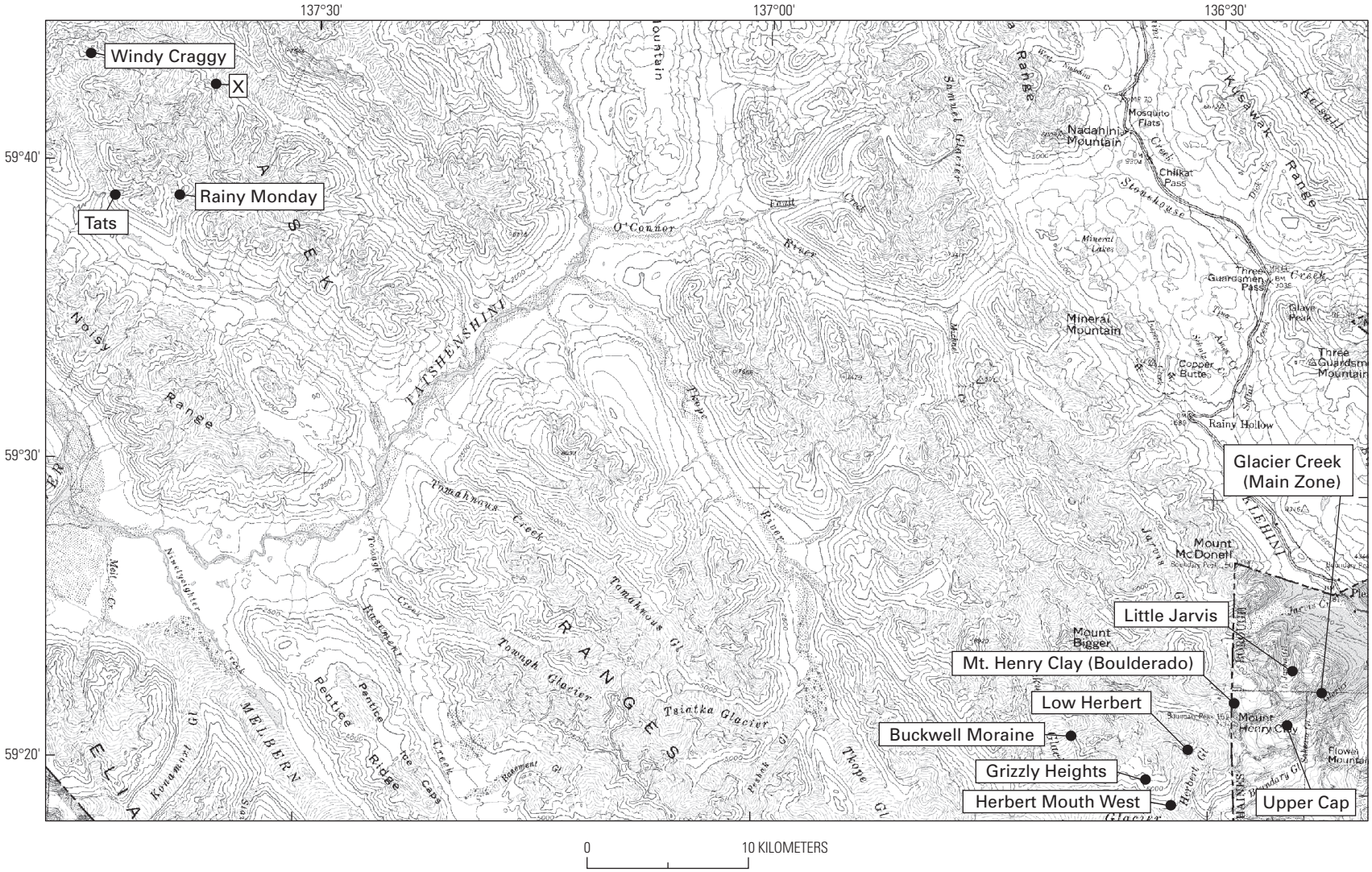

Figure 1, inset f. Detailed map of the northern ATMB showing the locations of mines, mineral deposits, and mineral occurrences and other features discussed in the text between the Mt. Henry Clay area and Windy Craggy.

Cu-Zn ± Au-Co-Ni and are similar to many Besshi-type ores (for example, Slack, 1993). The Frenchie VMS occurrence (St. John's Harbor) may be the southernmost of this type, and deposits of both descriptions occur on either side of the international border in the Mt. Henry Clay area. By the latitude of about the Tatshenshini River, the majority of the deposits are Besshi-like with Windy Craggy being the notable example. The Greens Creek deposit itself is unusual in that it exhibits a range of syngenetic, diagenetic, and epigenetic features that are transitional between VMS, sedimentary exhalative (SEDEX; see review by Goodfellow and others, 1993), and Mississippi Valley-type (MVT; see review by Leach and Sangster, 1993) genetic models (Taylor and others, 1999).

In the several locations where the host rocks of the ATMB have been studied, data uniformly suggest that the environment of deposition was some type of intra-arc or back-arc setting. Trace and REE chemistry of the mafic volcanics is transitional between midocean ridge basalt (MORB) and island-arc basalt (IAB), with discriminant plots based on immobile elements showing tectonic environments from MORB to within-plate basalts. Radiogenic isotopic data are indicative of a juvenile (mantle ?) source for the basalts. The several tectonic settings suggested to have produced these host rocks are variably: a brief episode of Late Triassic rifting prior to final docking of outboard terranes to the continental margin, small pull-apart basins in response to transpressive motion along the margin, or a failed rift.

Under close examination, however, the correlation of host rocks throughout the 600-km-long ATMB is problematic. Traditionally, the central strip of Upper Triassic volcanics, from Annette Island to at least the latitude of mid-Admiralty Island, was placed in the Alexander terrane. The Upper Triassic rocks on the mainland to the east were assigned to the Taku terrane, and the strip of Upper Triassic greenstones at Goondip to the west were placed in the Wrangellia terrane (for example, Berg and others, 1972, 1978; Churkin and Eberlein, 1977; Gehrels and Berg, 1994). Tentative correlation of the Hyd Group rocks on Admiralty Island with the informally named Jarvis basalts at Mt. Henry Clay, and with the informally named Tatshenshini basalts on the Canadian side of the border, would extend the central strip of rocks at least as far north as Windy Craggy within the Alexander terrane. However, correlation of the basalts at Chilkat in the central strip with the basalts at Taku of the eastern strip near Juneau (Ford and Brew, 1993; Gehrels and Barker, 1993) and with possible Hyd Group-equivalent rocks on the north end of Admiralty Island (Ford and Brew, 1993), raises the possibility that all of the Upper Triassic rocks of the composite Alexander-Wrangellia terrane are genetically related and formed during the same igneous event.

As originally defined, the distinguishing difference between the Alexander and Wrangellia terranes is the age and character of the Upper Triassic volcanic rocks. Wrangellia terrane basalts, as exemplified by the Nikolai Greenstone, basalts at Chilkat, greenstones at Goondip, and Karmutsen Formation, are voluminous, subaerial to shallow subaqueous, flood basalts of Carnian (230 Ma) age that were extruded over a period of about 5 million years (Panuska, 1990; Richards and others, 1991). In contrast, the basalts of the Alexander terrane, as exemplified by the Hyd Group, the Hound Island Volcanics of the Hyd, and possibly the Jarvis basalts of the Mt. Henry Clay area and the Tatshenshini basalts of northern British Columbia, are much thinner flows of Norian (210 Ma) age that are intercalated with graywacke and graphitic/pyritic mudstone. Several competing models for the production of the basalts of the Wrangellia terrane include an episode of volcanism related to intra-arc or back-arc rifting (Barker and others, 1989; Sampson and others, 1991; Barker, 1994), or to production of an oceanic plateau flood-basalt province in response to initiation of a mantle plume beneath the Paleozoic arc (Richards and others, 1991). The Alexander terrane basalts have generally been ascribed to formation during a period of intra-arc or back-arc rifting.

Since the recognition that Pennsylvanian plutons stitch the two terranes into one Wrangellia supercontinent (Gardner and others, 1988), distinctions between the Alexander and Wrangellian Upper Triassic rocks have been glossed over, and they are generally regarded as probable lateral facies of the same extensive unit. The extreme structural dismemberment and juxtaposition of parallel strips of rocks in southeastern Alaska, and thus the rapid variation in thickness of the Upper Triassic section and the associated variation in the percentage of volcanic to sedimentary rock, are explained as having occurred primarily in the Tertiary as a result of lateral transport of terranes northward along the continental margin. Alternatively, the volcanism could have occurred at multiple sites of rifting during discrete intervals from Carnian to Norian time.

Whereas the lumping of all of the Triassic volcanic rocks into one related package of rift- or plume-related rocks is convenient, it leaves unanswered the important question of why the belt of VMS deposits is only associated with basalts of the Alexander terrane. In this chapter we document the geology, stratigraphic setting, and mineral and host-rock geochemistry at a number of mineral occurrences within the ATMB. Our goal is to assemble a coherent metallogenic framework for the ATMB that will serve as a foundation for the more detailed chapters that follow on the Greens Creek deposit. This chapter treats a topic that was covered in a previous publication (Taylor and others, 2008), but it reports a greatly expanded chemical and isotopic database, many new figures, and extended descriptions and discussions.

Terrane Relationships

Host rocks to the ATMB are within the Admiralty and Craig subterranes of the Alexander terrane (Berg and others, 1972, 1978; Churkin and Eberlein, 1977). Terrane relationships in southeastern Alaska are shown in figure 2. The general evolution of the Alexander terrane has been discussed by Sampson and others (1989), who suggested that it has the characteristics of a wholly oceanic island arc. The terrane is

an allochthonous, continent-sized fragment of island arc crust that began forming in latest Precambrian time in low latitudes. It consists of as much as 35,000 feet of predominantly marine sedimentary and volcanic strata and plutonic rocks of latest Precambrian(?) to Middle(?) Jurassic age (Gehrels and Saleeby, 1987; Gehrels and Berg, 1994). By Devonian time the terrane had gone through two orogenies and a protracted period of quiescence marked by erosion and formation of extensive carbonate platforms. Paleomagnetic, paleontologic, and detrital zircon studies (Hillhouse, 1987; Hillhouse and Gromme, 1984; Haeussler and others, 1992; Bazard and others, 1994; Gehrels and others, 1994; Savage, 1994) suggest that by middle Permian time the terrane was outboard of a continental landmass and that depositional environments were characterized by shallow, tropical marine, possibly evaporitic, conditions.

Rift-fill stratigraphic sequences and bimodal volcanism along the eastern edge of the terrane (MacIntyre, 1986; Gehrels and others, 1986, 1987; Taylor and others, 2008) mark the beginning of an extensional tectonic event in the Late Triassic that either split the terrane or separated it from its low-latitude, offshore position and transported it to its present location on the western North American continental margin (Gehrels and Berg, 1994). The allochthonous Wrangellia terrane of Pennsylvanian to Late Triassic age (Jones and others, 1977), which is also of oceanic arc derivation (Sampson and others, 1990), adjoins the Alexander terrane on its western, northern, and northeastern sides. These terranes were stitched together by Middle Pennsylvanian plutons in southern Alaska (Gardner and others, 1988) to form the Wrangellia superterrane. Accretion of the Wrangellia superterrane may have commenced by the Early or Middle Jurassic (McClelland and Gehrels, 1990) or the Late Jurassic (Saleeby, 1994) and was complete by about middle Cretaceous time, as indicated by the intrusion of subduction-related, magmatic-epidote-bearing plutons and the development of the Jurassic-Cretaceous Chugach accretionary prism outboard of the superterrane.

Collision resulted in regional metamorphism and deformation related to underthrusting of the continental margin. This event produced relatively flat-lying, northwest-vergent thrust faults identified underground and in surface outcrops on Admiralty Island and throughout southeastern Alaska. Mapping of regional metamorphic facies by Dusel-Bacon (1994) places Triassic and older rocks in southeastern Alaska within the lower to middle greenschist facies. In early Tertiary time (Goldfarb and others, 1991; Miller and others, 1994), oblique subduction changed to right-lateral transcurrent motion along the margin, imparting the present structural grain to the country rocks and causing the formation of numerous, subparallel, high-angle, strike-slip faults that dismember the outboard terranes.

Stratigraphy of Host Rocks to Late Triassic Mineral Occurrences and Correlation Throughout Southeastern Alaska

The host rocks to the mines, deposits, and mineral occurrences examined during the course of this study are discontinuously exposed for approximately 600 kilometers along the eastern margin of the Alexander terrane, from Annette Island in the south, northward to Windy Craggy. In general, the stratigraphy within the ATMB consists of a 200–800-m-thick sequence of conglomerate, limestone, marine clastic sediment, volcanic rock, and tuff that are intercalated with and overlain by a distinctive unit of mafic pyroclastic rocks and pillowed flows (fig. 3). Faunal data bracket the age of the host rocks between Anisian (Middle Triassic) and late Norian (middle Late Triassic) time.

On Annette (fig. 4) and Gravina Islands (fig. 5) at the southern end, and in Keku Strait (fig. 6) in the middle portion of the ATMB, the base of the section is marked by a distinctive pebble conglomerate indicative of high-energy deposition in a near-slope or basin-margin setting. Clasts are polymictic, extremely immature, and are locally derived from the immediately underlying rocks. Features of the conglomerates indicate changing proximity to the source area. The median size and sorting of the clasts as well as the thickness and continuity of the units substantially change to the north. On Annette and Gravina Islands the dominant clast lithology is Silurian trondhjemite derived from the extensive pluton that underlies most of Annette Island and the south end of Gravina Island (Berg, 1972, 1973; Karl, 1992). Clast sizes range from pebbles to boulders 3 meters in diameter in continuous conglomerate sheets 30–45 meters thick (fig. 7). In Keku Strait clasts are dominantly composed of dolomite and chert from the underlying Pybus and Cannery Formations. Clasts are pebble- to boulder-sized (maximum of 0.3 m in long dimension) and occur in thin (0–6 m) discontinuous outcrops. In places, most notably on the northern shore of Hamilton Island, conglomerates occupy discrete scour channels that migrate laterally and vertically in a graywacke host.

A profound change in the character of the Upper Triassic stratigraphy occurs between Keku Strait and Duncan Canal. Both the sedimentary and volcanic units that comprise the section transition into rock types indicative of a position more distal to the Late Triassic rift margin. Whether this simply reflects a more seaward Late Triassic relative position of the Duncan Canal area to the east of Keku Strait or whether juxtaposition by faulting or folding of the two areas has occurred is not resolvable, given the current state of mapping and the

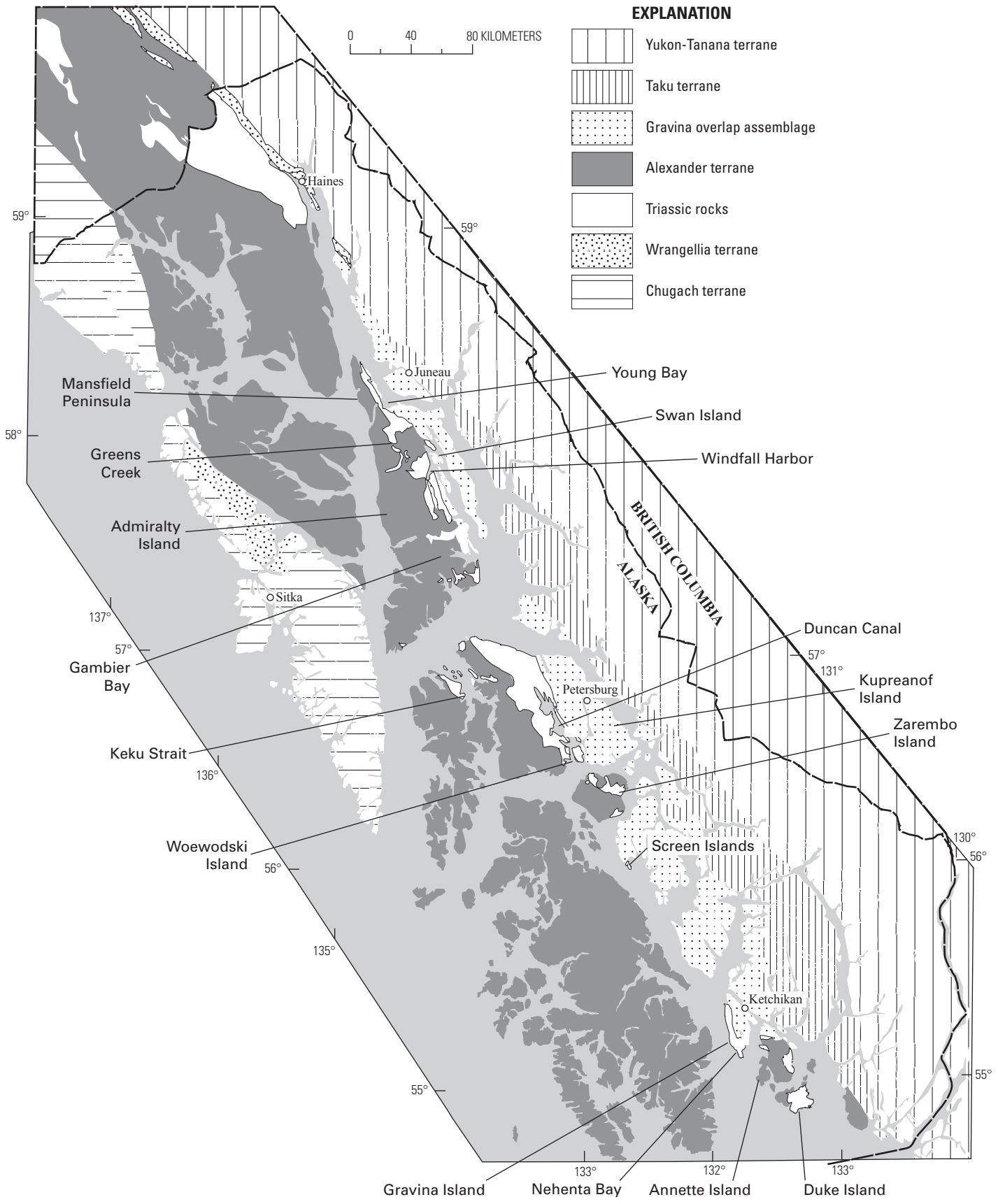

Figure 2. Tectonostratigraphic terranes of southeastern Alaska.

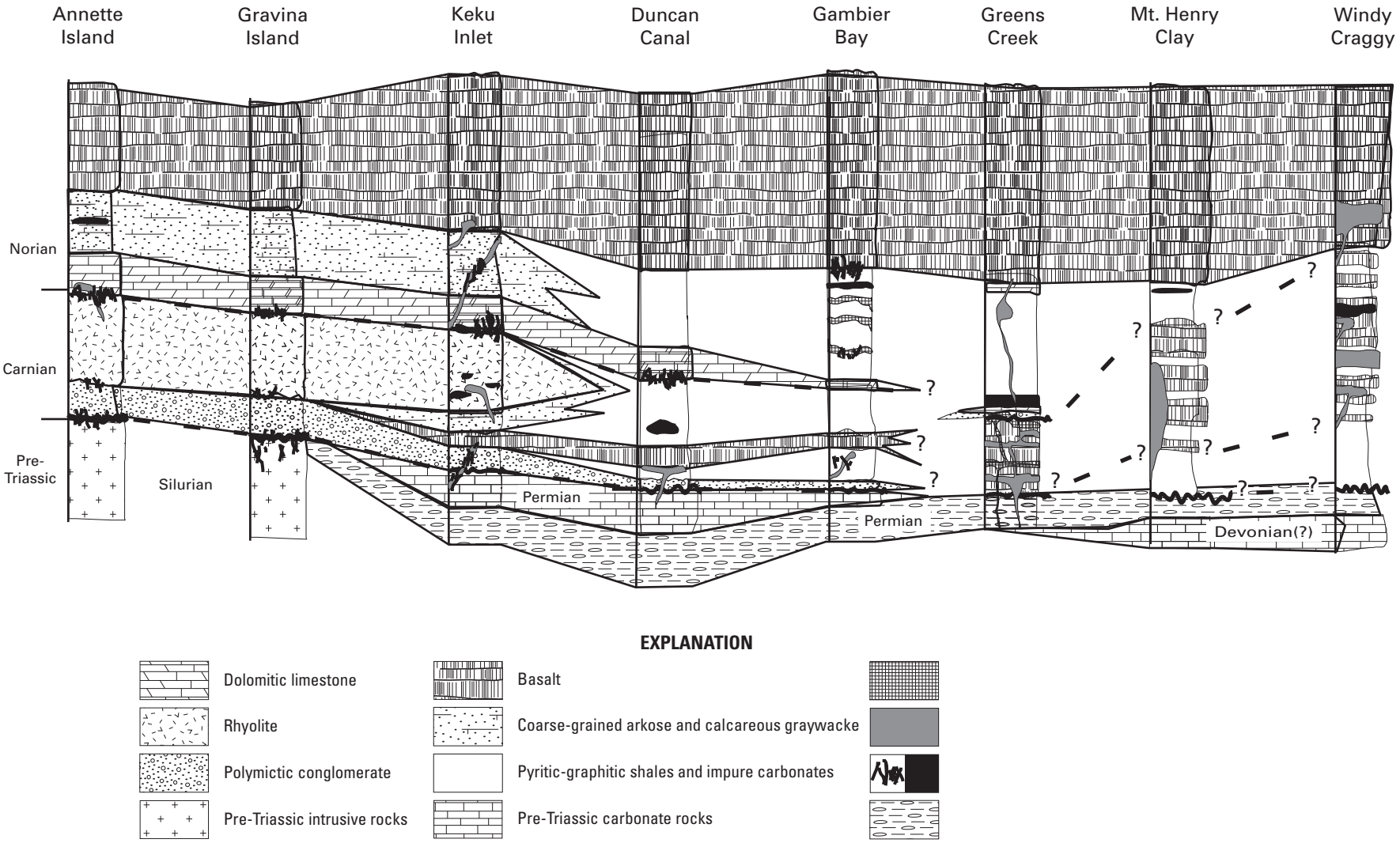

Figure 3. Stratigraphy and correlation of Upper Triassic host rocks in southeastern Alaska and adjacent British Columbia.

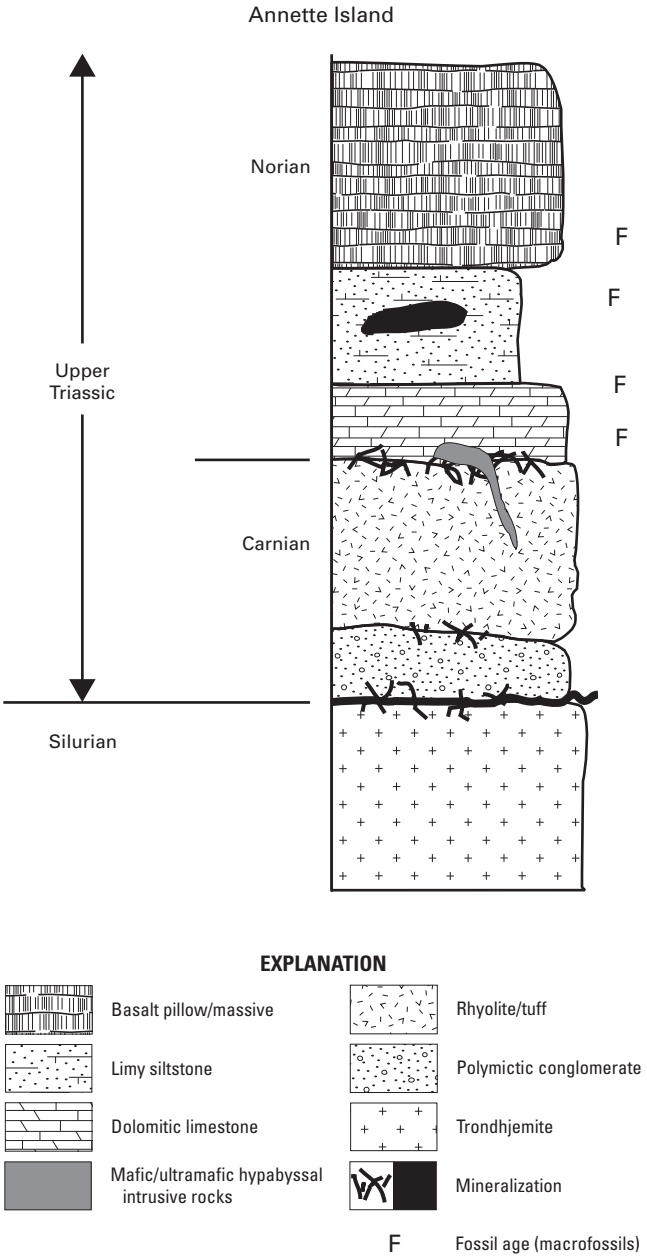

Figure 4. Composite stratigraphic column of the Upper Triassic section on Annette Island. Interpretation is based on Berg (1972), Gehrels and others (1987), Karl (1992), and this study.

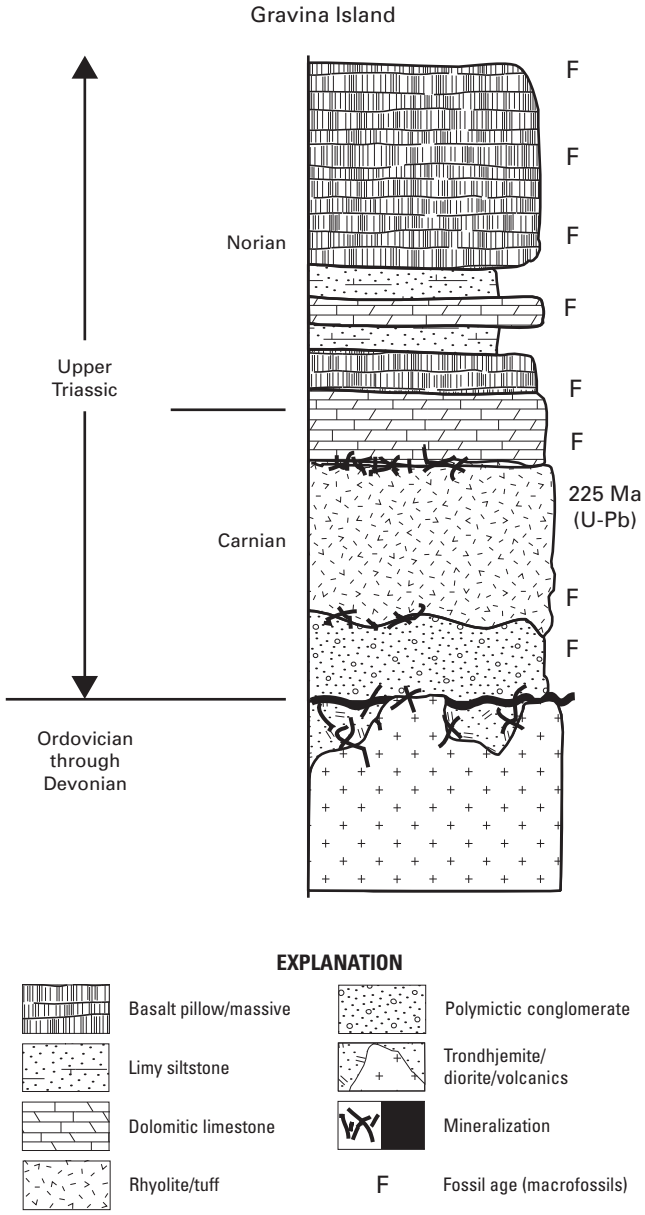

Figure 5. Composite stratigraphic column of the Upper Triassic section on Gravina Island. Interpretation is based on Berg (1973), Gehrels and others (1987), and this study.

generally poor exposure on most of Kupreanof Island. Tectonic shortening of a former basin is consistent with the synclinal structure proposed for the Keku Strait (Muffler, 1967) and is also compatible with the pattern of open folding and northwest-vergent thrusting documented by recent mapping in the Duncan Canal area (Karl and others, 1999a). Alternatively, juxtaposition of seaward (Duncan Canal) and landward (Keku Strait) areas of a northward-deepening rift basin may have resulted due to northward transport of the southern portion of the ATMB during Tertiary margin-parallel faulting.

When present, the basal polymictic conglomerate in Duncan Canal (fig. 8) reflects the character of a debris flow that is distal to its source. Clasts are millimeters to several centimeters in size and occur in thin (0–10 meters) discontinuous outcrops. However, clasts appear to be subrounded and somewhat more sorted than conglomerates to the south. Clasts are dominantly composed of white quartz pebbles and chert with a lesser but important component of black shale chips that are probably derived from the underlying Cannery Formation. In two outcrops examined, one on the northwestern shore of Woewodski Island and a second on the west side of Duncan Canal north of the Castle River, the clasts are stretched considerably and the sericitic matrix appears drawn out by shearing. This deformation, related to movement in the

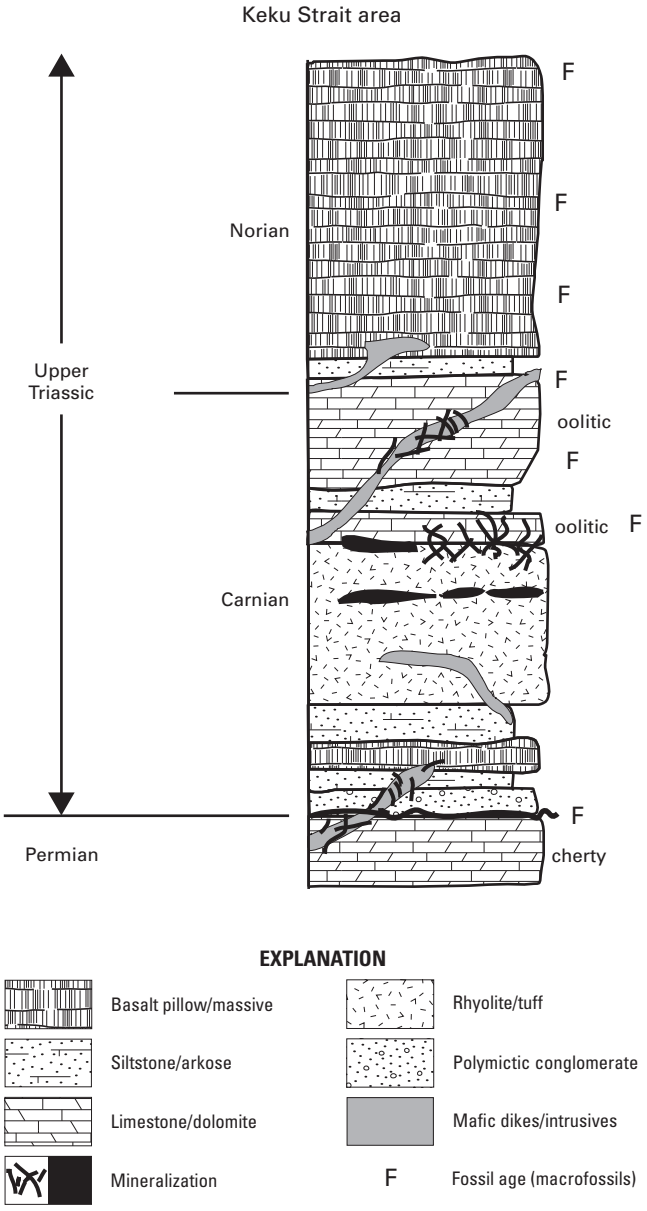

Figure 6. Composite stratigraphic column of the Upper Triassic section in the Keku Strait area. Interpretation is based on Muffler (1967), and this study.

Duncan Canal shear zone (McClelland and Gehrels, 1990; Haeussler and others, 1999), has imparted a platy, fissile character to the conglomerates not observed at the previously described locations.

By the latitude of Gambier Bay and Windfall Harbor on Admiralty Island the basal polymictic conglomerate is only locally present (fig. 9). Clasts are mostly pebble to cobble sized and are dominantly composed of chert and dolomite, derived from the underlying Permian units. Individual conglomerate horizons are no thicker than about 3 meters. Although thin and discontinuous conglomerate horizons occur in the northern half of Admiralty Island, their stratigraphic positions within the Triassic section are uncertain. In most cases, they are thought to be above the base of the section within the shales that constitute the middle sedimentary portion of the Triassic stratigraphy. Additionally, these midsection conglomerates are similar in clast composition and maturity to the more distal-looking conglomerates in the Duncan Canal area. Notable examples are the thin quartz pebble-rich horizons in the 720 access ramp underground at the Greens Creek mine (fig. 10), and the 2-m-thick horizon immediately west of the drill pad at the Little Sore prospect several kilometers north of the mine. The stretched quartz-pebble-rich conglomerate near Young Bay along the A-road may be an additional example.

The northernmost occurrences of a conglomerate "marker horizon" at the base of the Triassic section are on the eastern shore of Windfall Harbor immediately overlying the siliceous black shales of the Cannery Formation, and the debriite in Zinc Creek, described by Duke and others (chap. 4, the term debriite is used here to connote debris-flow deposits, following Warme and Kuehner, 1998). Our examination of this unit shows it to be a very poorly sorted, proximally derived polymictic conglomerate, composed of angular fragments of the immediately underlying lithologies. Abundant pyrite and iron carbonate in the matrix suggest the unit has been mineralized. Similarity to angular conglomerates in the footwall stratigraphy at the North Gambier pyritic copper-zinc-silver-barite occurrence (Taylor and others, 1992) suggests local fault control on the distribution of the basal conglomerates and on hydrothermal fluid flow. North of Admiralty Island, the basal conglomerate is absent, and no midstratigraphy conglomerate lenses are reported in the Triassic section.

In the southern end of the ATMB, dominantly felsic volcanic rocks immediately overlie the basal conglomerate. Thin basaltic flows are variably present as well near the bottom of the section and tend toward alkali basalt compositions. Massive and pillowed basalt flows occur within the sedimentary portion of the section on Gravina Island overlying the Puppets Formation. In the Keku Strait area we place thin basaltic flows within an interval of arkosic sediments immediately below the Keku Volcanics. Muffler (1967) also described mafic flows intercalated with the Keku Volcanics. On Annette and Gravina Islands the rhyolites are continuous, massive, flow-banded units; the cliff exposure of the Puppets Formation in Nehenta Bay is on the order of 150 meters thick. Berg (1973) estimated the unit to be 165 meters thick. On the Cornwallis Peninsula the Keku Volcanics is of uncertain thickness due to structural complexities but occupies an eastward-dipping belt 1.5 to 5 kilometers wide (Muffler, 1967). Drilling on the peninsula in 1995 by Sealaska Corporation was collared in the Keku Volcanics and penetrated over 366 meters of massive, flow-banded, volcaniclastic, and tuffaceous rhyolite without encountering a bottom contact. The position low in the section beneath the sedimentary and overlying mafic volcanic rocks, as well as the distinctive chemistry of the Keku Volcanics (discussed in succeeding

Figure 7. Photograph of the basal Upper Triassic conglomerate in Nehenta Bay, Gravina Island. Note abundance of light-colored clasts of Silurian trondhjemite derived from the pluton that underlies much of Annette and southern Gravina Islands.

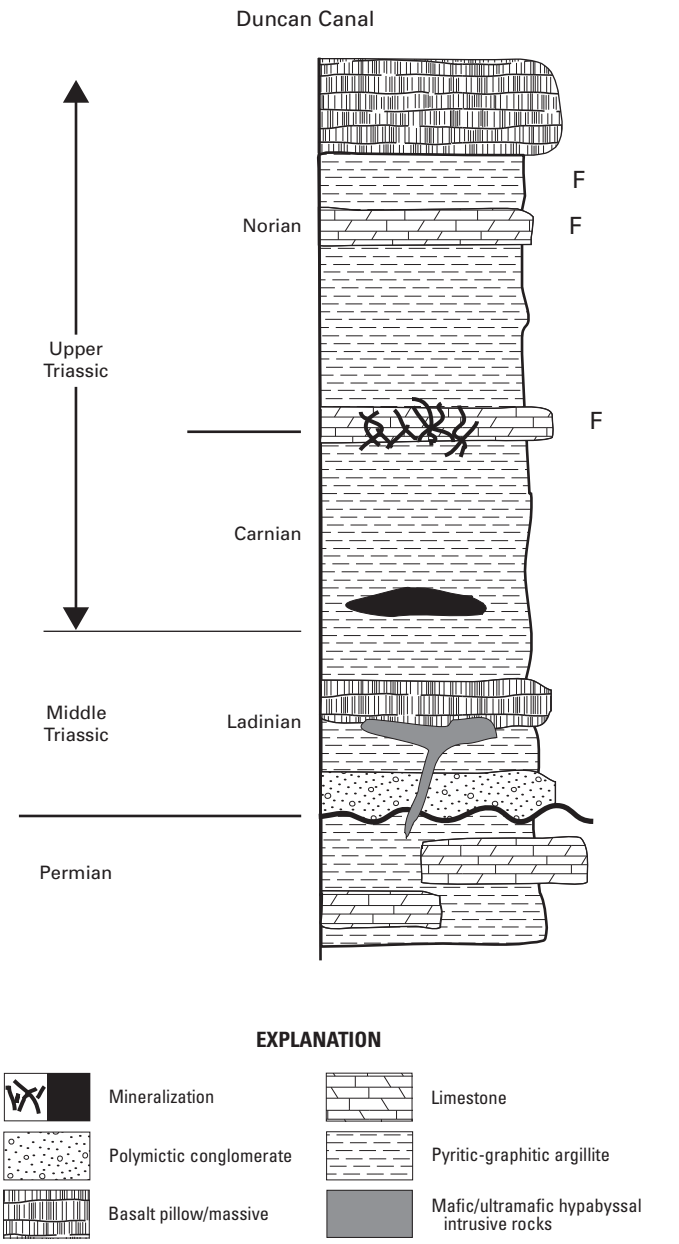

Figure 8. Composite stratigraphic column of the Middle and Upper Triassic section in the Duncan Canal area. Present interpretation is based on McClelland and Gehrels (1990), Karl and others (1999b), and this study.

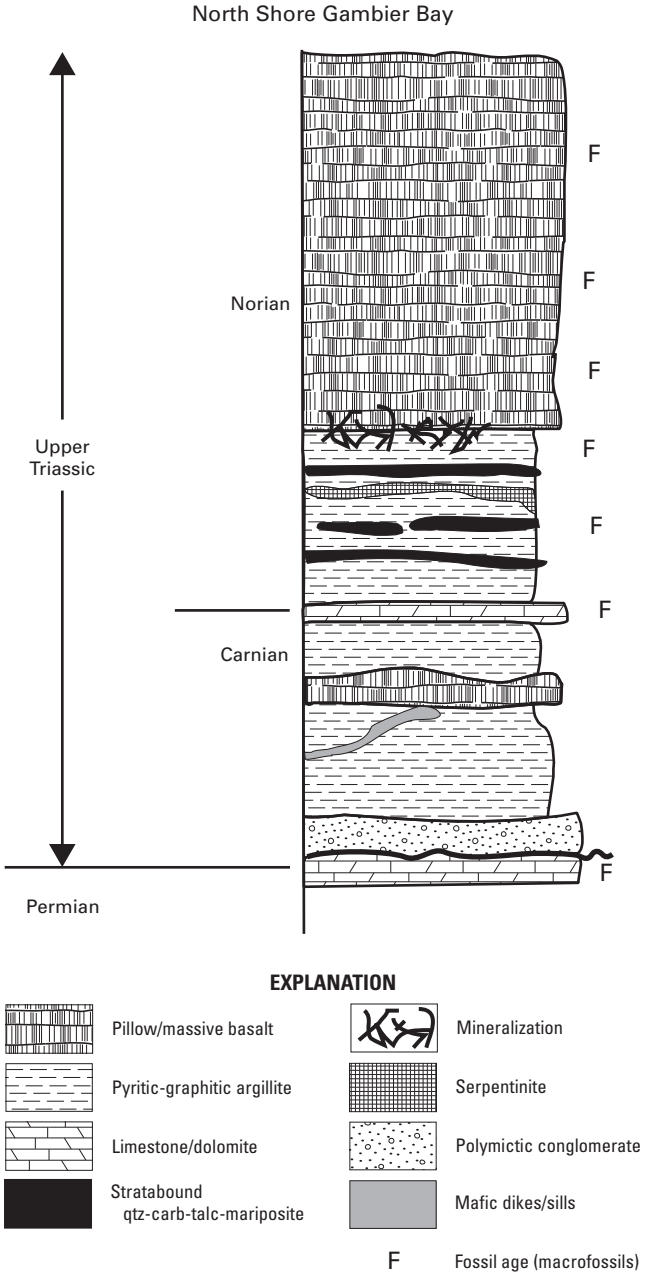

Figure 9. Composite stratigraphic column of the Upper Triassic section on the north shore of Gambier Bay, southern Admiralty Island. Interpretation is based on Loney (1964), Taylor and others (1992), and this study.

paragraphs), strongly suggest origins as bimodal volcanic rocks that were produced during the initiation of rifting.

In the Duncan Canal area, the stratigraphy is poorly constrained due to poor exposure. Rhyolites are largely absent north of Keku Strait, and their place low in the section is occupied instead by minor basalt flows interbedded with black shale. At the mouth of Castle River on the west side of Duncan Canal, thin (~4-m-thick) columnar-jointed basalt flows occupy a stratigraphic position just above the conglomerates. Similarly, pillowed basalt flows are present on the north tip of Little Castle Island immediately west of (underlying ?) the Castle Island barite deposit. On the northwest shore of Woewodski Island, a thin basalt flow lies immediately beneath a stretched pebble conglomerate lens that we interpret to be the Upper Triassic basal conglomerate. Black shales immediately overlying the conglomerate contain several 15-cm-thick horizons of pyritic felsic tuff. To the south on Woewodski Island, several crudely stratiform

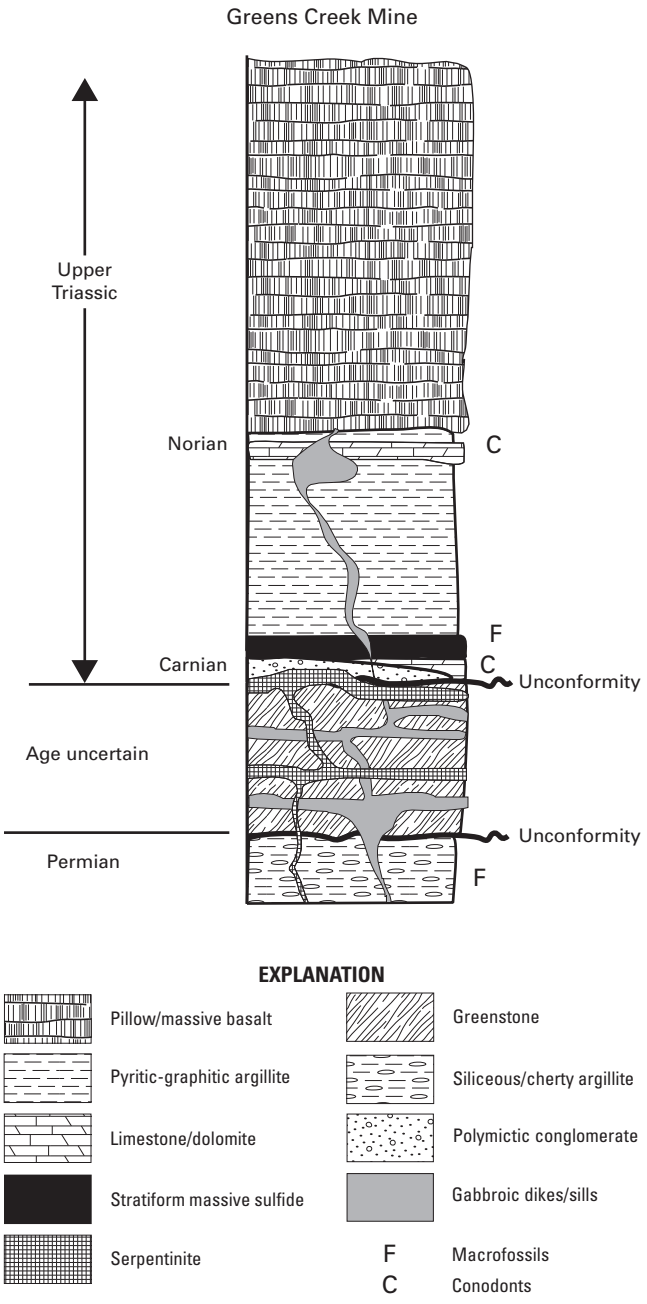

Figure 10. Composite stratigraphic column of the Upper Triassic section at the Greens Creek mine, northern Admiralty Island. Interpretation is based on this study.

mineral occurrences of probable Late Triassic age (for example, Lost Show and Brushy Creek) are hosted in highly altered volcanic rocks. Although protoliths are obscured, it is unlikely that the altered volcanics were rhyolites. Their chemistry (for example, 98DC–33, table 2) and mineralogy is most consistent with altered mafic volcanic rocks. Less altered country rocks consist of mafic volcanic, volcaniclastic, and tuffaceous rocks. Highly altered tuffaceous rocks at Brushy Creek and sericite schist in creek exposures several hundred meters south of the occurrence could represent felsic tuffs. Poor exposure precludes assignment of these volcanic rocks to a specific position within the Upper Triassic stratigraphy.

On Zarembo Island, Upper Triassic rocks occur in a northwest-trending swath of flat topography that limits exposures to creek banks and borrow pits along logging roads. Absence of a recognizable stratigraphic marker horizon at the Frenchie pyritic massive sulfide deposit prevents distinguishing the stratigraphic position. However, the host rock immediately overlying the Frenchie deposit is a 6- to 10-meter-thick unit of pyritic quartz-sericite schist; the immediate footwall contains a thin lens of muscovite schist overlying graphitic pyritic argillite. Relationships at the Round Point mineral occurrence to the southeast are similarly obscure. Like the volcanic-hosted deposits on Woewodski Island, Round Point is hosted in altered volcanic rocks of probable mafic parentage.

Felsic volcanic rocks in the ATMB north of the felsic tuffs on the northwest shore of Woewodski Island and the Keku Volcanics in Keku Strait are rare. Recent mapping (S.M. Karl, oral commun., 2004) has identified outcrops of rhyolite of probable Triassic age on central Admiralty Island along the shoreline of Seymour Canal west of Swan Island, and vicinity. Thin units of quartz-sericite-pyrite altered trachyandesite, rhyolite, and felsic tuffaceous rocks associated with the RW zone (also called the Little Jarvis occurrence) of the Glacier Creek (Main) deposit (fig. 11) (Green and others, 2003) constitute the northernmost occurrence of Upper Triassic felsic volcanic rocks.

North of the Duncan Canal area, the position low in the Triassic section occupied by the rhyolites is filled by mafic lava flows. On the north shore of Gambier Bay, at least two separate pillowed flows are present in graphitic sediments above the basal conglomerate (fig. 12). Similarly, an outcrop of pillow basalt is present between the conglomerates and sediments in the footwall section of the North Gambier occurrence, 2.5 kilometers to the north (Taylor and others, 1992). At Greens Creek, the age of the footwall phyllites remains the major unanswered question of the current research effort. The position of the phyllites immediately below and in apparent conformable contact with the argillites suggest that they represent a locally thickened accumulation of mafic volcanics low in the section, as observed in Gambier Bay and elsewhere. The presence of the conglomerate horizons, both in the footwall and in the immediate hanging wall as previously described, does little to clarify the problem, as they are not clearly identifiable as the locally derived, polymictic conglomerate marker horizon commonly present at the base of the section. The highly altered and foliated nature of the footwall phyllite also distinguishes it from other mafic volcanics low in the section and invites comparison to other, older mafic units that display similar styles of deformation. Current mapping by Duke and others (chap. 4) assigns the footwall phyllites to the Middle(?) Devonian Retreat Group. Karl and others (S.M. Karl, oral commun., 2004) map a metamorphic unit of mixed lithologies including black phyllite, greenschist, and Devonian metalimestone on the north side of Greens Creek, stratigraphically beneath the Cannery Formation

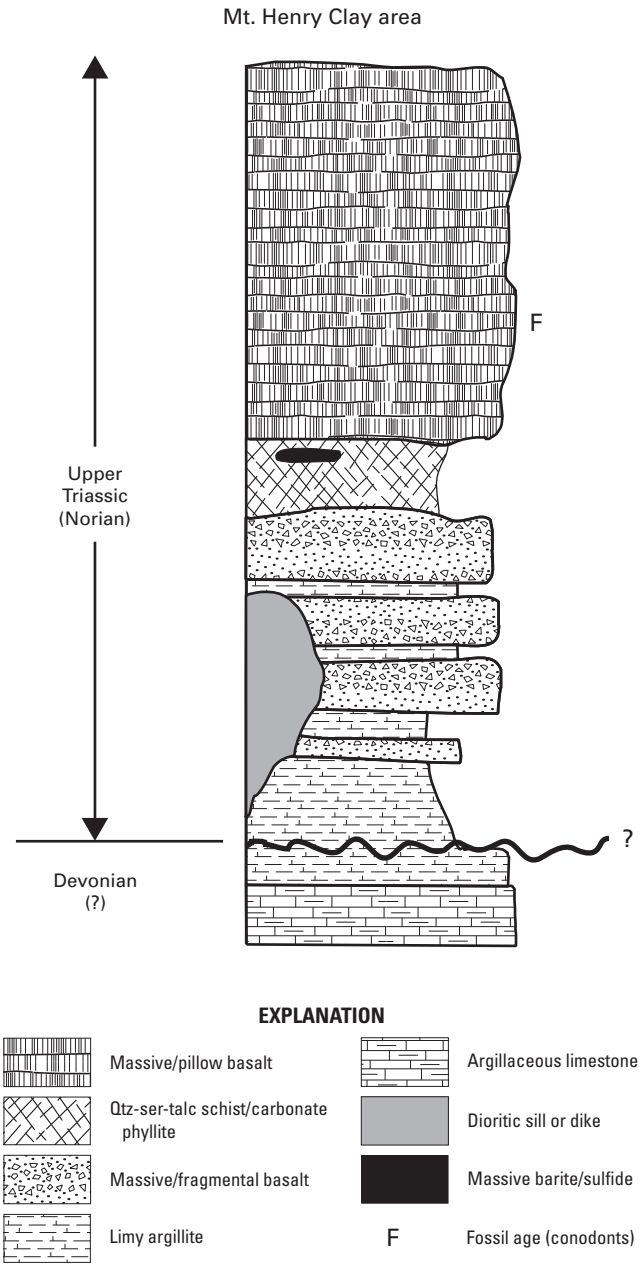

Figure 11. Composite stratigraphic column of the Upper Triassic section in the Mt. Henry Clay area, northern southeastern Alaska and northwestern British Columbia. Modified from MacIntyre and Schroeter (1985).

and Hyd Group. We note the evidence to suggest a Late Triassic age for the footwall; however, in the absence of direct evidence of a Late Triassic age we assign the footwall to an uncertain Late Triassic, Permian, or older lithologic association (fig. 10). At both Mt. Henry Clay and Windy Craggy (fig. 13), felsic volcanic rocks are absent, and their position low in the section is occupied by mafic volcanic rocks (MacIntyre and Schroeter, 1985; Forbes and others, 1989; Peter and Scott, 1999).

In the southern portion of the ATMB the rhyolites are overlain by dolomitic limestones that in places contain ooids (Muffler, 1967) and abundant fossils (Muffler, 1967; Berg, 1973), indicative of a shallow marine depositional environment (Muffler, 1967). The carbonate portion of the section also contains carbonate turbidites and carbonate breccias with fining-upwards sequences (for example, Nehenta Bay of Gravina Island, Screen Islands) indicative of the destruction of a shallow carbonate ramp during the onset of rifting. The limestones are present as 15-meter-high cliffs on the Cornwallis Peninsula, but thin substantially northward. They occur discontinuously in the Duncan Canal area and across Admiralty Island. In Gambier Bay the limestones are present as a locally exposed carbonate/dolomite breccia near the base of the section. In the Cliff Creek Cirque and in several locations along Gallagher Ridge immediately south of the Greens Creek mine, thin carbonate beds lie just below and are intercalated with the capping Hyd basalts. Underground at Greens Creek, thin discontinuous beds of fossiliferous limestone with *Halobia* fragments establish a Late Triassic age for carbonates in the footwall of the orebody and represent additional evidence for a Triassic age of the underlying phyllites. Unfortunately, the highly altered nature of the footwall carbonate rocks and their commonly brecciated texture yields uncertainty regarding the nature of the phyllite-carbonate contact. The footwall carbonate rocks may well be carbonate debris flows and thus could be stratigraphically equivalent to the basal conglomerate. North of Admiralty Island, discrete limestone units appear to be missing from the section.

The disappearance of the limestones from the section is accompanied by a corresponding increase in carbonaceous shales, indicative of deeper water settings. As far north as Keku Strait, the middle portion of the section is composed of very limy, arkosic sediments characteristic of a proximal, carbonate-rich source on the flanks of the Alexander terrane. From Zarembo Island northward the sediments contain more graphitic, pyritic black shale, indicative of an anoxic to euxinic, sediment-starved depositional environment distal to the flanks of the rift. At Greens Creek the shales (argillites) are intercalated with dolomitic limestone, and at Windy Craggy the black shales are markedly calcareous (Peter and Scott, 1999).

Most everywhere throughout southeastern Alaska and adjacent British Columbia the Triassic stratigraphy is capped by a thick (200–600 m) sequence of basalts. These basalts are massive to pillowed and commonly show spectacular volcaniclastic textures. In hand specimen and thin section, the basalts are vesicular and mostly aphanitic; minor porphyritic-aphanitic varieties contain relict phenocrysts of clinopyroxene, plagioclase, hornblende, and rare olivine. Compared to the generally foliated Paleozoic greenstones of the Alexander terrane, these Norian-age basalts are relatively undeformed. In the absence of the basal conglomerates, the thick sequence of greenstones overlying the sedimentary portion of the section is the most distinguishing feature of the Upper Triassic stratigraphy. Although the basalts have a variety of names throughout the ATMB—Chapin Peak Formation of Hyd Group on

Figure 12. Pillowed basalt flow near the base of the Upper Triassic section on the north shore of Gambier Bay, southern Admiralty Island.

Gravina Island (Berg, 1973); Hound Island Volcanics in the Keku Strait (Muffler, 1967); Hyd Group basalts on Admiralty Island (Lathram and others, 1965); Jarvis basalts (informal) in the Mt. Henry Clay area (Forbes and others, 1989); Tatshenshini basalts (informal) of northwestern British Columbia (MacIntyre and Schroeter, 1985)—they are all related by similar age, chemistry, and stratigraphic position.

Geochemistry of Upper Triassic Basalts and Rhyolites of Southeastern Alaska

Whole-rock geochemical data for Upper Triassic igneous rocks at mineral occurrences and unmineralized outcrops throughout southeastern Alaska were obtained in order to evaluate the petrogenetic setting of the ATMB. Major, minor, and trace-element abundances were determined by XRF, lithium metaborate fusion ICP–MS, and ICP–AES in the USGS laboratories in Denver. Summary data for a number of key locations are given in table 1; all the data are presented in table 2. General analytical methods and information on accuracy and precision of each method are described in Taggart (2002). Specific information on the lithium metaborate fusion ICP–MS analytical method used to obtain rare-earth and high field-strength elemental data critical to the tectonic discriminant analysis presented herein is available in Meier and Slowik (2002). Lower limits of detection (LOD) are represented in table 2 as less-thans and are 3 sigma values that are calculated for each instrument run based on multiple analyses of reagent blanks. Multiple analyses of internal laboratory standards are used to calibrate the instrument response, and then accuracy and precision of the analyses are verified to be within published limits by analysis of several USGS standard reference materials that are included in each run. Due to the nature of the ICP–MS technique, lower limits of detection vary between analytical runs. Also, there was an instrumentation change during the course of this study, with a resulting order-of-magnitude increase in instrument sensitivity for analyses performed after 1994. Variation in LOD for most of the elements reported in table 2 are due to these factors and are a normal feature of ICP–MS analyses (P.J. Lamothe, oral commun., 2004). Additional discussion of the use of ICP–MS analysis for the determination of trace elements in igneous rocks is available in Longerich and others (1990), Jenner and others (1990), and Jenner (1996).

Table 1. Summary whole-rock geochemical data for Upper Triassic basaltic rocks at key locations in southeastern Alaska.

Location	Annette Island	Gravina Island	Gravina Island	Keku Strait	Duncan Canal	Gambier Bay	Central Admiralty Island	Greens Creek south	Greens Creek north	Mansfield Peninsula	Mt. Henry Clay	Windy Craggy
Lithology	basalt	basalt	gabbro	basalt	basalt	basalt	basalt	basalt	basalt	basalt	basalt	basalt
Number (n)	7	2	2	7	21	6	7	13	4	5	9	3
SiO_2	50.1	44.3	44.4	45.8	48.4	45.7	52.1	51.9	46.6	47.3	48.9	42.9
Al_2O_3	17.6	14.3	17.4	14.8	13.6	15.4	15.0	15.8	16.4	14.6	14.0	16.1
Fe_1O_3	10.2	10.8	11.1	13.4	13.1	10.4	10.9	10.1	11.4	11.4	12.0	14.3
MgO	3.6	4.3	8.7	6.1	6.1	5.1	6.9	6.4	6.6	6.7	4.9	10.1
CaO	6.5	12.3	10.1	7.5	9.1	11.8	5.3	4.4	6.6	11.0	7.3	4.7
Na_2O	3.7	3.0	2.4	3.3	3.1	2.9	3.1	4.3	2.8	2.3	2.7	2.9
K_2O	2.2	1.1	0.3	0.8	0.7	0.6	1.0	1.3	1.9	0.9	0.8	0.4
TiO_2	0.9	2.0	1.3	2.4	1.9	1.2	1.1	0.8	1.4	1.6	1.1	1.0
P_2O_5	0.3	0.6	0.2	0.4	0.2	0.2	0.2	0.2	0.3	0.2	0.2	0.5
MnO	0.2	0.2	0.2	0.2	0.2	0.2	0.1	0.2	0.2	0.2	0.2	0.1
CO_2	1.7			1.6	0.9	2.7						
Total H_2O	3.3			4.9	3.1							
LOI	4.1	6.5	3.9	4.8	2.7	5.7	3.8	4.1	5.6	3.4	7.0	6.2
Sum	100.2	99.4	99.9	101.1	100.4	101.9	99.5	99.4	99.8	99.4	99.1	99.0
La	11.4	17.4	5.4	13.4	9.3	9.4	10.6	11.9	8.6	7.1	9.3	24.7
Ce	25.6	43.0	15.0	31.0	22.2	21.5	22.4	22.8	22.0	18.4	20.4	48.7
Pr	3.4	6.4	2.4	4.5	3.2	3.1	3.0	2.7	3.4	2.7	2.6	5.5
Nd	15.1	31.0	11.5	20.0	15.3	14.2	13.0	11.4	16.0	13.0	11.5	21.3
Sm	3.5	7.8	3.4	5.2	4.2	3.7	3.3	2.6	4.4	3.6	3.0	3.8
Eu	1.0	2.6	1.3	1.8	1.4	1.1	1.0	0.8	1.5	1.3	1.0	0.9
Gd	3.5	8.9	3.9	6.5	5.0	4.2	3.8	3.1	4.6	4.4	4.0	3.9
Tb	0.6	1.4	0.6	1.1	0.9	0.7	0.7	0.5	0.8	0.7	0.7	0.6
Dy	3.8	8.3	3.8	6.5	5.0	4.1	3.9	3.4	4.5	4.4	4.5	3.8
Ho	0.8	1.8	0.8	1.2	1.0	0.9	0.8	0.8	0.9	0.9	1.0	0.8
Er	2.4	4.9	2.1	3.7	2.8	2.5	2.4	2.3	2.6	2.6	2.9	2.4
Tm	0.4	0.7	0.3	0.6	0.4	0.4	0.4	0.3	0.4	0.4	0.5	0.4
Yb	2.4	4.5	1.8	3.6	2.8	2.4	2.4	2.5	2.4	2.3	3.0	2.3
Hf	2.3	4.3	1.9	4.7	3.6	2.3	3.2	2.3	2.8	3.2	2.7	3.3
Ta	0.4	0.6	0.4	0.7	0.8	0.5	1.3	0.4	0.6	0.6		
Rb	43.6	19.5	4.3	14.5	14.5	16.0	20.5	19.6	53.1	14.4	18.1	5.7
Y	21.0	42.0	17.5	34.0	28.5	22.5	23.4	19.4	22.5	22.6	25.2	24.0
Zr	54.0	205.0	90.0	140.3	124.1	78.8	134.0	85.3	109.8	105.0	69.7	88.7
Nb	3.4	5.3	2.2	11.8	7.2	4.8	7.1	5.7	4.8	5.6	6.0	20.0
Ba	562.9	270.0	140.0	1017.1	956.4	791.8	378.6	633.8	467.8	174.0	397.8	178.0
Th	2.7	3.2		1.1	1.1	0.9	1.8	2.6	1.1	0.8	3.9	4.1
Sc	28.3	27.0	27.0	37.6	41.5	29.2	31.0	28.4	30.5	33.8	37.6	28.7
V	268.6	219.5	255.0	358.6	434.5	333.3	295.7	222.3	307.5	382.0	303.3	196.7
Cr	53.7	120.0	97.0	121.3	185.6	578.0	200.7	314.6	875.0	770.0	49.6	336.7
Ni	19.4	51.0	142.5	43.3	71.9	46.5	47.3	44.2	67.3	70.6	30.7	118.3
Co	29.6	52.0	68.0	44.4	50.1	45.0	39.0	38.7	44.5	47.6	39.2	33.3
Cu	123.4	48.5	62.5	59.7	167.3	219.5	45.8	83.5	80.3	107.4	112.0	249.7
Zn	174.6	135.0	90.0	115.6	112.0	84.3	130.9	111.1	92.0	92.2	336.7	51.0
Ga	20.7			24.0	21.0	17.0					17.7	25.0
Sr	727.1	425.0	365.0	468.6	307.2	773.3	152.9	146.6	330.0	362.0	240.3	251.0
Cs	0.5	0.4	0.3	0.9	0.5	1.4	1.2	0.8	2.0	0.4		
Pb	12.3	3.2		27.0	3.8	6.5	5.3	8.0	4.7	5.2	10.9	4.3
Sn		2.5	0.9	2.0	2.4	0.9	3.5	3.7	0.7	1.4		
W	0.1	0.4	0.3		2.3	1.4	0.9	0.8	0.3	0.4		
U	0.3	0.7	0.1	0.6	0.4	0.2	0.7	0.7	0.4	0.4		

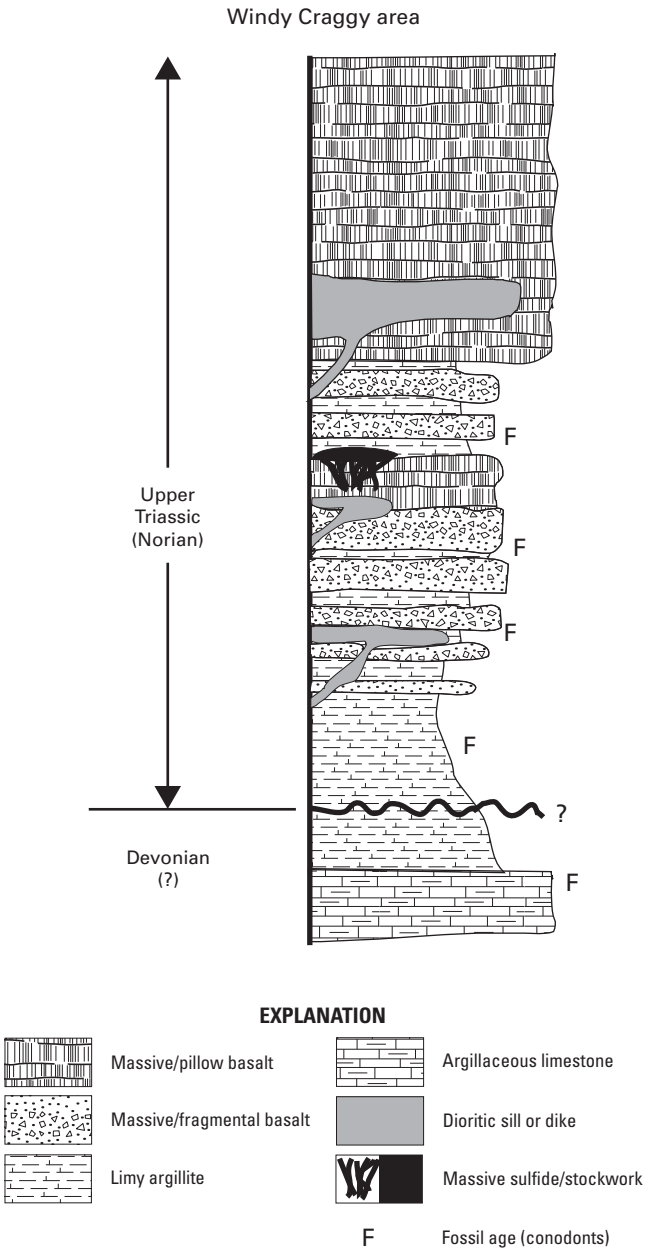

Figure 13. Composite stratigraphic column of the Upper Triassic section at the Windy Craggy deposit, northwestern British Columbia. Modified from MacIntyre and Schroeter (1985).

In the presentation that follows we attempt to shed additional information on the nature of the tectonic setting of the ATMB through the use of immobile-element-based tectonic discriminant diagrams. In general, we have followed the recommendations and cautions regarding the use of such diagrams as explained by Pearce (1996). The literature is full of examples of the use and misuse of discriminant diagrams (for example, Wood, 1980; Arculus, 1987; Dudas, 1992; Rollison, 1993) in developing petrogenetic models for the origin of suites of igneous rocks. Our purpose is not to attempt rigorous petrogenetic modeling but rather to make a first-order assessment of tectonic settings suggested by the immobile-element geochemistry of igneous rocks of the ATMB, and to look for consistency with the volcanosedimentary, metallogenic, and radiogenic isotopic characteristics that we describe here and in later chapters of this volume.

In acknowledgment of the difficulty of obtaining reliable data at the low abundance levels of the immobile elements commonly used in discriminant diagrams, we have made every effort to be conservative in the representation of our geochemical data. After removing all obviously veined, mineralized, altered, and nonigneous rocks, the data set was stripped of all potential sediments and cumulate rocks using the geochemical criteria of Pearce (1996). The primary geochemical compositions of the volcanic host rocks have been modified by sea-floor alteration as well as by middle-greenschist-facies regional metamorphism during collision and underthrusting of the Alexander terrane with the North American continental margin. The resulting moderate to extreme alteration (loss on ignition-LOI, commonly 4–10 weight percent and as high as 30 weight percent) precludes the use of major element data for identification and tectonic discrimination of the volcanic rocks. Therefore, in order to maximize the utility of the immobile-element chemistry, all extremely altered samples with LOI greater than 10 weight percent also were removed from the database. An additional conservative control was placed on our use of the data by selecting a plotting routine that assigns a null value to all data at the LOD; thus, only data at abundances above the LOD are considered during the discriminant analysis. As a final check on the utility of our data, we have plotted the analyses of the USGS basalt standards BIR–1, BCR–2, and BHVO–2 and of two replicate standards that were inserted as blind standards throughout the duration of the study (fig. 14) onto the suite of discriminant diagrams used in this analysis. We note the acceptable size of the error elipses relative to the various discriminant fields (Dudas, 1992) and suggest that these plots demonstrate the sufficiency of our data for discriminant analysis.

For plotting purposes, the data in table 2 have been organized by rock type, by known or inferred age (for example, Triassic vs. Triassic(?)), and by principal location. Figure 15 shows the known Upper Triassic igneous whole-rock data plotted on the immobile-element classification diagram of Winchester and Floyd (1977). The most important feature of the data is that a bimodal suite of rocks is clearly distinguishable. Further, basalt-rhyolite suites are evident on Annette Island and on the Cornwallis Peninsula, the latter constituting the western shore of Keku Strait. North of Keku Strait, rhyolites are absent and the volcanic rocks are entirely basaltic. Such bimodal suites of volcanic rocks are a common feature of rift-related tectonic environments worldwide (Wilson, 1989) and are commonly associated with VMS mineral districts (Lentz, 1998; Barrett and MacLean, 1999). These compositions provide first-order evidence of the rift-related origin of the Upper Triassic volcanic rocks of the ATMB. The basaltic rocks (fig. 15) mainly plot in the subalkaline basalt and basaltic andesite fields, with a few examples of alkaline basalts.

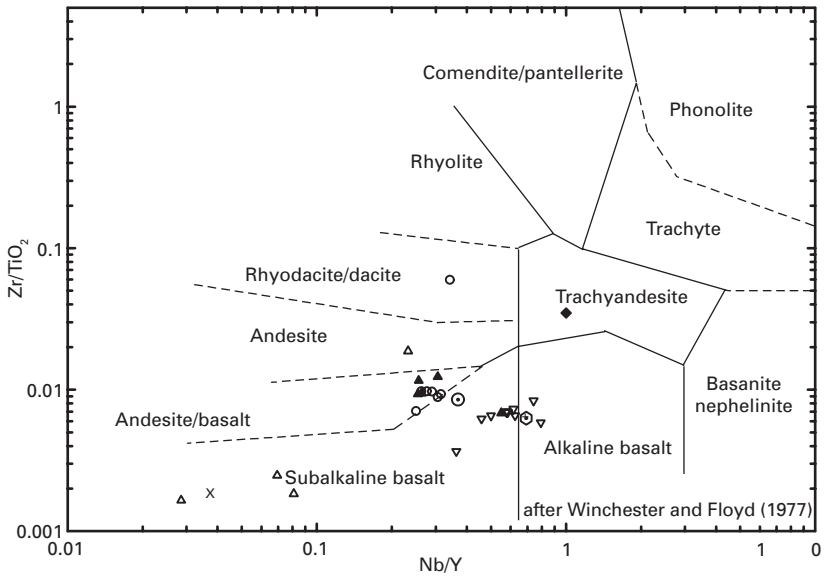

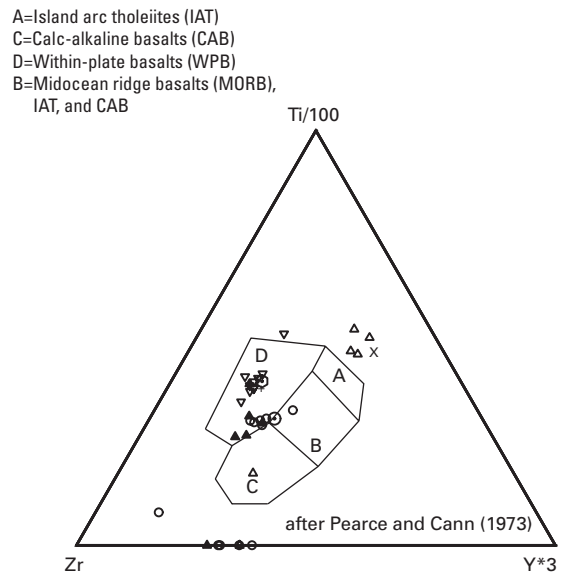

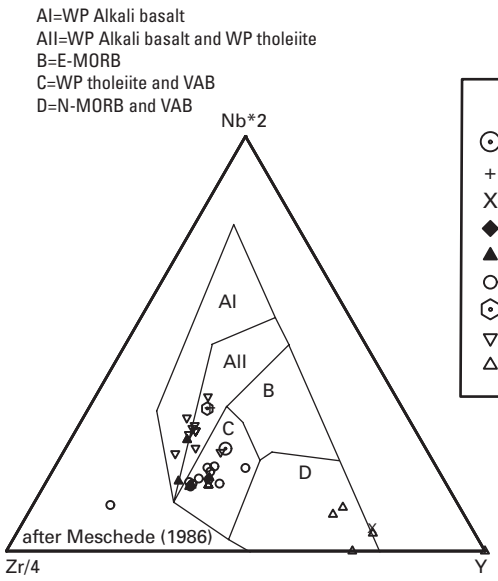

EXPLANATION

- BCR-1 published values
- BHVO-1 published values
- BIR-1 published values
- blind standard 93KK-37 altered Keku rhyolite
- blind standard 93KK-66 Hound Island basalt
- blind standard BCR-2
- BHVO-2 published values
- blind standard BHVO-2
- blind standard BIR-1

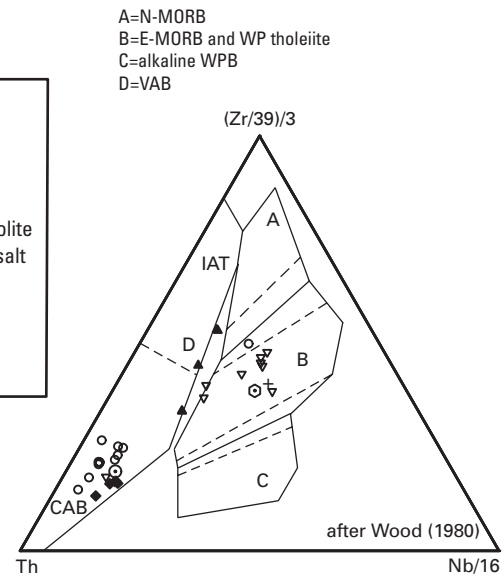

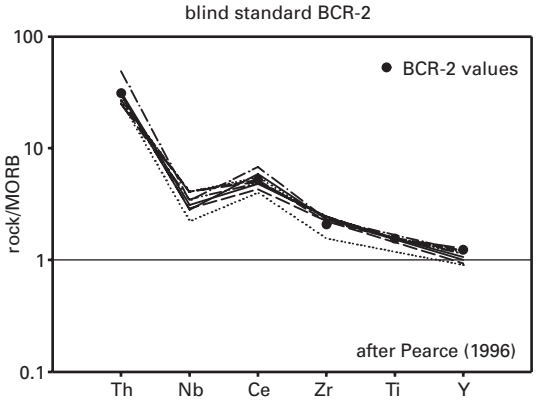

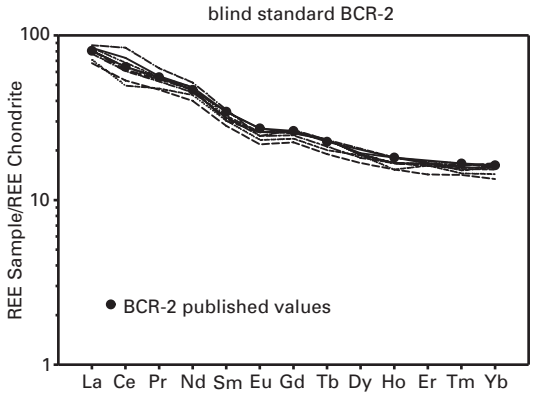

Figure 14 (facing page). Accuracy and precision of blind standards plotted on the diagrams used in the text as compared to accepted values. Multiple analyses of the USGS standards BIR-1, BHVO-2, and BCR-2 inserted as blinds into analytical batches throughout the duration of the study are shown on the immobile-element-based rock type diagram of Winchester and Floyd (1977) and on the tectonic discriminant diagrams of Pearce and Cann (1973), Meschede (1986), and Wood (1980). Multiple analyses of BCR-2 are also shown on the MORB-normalized, abbreviated trace-element plot of Pearce (1996) and on a standard chondrite-normalized REE diagram (using the chondrite values of Boynton, 1984). Note the acceptably small size of the data clusters for a given standard relative to the discriminant fields of the diagrams. Acceptable accuracy and precision are also demonstrated by multiple analyses of BCR-2 on the trace and REE plots.

The felsic volcanic rocks on Annette and Gravina Islands are typical calc-alkaline rhyolites with bulk compositions similar to those of island arc rocks. However, data for the rhyolitic rocks at Keku Strait (Cornwallis Peninsula–Keku Strait area, fig. 15) consistently fall into the comendite/pantellerite to trachyte fields of Winchester and Floyd (1977). Whereas the peralkaline composition of the Keku Volcanics rhyolites is difficult to confirm due to a high degree of brecciation and alteration, at least some of the samples approach the excess of $Na_2O + K_2O$ over Al_2O_3 that characterizes such rocks (Cole, 1978). This is an important observation due to the relatively distinctive tectonic setting of such rocks, which commonly occur in rift-related environments and are often the indicators of incipient rifting (for example, Mayor Island in the Bay of Plenty, New Zealand, and the D'Entrecasteaux Islands west of the Woodlark Basin, Papua, New Guinea, Smith and others, 1977; Smith and Johnson, 1981; also Civetta and others, 1984; Mahood and Baker, 1986; Pin and Paquette, 1997). The occurrence of felsic volcanism prior to basaltic volcanism throughout the southern portion of the ATMB and the peralkaline composition of the rhyolites of Keku Strait are typical features of intra- and back-arc rifts. The transition from calc-alkaline rhyolites to

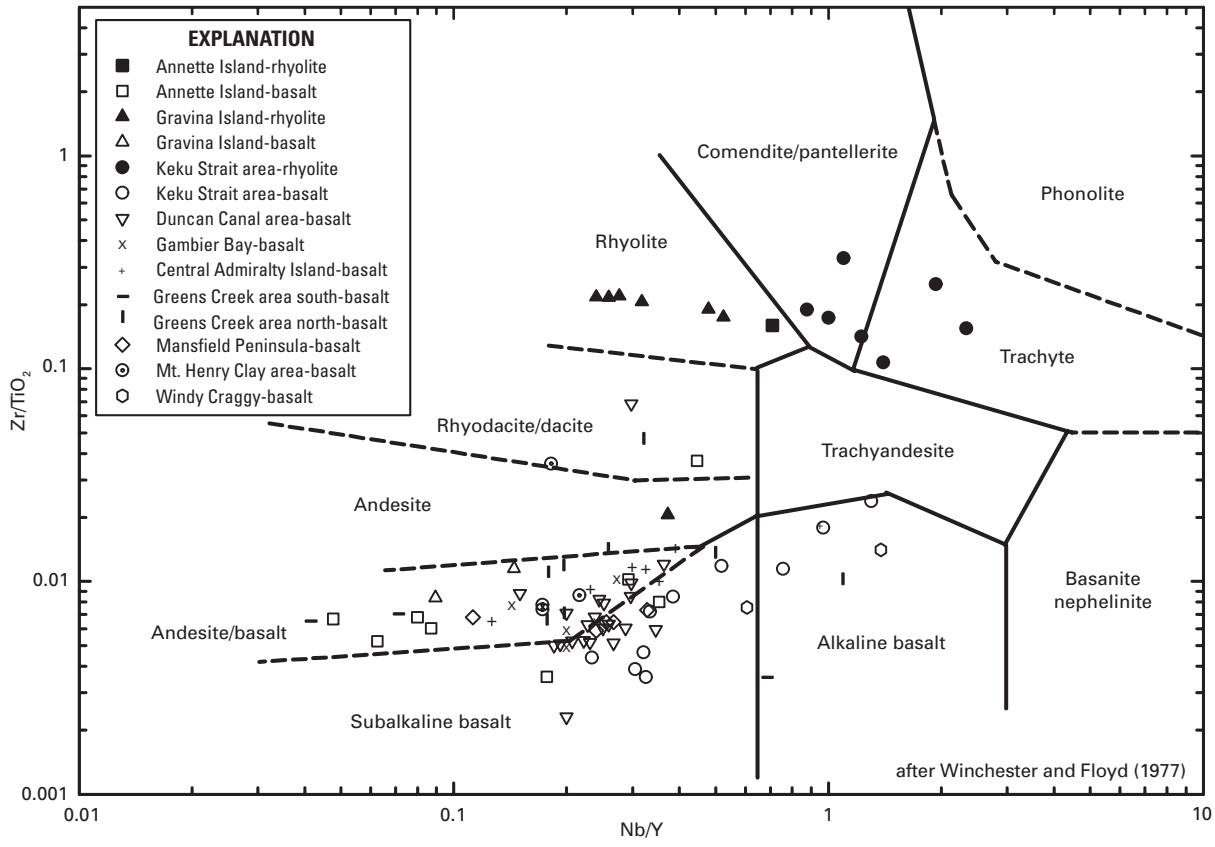

Figure 15. Volcanic rock classification diagram of Winchester and Floyd (1977) based on immobile-element ratios, showing the composition of southeastern Alaska Upper Triassic volcanic rocks analyzed for this study. Note the distinctly bimodal basalt-rhyolite distribution of data, and the comendite-pantellerite to trachytic compositions of the Keku Volcanics rhyolites (Cornwallis Peninsula suite).

peralkaline rhyolites northward along the ATMB is also consistent with a shift from a proximal-arc to an arc-slope or basin-margin setting. The peralkaline Keku rhyolites are indicative of small degrees of partial melting of a deep, garnet-bearing source during the earliest stages of rifting, followed by extreme fractionation and eruption from a shallow magma chamber (for example, Smith and Johnson, 1981; Mahood and Baker, 1986).

Application of discriminant analysis to the basaltic rocks of the ATMB provides additional information regarding their petrotectonic origins. We use a progression of three ternary plots based upon the immobile elements Ti, Zr, Th, Nb, and Y (fig. 16 a–f), and follow with the MORB-normalized trace-element plot recommended by Pearce (1996) and chondrite-normalized REE plots (fig. 17 a–v). The diagram of Pearce and Cann (1973), which is shown in figures 16a and d, is most effective for separating within-plate basalts (WPB) from those showing either destructive plate margin (volcanic arc basalt—VAB, including both calc-alkaline and tholeiitic trends; CAB and IAT, respectively) or MORB compositions. This discriminant is based largely on the effect of melting and residual enrichment of yttrium in a mantle garnet lherzolite source. Thus, WPB compositions on this diagram are suggestive of small degrees of melting from a deep source. In contrast, compositions in the MORB–VAB fields are largely controlled by partial melting at shallower levels of a spinel lherzolite source. Transitional processes such as attenuation of continental lithosphere cause trends from the WPB to the MORB field (due to progressively shallower and increased degrees of partial melting), and assimilation of upper crust results in trends from these compositions toward the CAB field (Pearce, 1996). The Meschede plot (1986), which is shown in figures 16b and e, is similar to the first plot but has the advantage of providing a discriminant between normal and enriched (or transitional) MORB compositions.

The discriminant diagram of Wood (1980), which is shown in figures 16c and f, is most efficient at separating VAB from MORB–WPB compositions and at separating calc-alkaline and tholeiitic VAB trends. As with the previous two diagrams, complex tectonic settings result in transitional data arrays between fields. Lavas erupted on attenuated continental lithosphere are perhaps the most problematic as they occupy overlapping fields in the center of the diagram. Syn- and postcollision zone magmas define a field that stretches from the center of the diagram toward the CAB end of the VAB field, reflecting the assimilation of upper crust by enriched MORB or intraplate magmas. Petrogenetic vectors toward or away from the zirconium apex from the within plate fields of the diagram are controlled by variations in the degree of partial melting and enrichment or depletion of the mantle source. Mantle enrichment and(or) low degrees of partial melting shift basalt compositions toward lower zirconium abundances. VAB compositions are controlled by the characteristic depletion in niobium with increasing input of a subduction component reflected by vectors moving toward the thorium apex (Pearce, 1996).

Data for volcanic rocks from the ATMB fall most readily into two basic groups based on how they plot on this series of discriminants. Lavas from locations predominantly in the central portion of the ATMB (Keku Strait to the Mansfield Peninsula) show a transitional nature with compositions characteristic of WPB that exhibit a spread between variably enriched or depleted MORB and CAB. The second group is composed of rocks from the southern and northern ends of the ATMB and the area immediately surrounding the Greens Creek mine (Annette Island, Greens Creek area south, and Mt. Henry Clay area). This group plots in arrays suggestive of compositions transitional between CAB and variably enriched MORB. Several areas along the ATMB (Gravina Island, Gambier Bay, Greens Creek area north, and the Mansfield Peninsula) exhibit examples of both groups. Notable exceptions are the rocks from Keku Strait which exhibit a shift toward alkaline intraplate compositions on the Wood (1980) diagram, and the consistent display of NMORB to EMORB or alkaline intraplate compositions of the Windy Craggy rocks.

Trace and REE plots of the basaltic rocks of the ATMB (fig. 17 a–v) generally support the division of rocks into two groups. The first group of rocks that plot in the transitional WPB/EMORB to CAB array exhibit the gently sloping profile from enriched thorium, niobium, and zirconium, to depleted yttrium that is characteristic of intraplate rocks and of complex tectonic settings. Similarly, the REE patterns show uniformly smooth slopes without negative europium anomalies. The second group of rocks that exhibit an array transitional between CAB and NMORB on the discriminant plots are all characterized by depletions in niobium, zirconium, titanium, and yttrium that are the hallmark of destructive margin basalts. The REE profiles of these rocks generally have steeper LREE profiles and a slight negative europium anomaly, which probably indicates separation of plagioclase and input of a subduction component to the melt.

We note that there is some consistency in the tectonic environments suggested by the discriminant diagrams and trace and REE plots. On both the Pearce and Cann (1973) and the Wood (1980) plots, the first group of rocks occupy fields that are characteristic of attenuated continental lithosphere, whereas the second group occupy fields defined by rocks produced in syn- and postcollisional environments (Pearce, 1996). In both cases, the data form arrays that are best described as transitional and are indicative of tectonic settings that are more complex than the midocean ridge, intraplate, or destructive margin settings that compose the fields of most of discriminant diagrams. We know that the pre-Jurassic history of the Alexander terrane involved the formation and transport of a continent-sized fragment of island-arc crust to a position just outboard of a subduction zone prior to the Late Triassic. Whether collision and partial subduction (or obduction) of the Alexander terrane occurred is uncertain; however, by Late Triassic the production of ATMB volcanic rocks indicate that a period of crustal relaxation outboard of the destructive margin had occurred, resulting in lithospheric extension and incipient rifting in the Alexander terrane. We suggest that the Alexander terrane must have been thick enough that initial rifting resulted in deep melting of a relatively enriched mantle and that the first melt products

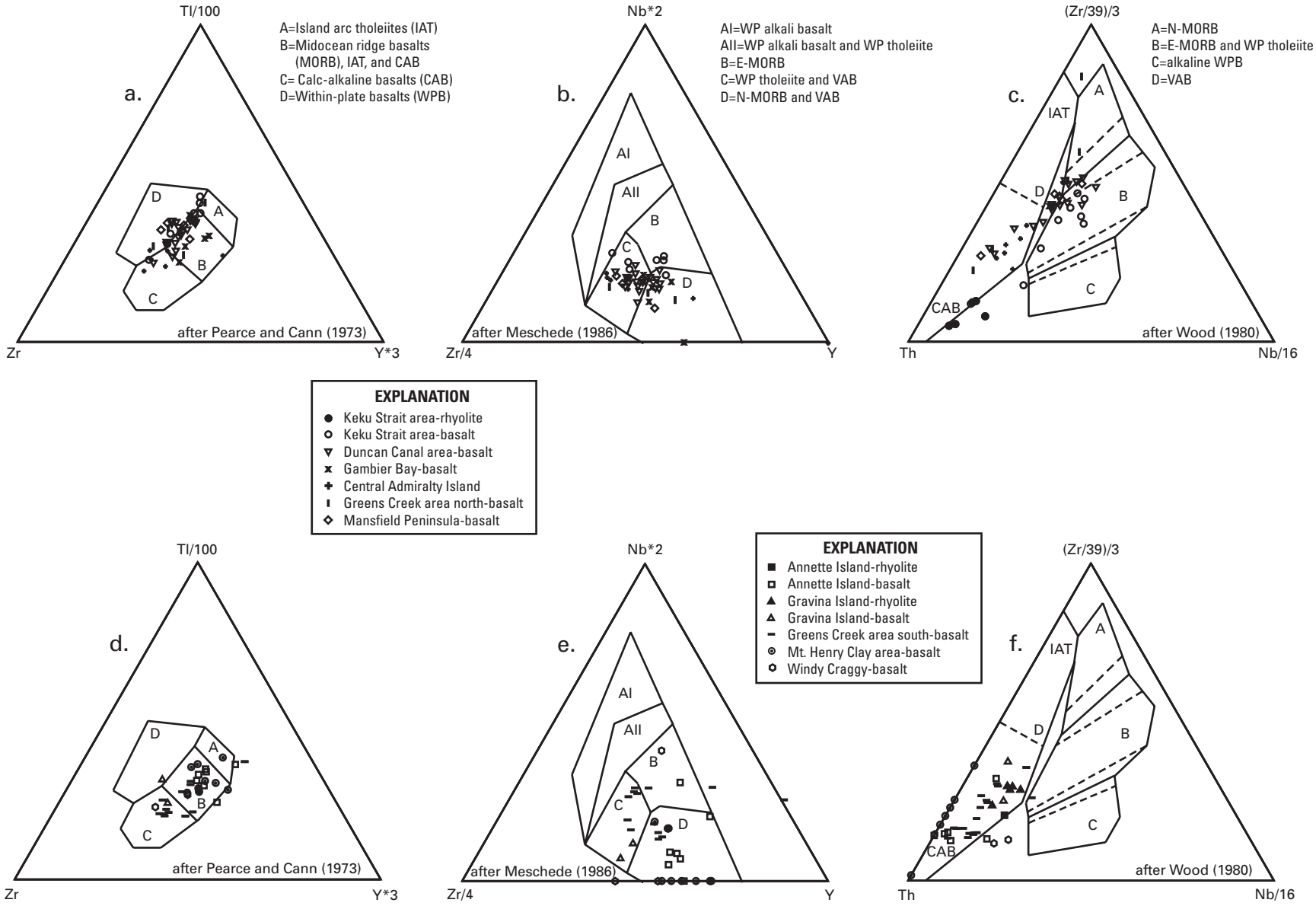

Figure 16 a–f. Discrimination diagrams showing compositions of southeastern Alaska Upper Triassic basalts and rhyolites (on the Wood, 1980, diagram only) analyzed for this study. Diagrams a–c show data from locations within the central ATMB and are characterized by transitional chemistry that reflects a stronger intraplate signature than samples from the north and south end of the ATMB and from the ridge south of the Greens Creek mine as shown in diagrams d–f. The second set of diagrams indicate chemistries transitional between that of WPB and/or EMORB and CAB.

thus have chemistry similar to WPB and EMORB depending upon how much assimilation of the overlying island-arc crust occurred. In places where attenuation or rifting of the crust was more pronounced, shallower melting of variably enriched mantle at variable degrees of partial melting produced the data array between arclike CAB and NMORB of the second group. Thus the transitional chemistry of the ATMB volcanic rocks are a product of a combination of variable depths and degrees of partial melting beneath the rifting Alexander landmass and of variable amounts of crustal assimilation (to achieve the CAB signature).

As with previous radiogenic isotopic studies (Sampson and others, 1989, 1990, 1991), Sr-Nd-Pb isotope analyses of pre-Triassic rocks of the Alexander terrane (Premo and Taylor, unpub. data, 2004) and of footwall host rocks at Greens Creek (chap. 11) suggest derivation from a depleted mantle source and are consistent with isotopic signatures of oceanic island arcs. Initial niodymium compositions at 215 Ma (average age of host rocks) of metabasalts and gabbros vary between ε_{Nd} = +4 to +9, and initial $^{206}Pb/^{204}Pb$ and $^{87}Sr/^{86}Sr$ = 18.45 to 18.92 and 0.7037 to 0.7074, respectively, and are enriched compared to MORB or oceanic island basalt (OIB) sources. Isotopic data for Permian and Triassic argillites are similarly enriched and indicate derivation from an island-arc terrane with input of older, more radiogenic source material. Interestingly, radiogenic isotopic data on footwall phyllites at Greens Creek are bimodal (ε_{Nd} ~ +8 and +2), which we interpret to indicate the intrusion of Late Triassic gabbroic sills into the footwall basaltic pile. Hyd Group basalts exhibit a relatively primitive isotopic signature (ε_{Nd} = +8 to +9) consistent with derivation from a mantle source (chap. 12).

Results of the tectonic discriminant analysis, in combination with the fairly primitive and transitional trace, REE, and radiogenic isotopic geochemical signatures, are consistent with rift-related basalt produced in an incipient intra-arc or back-arc setting. We note that basalts at several locations, especially in the southern end of the ATMB, the Greens Creek area, and at Mt. Henry Clay, have compositions that are similar to those of relatively unfractionated calc-alkaline basalts formed in an oceanic volcanic arc, whereas those in others, most notably in the central portion of the ATMB, display transitional chemistry consistent with derivation from EMORB or OIB sources and variable assimilation of preexisting arc crust. Similar to the trends for the mafic volcanic rocks, the felsic volcanic rocks show a transition from more arclike compositions in the southern end of the ATMB to intraplate compositions in the center of the ATMB. The most MORB-like rock compositions in the ATMB are displayed by Tats Group basalts at Windy Craggy. Consistent with the extensive geochemical data of Peter and Scott (1999) we note elevated LREE compositions and lower ε_{Nd} compositions for the Tats Group as compared to Triassic basalts to the south. Peter and Scott (1999) interpret the tectonic setting at Windy Craggy at the time of ore formation as a mature back-arc basin.

The Geochemistry and Significance of Late Triassic Hypabyssal Mafic-Ultramafic Intrusive Rocks

An important and largely unrecognized feature of many of the mineral occurrences that has important genetic implications is their spatial and temporal relationship to a mafic-ultramafic suite of hypabyssal (probably rift-related) intrusions. Throughout the ATMB there are numerous mapped outcrops of gabbros, microgabbros, and less commonly, ultramafic intrusive rocks of either Triassic or uncertain age. Notable examples are the Duke Island ultramafic complex lying immediately south of Annette Island, and the microgabbros on the southwestern shore of Bostwick Inlet on Gravina Island. Microgabbros on Hare Island, just west of Hound Island in Keku Strait, are mapped as Cenozoic igneous rocks; however, we note the similar geochemical compositions of these rocks to those of the Upper Triassic basalts of Hound Island Volcanics. More strikingly perhaps is the growing realization that a significant portion of the capping Triassic basaltic unit throughout the ATMB is composed of gabbroic sills and that immediately underlying serpentinite bodies are probably the residual cumulate sources of these voluminous flows. Both serpentinite and gabbro bodies are commonly intersected by underground mine workings and are seen to crop out at Greens Creek (chaps. 6, 7). Similarly, the stratigraphic sequence at Windy Craggy is composed of interbedded gabbro sills, sediments, and basalts (MacIntyre and Schroeter, 1985).

Even more compelling is the observation that many of the mineral occurrences are within, or are in close proximity to, barite-sulfide-mineralized mafic sills and dikes that have strikingly similar chemistry to the overlying basalts. Figure 18A is a photograph of a heavily carbonate altered gabbroic sill hosted in late Upper Triassic sedimentary rocks at a mineral occurrence (Berg #17, Berg, 1972) on the Sylburn Peninsula of Annette Island. The altered sill sits immediately beneath a large, discontinuous pod of barite accompanied by minor sphalerite, and galena. Similarly, the Ladder vein occurrence (Muffler, 1967) in the Keku Strait and at least two other similar occurrences represent instances of mineralized basaltic intrusions that are spatially associated with Late Triassic mineral occurrences. The Ladder vein (fig. 18B) consists of a basaltic dike cutting Permian and Triassic(?) conglomerates and sedimentary rocks that have distinctive, associated, 2.5-cm-thick, massive sphalerite veins crosscutting the dike and occurring along its margins. A similar sill several hundred meters to the south exhibits peperitic margins with the host (upper Upper Triassic?) sedimentary strata, indicating that the sediments were unlithified and water saturated at the time of intrusion (fig. 18C).

Some of the best examples of both mineralized basaltic dikes and mineralized and altered ultramafic intrusions are in Gambier Bay (fig. 1, inset d). In the southwest arm of the bay at Cave Mountain Point, several 1–2-meter-wide basaltic dikes (fig. 18D) intrude Devonian limestone and Upper Triassic

sedimentary rocks. Veins up to 15 centimeters wide consisting of barite, quartz, iron carbonate, chalcopyrite, sphalerite, and galena are present along the dike margins, locally forming replacement bodies in the limestone. Outcrops of altered serpentinite sills are a striking feature of the Upper Triassic section on the north shore of Gambier Bay and occur as distinctive, orange-weathered outcrops consisting of green and white quartz, magnesite, iron carbonate, sericite, and bright green fuchsite (fig. 18E). Often misidentified as exhalite beds or altered dolomite bodies, the presence of relict chromian spinel and olivine in the altered rocks, the compositionally distinct mafic-ultramafic element suite, and the preservation of serpentinite enclaves and breccia clasts within the altered bodies identify them as heavily carbon dioxide-metasomatized serpentinites. Although attempts to directly date relict serpentinite enclaves (fig. 18F) within these altered ultramafic bodies were unsuccessful, they are thought to be part of the mafic-ultramafic hypabyssal intrusive event related to Triassic rifting (chap. 11). An $^{40}Ar/^{39}Ar$ isotopic age for fuchsite separated from a quartz-iron carbonate-fuchsite altered body in Gambier Bay yielded an apparent plateau age of 210.3 ± 0.3 Ma (chap. 11), thus demonstrating that emplacement had occurred by the Late Triassic, and suggesting that alteration and mineralization of the intrusives were nearly synchronous. This relationship and the presence of skarn minerals in the aureoles of serpentinites in the Greens Creek area (N.A. Duke, oral commun., 1997), suggest that the precursor ultramafic rocks were emplaced hot in the shallow subsurface during Late Triassic time. Associated mineralization includes barite, pyrite, chalcopyrite, sphalerite, galena, tetrahedrite, siegenite, nickel bloom, and anomalous gold values, further suggesting that the ultramafic precursor intrusives drove hydrothermal circulation and in the process were themselves altered. Similar examples of mineralized and altered mafic-ultramafic hypabyssal intrusions occur on Zarembo and Woewodski Islands, and in Duncan Canal (Taylor, 2003), and at numerous locations across Admiralty Island, notably at the North Gambier occurrence, Yellow Bear Mountain, Etta prospect, Mariposite Ridge just north of Greens Creek (fig. 18G), and at several localities on the Mansfield Peninsula.

Late Triassic Mineral Occurrences in Southeastern Alaska

The northward change in depositional environment and volcanic host-rock chemistry in Upper Triassic strata is accompanied by a northward transition from epithermal-type base-metal occurrences having a relatively simple mineralogy, to sulfosalt-enriched polymetallic VMS occurrences, and finally to larger copper-cobalt-bearing deposits with more clearly stratiform morphologies. In the following sections we describe some of the more important mineral occurrences that demonstrate the evolving nature of the Late Triassic metallogeny from south to north in the ATMB.

Mineral Occurrences in the Southern ATMB

Occurrences on Annette and Gravina Islands are typified by structurally controlled, discontinuous veins, breccias, and pod-shaped bodies, and less commonly, by small stratiform lenses. The occurrences are Pb-Zn-Ag-Ba-(Cu)-enriched with a relatively simple sulfide mineralogy, at or near the contact between felsic volcanic rocks and overlying fossiliferous and locally oolitic limestone. In places, the limestone is dolomitized and brecciated. A pervasive orange to black, iron- and manganese-rich hydrothermal alteration locally colors the otherwise medium gray dolomite (for example, Nehenta Bay on Gravina Island; fig. 19A). Where this alteration is most intense, the matrix of the dolomite breccia consists of quartz and iron-rich dolomite cement with sparsely disseminated sulfides. Solution cavities are present and commonly have inward-projecting euhedral crystals of quartz, late dolomite, and sulfides. Texturally, the hydrothermal features exhibited in such outcrops of shallow platform carbonates are similar to those in Mississippi Valley-type deposits of the U.S. midcontinent region (Leach and Sangster, 1993).

Examples of the pod-shaped and veinlike occurrences are numerous, especially on Annette Island, and include the previously described barite-chalcopyrite-sphalerite-galena pods (fig. 18A) associated with the altered gabbroic dike at Berg #17 (Berg, 1972). Another weakly mineralized, pod-shaped barite occurrence at Japan Bay on the Sylburn Peninsula (Berg #18) has a similar mineralogy, and botryoidal textures suggestive of growth in open space or in unlithified sediments during early diagenesis (fig. 19C). Interestingly, in 1976, 181.4 meters of diamond core was drilled in five holes at three different locations on the Sylburn Peninsula to test for the presence of minable quantities of barite and Pb-Zn-Ag. Of these, four holes at two locations intersected low-grade stratabound barite-sulfide intervals dipping west under the peninsula at 25 degrees. At

Figure 17 a–v (following pages). MORB-normalized abbreviated immobile-trace-element (after Pearce, 1996) and REE plots of data for samples from locations throughout the ATMB corresponding to the samples and locations shown on the discriminant plots. Chondrite values from Boynton (1984). Note that arc-type trace-element patterns and steeper LREE patterns with slight to moderate negative europium anomalies characterize the samples from the northern and southern ATMB and the ridge south of the Greens Creek mine, consistent with data shown on the discriminant diagrams. Trace-element patterns consistent with transitional mixtures of intraplate rocks and CAB, as are often seen in areas of attenuated lithosphere and in syn- and postcollision settings, are exhibited by samples from locations in the central ATMB. Corresponding REE patterns are generally flatter and do not exhibit europium anomalies.

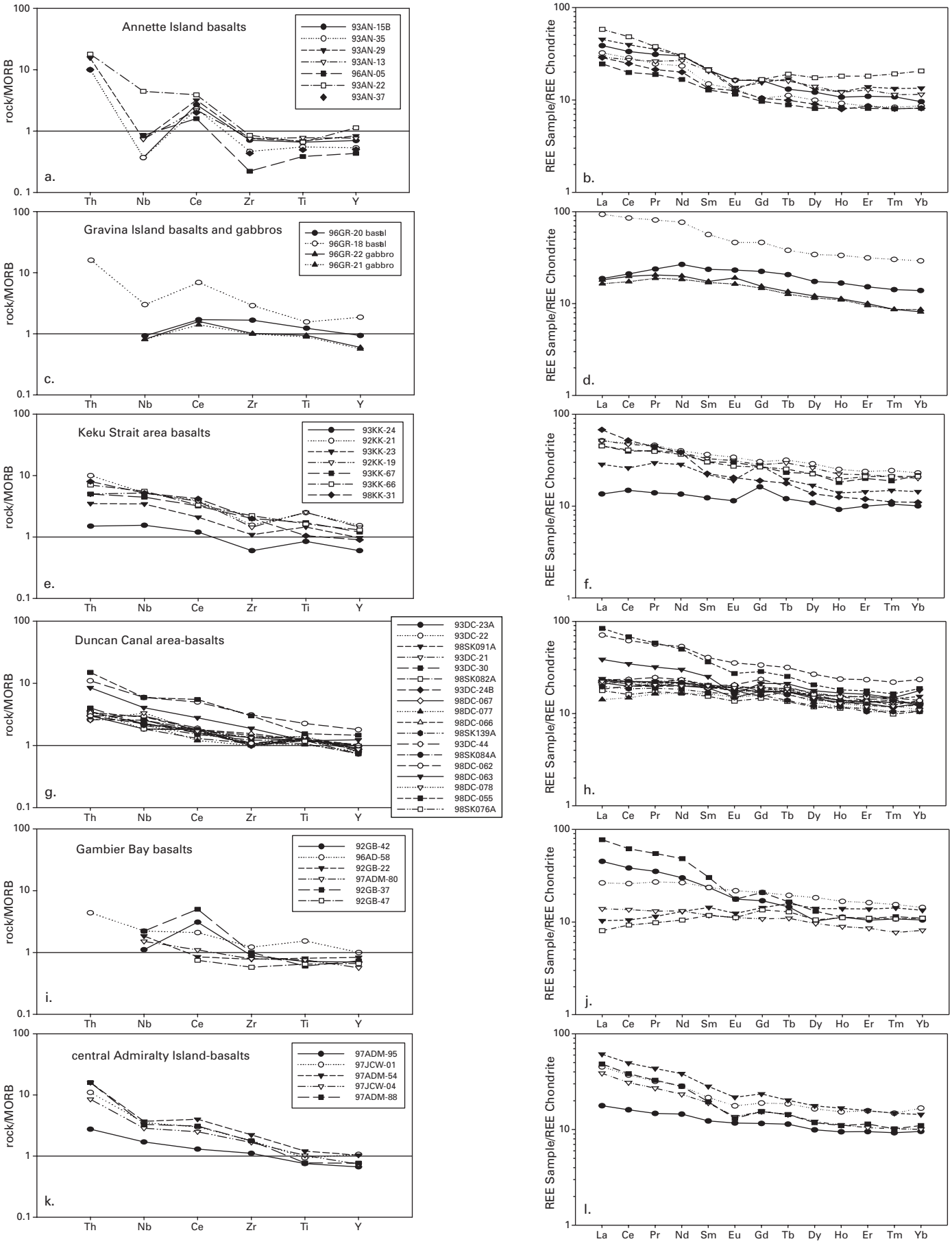
Annette Island basalts
93AN-15B
93AN-35
93AN-29
93AN-13
96AN-05
93AN-22
93AN-37
a.
b.
Gravina Island basalts and gabbros
96GR-20 basalt
96GR-18 basalt
96GR-22 gabbro
96GR-21 gabbro
c.
d.
Keku Strait area basalts
93KK-24
92KK-21
93KK-23
92KK-19
93KK-67
93KK-66
98KK-31
e.
f.
Duncan Canal area-basalts
93DC-23A
93DC-22
98SK091A
93DC-21
93DC-30
98SK082A
93DC-24B
98DC-067
98DC-077
98DC-066
98SK139A
93DC-44
98SK084A
98DC-062
98DC-063
98DC-078
98DC-055
98SK076A
g.
h.
Gambier Bay basalts
92GB-42
96AD-58
92GB-22
97ADM-80
92GB-37
92GB-47
i.
j.
central Admiralty Island-basalts
97ADM-95
97JCW-01
97ADM-54
97JCW-04
97ADM-88
k.
l.
rock/MORB
REE Sample/REE Chondrite
Th Nb Ce Zr Ti Y
La Ce Pr Nd Sm Eu Gd Tb Dy Ho Er Tm Yb

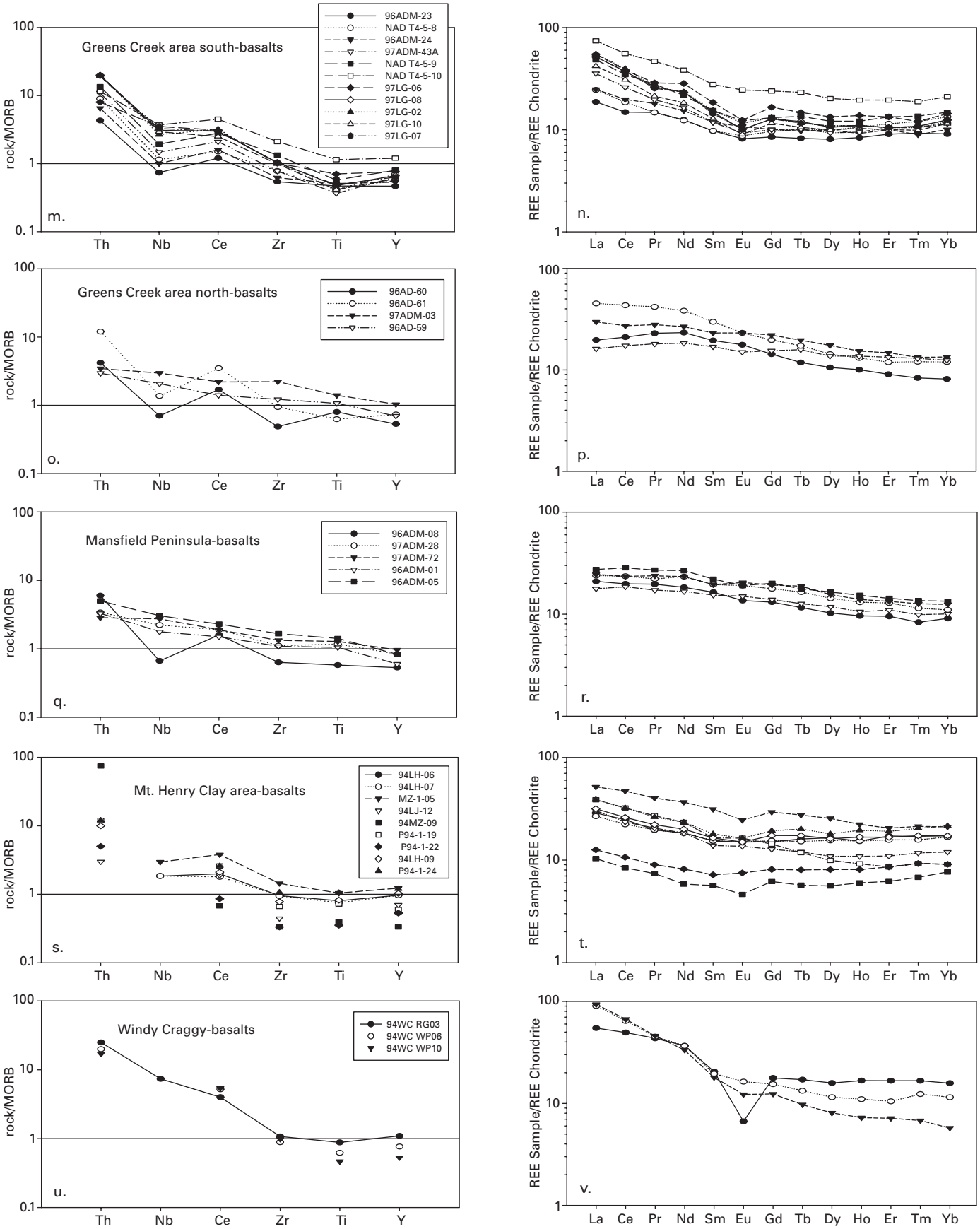
Greens Creek area south-basalts
96ADM-23
NAD T4-5-8
96ADM-24
97ADM-43A
NAD T4-5-9
NAD T4-5-10
97LG-06
97LG-08
97LG-02
97LG-10
97LG-07
rock/MORB
m.
Th Nb Ce Zr Ti Y
REE Sample/REE Chondrite
n.
La Ce Pr Nd Sm Eu Gd Tb Dy Ho Er Tm Yb
Greens Creek area north-basalts
96AD-60
96AD-61
97ADM-03
96AD-59
o.
p.
Mansfield Peninsula-basalts
96ADM-08
97ADM-28
97ADM-72
96ADM-01
96ADM-05
q.
r.
Mt. Henry Clay area-basalts
94LH-06
94LH-07
MZ-1-05
94LJ-12
94MZ-09
P94-1-19
P94-1-22
94LH-09
P94-1-24
s.
t.
Windy Craggy-basalts
94WC-RG03
94WC-WP06
94WC-WP10
u.
v.

the first location (Berg #18, previously described), geochemical analyses indicate the presence of a 14.6- to 15.5-meter-thick interval grading 25.8- to 38.3-percent barite with minor lead, zinc, and silver. At the second location 120 meters to the south, drilling revealed a structurally complicated, lower grade mineralized section that may also dip 25 degrees to the west. Geochemical analyses indicate a 21.3-meter-thick interval having an average grade of 16 percent barite and minor lead, zinc, and silver. Within this interval is a 5.8-meter-thick section grading 45.2 percent barite, 3.4 percent lead, and 34 parts per million silver (D.C. McCrillis, written commun., 1976; Berg and Clautice, written commun., 1982). Estimation of size and grade based on the drilling results and the persistence of soil geochemical anomalies indicate a 1–2 million metric tonne deposit averaging 32 percent barite, 2–3 percent combined lead and zinc, and 28 grams per metric tonne silver could be present (A.L. Eng, written commun., 1983; Taylor, 1993). A second, very small stratabound occurrence was noted during this study at the mouth of Nehenta Bay, Gravina Island, enclosed within the gritty limestone sequence overlying the basal conglomerate. Several stacked horizons of bladed barite up to 7 cm thick and 10 m long are present and provide additional evidence for stratabound, early diagenetic if not exhalative mineralization (fig. 19*C*).

Clearly epigenetic, veinlike mineral occurrences are also common on Annette and Gravina Islands and are typified by occurrences in the Crab Bay area on the east side of Annette Island. As on the Sylburn Peninsula, mineralization occurs predominantly at and near the contact of rhyolitic volcaniclastic rocks and locally dolomitized limestone. Discontinuous and generally small ribbon and ladder quartz veins occurring as en echelon sets tens to 100 meters long are best developed within the limestone (Hawley and Associates, written commun., 1975). They contain sphalerite, galena, and rare chalcopyrite, malachite, tetrahedrite, barite, and possibly stibnite. Most of the veins in the Crab Bay area are too discontinuous and poorly mineralized to be of economic interest (Hawley and Associates, written commun., 1975; A.L. Eng, written commun., 1983; Taylor, 1993). The largest vein is 0.45 meter thick and contains 30 to 50 percent sulfides over an exposed length of 6 meters. A minor amount of galena and sphalerite also is disseminated locally within the limestone. In general, mineral occurrences in the southern end of the ATMB, regardless of morphology, are characterized by an anomalous geochemical signature of Pb, Zn, Cu, Au, Ag, Ba, and minor Sb, As, Cd, Bi, and Ni (Taylor, 1993). Comparison of this geochemical suite to that which characterizes the Greens Creek deposit (chap. 6) demonstrates their similarity and possible genetic relationship.

Mineral Occurrences in the Northern ATMB

Relative to the southern end, the northern end of the ATMB is characterized by larger and more clearly stratiform occurrences of pyrite-pyrrhotite-(chalcopyrite-sphalerite) with Cu-Zn-(Co-Au)-enrichments. They are hosted by thick sections of argillite intercalated with basaltic flows and sills, or by the uppermost Triassic sequence of mafic volcanic rocks. The best example is the giant Windy Craggy massive sulfide deposit in northwestern British Columbia, approximately 100 km north of the international border. Published data for Windy Craggy indicate a minable resource of 297 million metric tonnes at 1.38 percent copper, 0.07 percent cobalt, 0.2 gram per metric tonne gold, and 3.8 grams per metric tonne silver (Peter and Scott, 1999). The total resource estimate is thought to be in excess of 500 million metric tonnes (Gerald Harper, oral commun., 1995). Currently regarded as the largest Besshi-type VMS deposit in the world (Peter and Scott, 1999), Windy Craggy is hosted in a rift-succession (Mihalynuk and others, 1993) of mafic flows, sills, and argillites (fig. 20*A*) which, based on the presence of Norian conodonts both below and immediately above the massive sulfide lenses, can be confidently correlated with the ATMB in southeastern Alaska. Windy Craggy consists of three stratiform massive sulfide lenses composed predominantly of pyrite and pyrrhotite with lesser and variably distributed chalcopyrite, sphalerite, marcasite, galena, digenite, arsenopyrite, an unidentified bismuth telluride, cobaltite, cubanite, electrum, and native gold and silver. Each sulfide lens is associated with a well-developed sulfide stringer zone (Peter and Scott, 1999). Typical massive ore consists of fine- to medium-grained (about 50–500 micrometers) primary-textured to variably recrystallized pyrite and pyrrhotite in a volumetrically minor gangue of quartz, calcite, and siderite gangue (fig. 20*B*). In striking contrast to many of the Late Triassic occurrences to the south, tetrahedrite-bearing, gangue-rich white ores are absent at Windy Craggy, and barite only occurs in trace amounts. Interestingly, hydrothermal sediments (exhalites) are present at the base of the massive sulfide lenses and suggest that hydrothermal fluids breached the sediment/water interface early in the ore-forming process (Peter and Scott, 1999). Early fluid exhalation may also have occurred at Greens Creek (chap. 15).

Numerous other deposits in the northern end of the ATMB consist of similar stratiform accumulations of pyrite-pyrrhotite massive sulfide characterized by Cu-Zn (-Au-Co-Ag) enrichments. The Tats, X, and Rainy Monday occurrences (Peter and Scott, 1999; Mihalynuk and others, 1993) in the vicinity of Windy Craggy, and several others on the Canadian side of the border in the Mt. Henry Clay area such as the Herbert Mouth West, Grizzly Heights, and Buckwell Moraine (MacIntyre and Schroeter, 1985), all display features similar to Windy Craggy. Notably, they are all hosted in Upper Triassic strata dominated by distal turbiditic sediments, and by mafic sills and flows with transitional chemistry indicative of rifting. At Mt. Henry Clay on the U.S. side of the border, the stratigraphic setting is similar to that in the Windy Craggy area; however, occurrences mostly consist of stratiform lead-zinc-silver-barite deposits such as Glacier Creek (Main) and upper Cap. The Little Jarvis occurrence on the opposite side of the ridge from the Glacier Creek deposit contains pyrite-pyrrhotite-chalcopyrite-sphalerite-bearing semimassive sulfides that may be more similar to the northern group of occurrences. Massive sulfide boulders at the Mt. Henry Clay (Boulderado)

occurrence are difficult to place in stratigraphic context due to their occurrence as float on a moraine. However they are mineralogically and texturally (fig. 20*C*) more like Windy Craggy than the stratiform lead-zinc-silver-barite occurrences in the Mt. Henry Clay area and to the south.

The southernmost occurrences of the northern type may be the numerous small stratiform pyritic bodies in the Duncan Canal and Woewodski and Zarembo Islands area in the central portion of the ATMB. The Junior Creek occurrence on the eastern shore of Duncan Canal consists entirely of semimassive pyrite lenses hosted in Upper Triassic graphitic argillites. On the west side of Woewodski Island, a 0.5- to 1-m-thick pod of pyritic massive sulfide is sandwiched between apparently conformable footwall and hanging-wall rocks composed of highly altered greenschist at the Helen-S occurrence (Taylor, 2003). As described herein, the Frenchie deposit on Zarembo Island is difficult to place in stratigraphic context. It is one of the larger and more clearly stratiform deposits within the ATMB, however, and has mineralogical and textural features most closely associated with the pyritic deposits in the Mt. Henry Clay and Windy Craggy areas. The Frenchie deposit consists of a 2–3-m-thick, ~250-m-long massive sulfide lens (fig. 20*D*) composed primarily of pyrite with lesser and variable chalcopyrite, sphalerite, and barite (fig. 20*E*; Taylor, 2003), much like the Windy Craggy and Mt. Henry Clay (Boulderado) deposits. At the adit the massive sulfide lens is approximately 3 meters thick and consists predominantly of coarsely recrystallized pyrite with minor chalcopyrite and sphalerite in a siliceous quartz-carbonate gangue. Along strike 50 to 100 meters upstream, the lens becomes semimassive and then dies out into the hanging-wall quartz-sericite schist. Along strike in the down-creek (westerly) direction for approximately 75 meters the lens maintains its thickness. However, over this interval the massive sulfide becomes finely crystalline, more sphalerite rich, and exhibits a footwall to hanging-wall zonation. Minor barite was observed in the footwall margin of the lens 45 meters west of the adit. Massive sulfide overlying the barite is sphalerite rich compared to the massive pyrite at the adit. The center of the lens becomes more pyritic and then grades into more galena-rich pyritic massive sulfide toward the hanging wall. Remobilization of ductile sulfides into fractures in the immediately overlying, more brittle quartz-sericite schist has caused local chalcopyrite and galena accumulations in the hanging wall. The massive sulfide lens is truncated by a fault oriented N. 65° E., 60° N. (Buddington, 1923) 75 meters downstream from the adit, and then reappears in the north creek bank approximately 150 meters downstream from the adit. The lens is continuous downstream for approximately another 100 meters and is approximately 2 meters thick. Samples collected from the downstream end of the lens in the south bank and from the downstream end of the portion of the lens in the north bank become increasingly sphalerite rich, indicating that a proximal-distal zonation exists as well. From the adit (proximal) to the distal downstream end, the massive lens is zoned from copper-gold to zinc. From footwall to hanging wall the lens is zoned from Zn-Mn-Ba, to Fe-Cu-Au, to Pb. In addition to the zonation described, the Frenchie occurrence has a geochemical signature containing Fe, Zn, Cu, Au, Fe, (Hg, Ag, As, Cd, Mo, Pb, and Sb; Taylor, 2003).

Mineral Occurrences in the Central ATMB

Mineral occurrences in the middle of the ATMB are transitional and define an overlap area between structurally controlled types that we believe formed in a shallow water, near-arc setting, to those having a more stratiform appearance, reflecting a deeper water, rifted basin-margin setting. Examples of structurally controlled mineral occurrences, similar to those described as characteristic of the southern end of the ATMB, extend northward to about the latitude of Keku Strait, Woewodski Island, and southern Admiralty Island. They include galena-sphalerite breccias in limestone at the contact with felsic volcanics, and galena-sphalerite-bearing mafic dikes on the Cornwallis Peninsula, weakly stockwork-mineralized tuffaceous mafic volcanics at the Lost Show and Brushy Creek on Woewodski Island, and similarly mineralized mafic dikes and chalcopyrite-bornite-tetrahedrite-barite-bearing, quartz-carbonate stockwork veins in mafic volcanics in the Gambier Bay area. Stratiform deposits in this transition region tend to be Pb-Zn-Ag-Ba (-Cu-Au)-rich and are typified by Greens Creek, described in detail in this volume. Other examples of these increasingly larger, polymetallic, silica-barite-carbonate gangue-rich, more obviously stratiform occurrences include silica-barite-sulfide-sulfosalt-rich occurrences on Zarembo Island (Frenchie occurrence described previously) and Woewodski Island, Duncan Canal, Pyrola, Greens Creek, as well

---

Figure 18 *A*–*G* (pages 44–45). Photographs of outcrops throughout the ATMB demonstrating the spatial relationship between mineral occurrences and mafic-ultramafic hypabyssal sills, dikes, and intrusions. (*A*) Altered gabbroic sill beneath barite-sulfide pod. Berg # 17 occurrence, Sylburn Peninsula, Annette Island. (*B*) The Keku Islet Ladder vein occurrence. Altered basaltic dike intrudes Permian-Triassic conglomerates and sedimentary rocks and is cut by dark reddish-brown sphalerite veins. (*C*) Peperitic margin of altered dike intruding Permian-Triassic sedimentary rocks on Keku Islet, south of the Ladder vein occurrence. (*D*) Basaltic dike cutting Devonian limestone and Upper Triassic sedimentary rocks and basalts in the south arm of Gambier Bay, southern Admiralty Island. Barite-quartz-carbonate-sulfide veins occupy the selvages of the dike and also cut the dike. (*E*) Quartz-iron carbonate-magnesite-fuchsite-altered ultramafic sills intruding the Upper Triassic sedimentary sections on the north shore of Gambier Bay, southern Admiralty Island. (*F*) Relatively unaltered enclave of serpentinite within a large body of altered ultramafic rock on the north shore of Gambier Bay, southern Admiralty Island. (*G*) Quartz-iron carbonate-magnesite-fuchsite-altered ultramafic intrusion on Mariposite Ridge 1 kilometer north of the Greens Creek mine.


A


B


C


D


E


F


G

Figure 19 *A*–*C*. Photographs of outcrops and polished rock slabs from mineral occurrences in the southern portion of the ATMB. (*A*) Pervasive orange-black, hydrothermal iron and manganese alteration of the Nehenta Formation limestone and carbonate debris flows in Nehenta Bay, southern Gravina Island. Note pod-shaped occurrence of bladed white barite and minor sulfides to the right of the hammer. (*B*) Stratiform horizons of bladed barite in iron- and manganese-altered calcareous sedimentary rocks of the Nehenta Formation near the mouth of Nehenta Bay, southern Gravina Island. (*C*) Massive botryoidal barite and galena from the Berg # 18 occurrence in Japan Bay of the Sylburn Peninsula, Annette Island. Texture of the barite and the fine-scale galena bands suggest growth in open space or into unconsolidated sediments during diagenesis.

Figure 20 *A*–*E*. Photographs of outcrops and polished rock slabs from mineral deposits in the northern portion of the ATMB. (*A*) South side of Windy Peak at the Windy Craggy deposit in northwestern British Columbia. Light and dark subhorizontal layering composes intercalated mafic sills and flows with calcareous black argillites. (*B*) Typical pyritic massive sulfide with minor pyrrhotite and chalcopyrite in a quartz-carbonate gangue, from the north crosscut of the Windy Craggy deposit in northwestern British Columbia. The black elongate inclusion in the lower right part of the sample is an argillite clast. (*C*) Pyrite- and sphalerite-rich massive sulfide from a boulder found at the Mt. Henry Clay (Boulderado) occurrence in northern southeastern Alaska. (*D*) Massive sulfide lens at the Frenchie deposit on Zarembo Island, central southeastern Alaska. Timbers in the adit are about 2 meters high and are holding up a hanging wall of graphitic quartz-sericite schist. (*E*) Massive sulfide from the Frenchie deposit. Top sample is dominantly pyritic and characterizes the majority of the sulfide lens. The center sample is more sphalerite- and galena-rich; the bottom sample has significant barite. As shown, the three samples mimic the ore stratigraphy in the distal downstream portion of the lens.

as the Glacier Creek (Main), upper Cap, and other deposits on either side of the border in the Mt. Henry Clay area described.

Numerous small, clearly epigenetic barite-sphalerite-galena (-chalcopyrite) occurrences dot the islets and shoreline of the Cornwallis Peninsula in the Keku Strait area. The majority of the occurrences consist of weakly mineralized, irregular pods and veins composed of massive to bladed, pink to white barite with minor sulfides. Less commonly, colloform banded textures suggestive of mineral growth in open space or in unlithified sediments are observed (fig. 21*A*), similar to the textures in the barite-rich occurrences on Annette Island. The colloform banded vein shown in figure 21*A* also exhibits a close spatial relationship with a 1-m-wide mafic dike that contains 1-cm-thick galena veins along its margins.

With few exceptions these occurrences are localized at the contact between the Keku Volcanics and the overlying Cornwallis Limestone. Two of the more highly mineralized occurrences are at the rhyolite/limestone contact along creeks roughly 300 meters from the shoreline. One is generally referred to as the Kuiu zinc deposit, the second is an undescribed occurrence located about half way up the second tributary entering Hungerford Creek south from its mouth. Both occurrences are characterized by stockwork- and breccia-textured Cornwallis Limestone cemented and replaced by sphalerite, galena, and pyrite (fig. 21*B*). A similar breccia composed of greenstone clasts in a matrix of pink barite, dolomite, and fine bands of galena occurs in the creek bed at the mouth of Hungerford Creek. Whereas all of the occurrences in the Keku Strait area are clearly epigenetic in style, it is worth noting that iron- and manganese-rich hydrothermal alteration is widespread at the rhyolite/limestone contact, which in many places is marked by clastic sediments and thin chert horizons (Muffler, 1967; this study).

A nearly identical style of mineralized limestone breccia associated with mafic dikes is present at the Taylor Creek occurrence on the west side of Duncan Canal. The occurrences are hosted entirely in a massive to thin-bedded, fractured, buff-colored to light gray dolomitic limestone. The limestone is in depositional contact with and overlies a penetratively foliated greenstone composed predominantly of a chlorite-calcite- (muscovite-quartz) phyllite. The units strike northwest to west-northwest and dip shallowly to moderately steeply to the northeast. Numerous north- to north-northeast-striking dikes of probable Tertiary-Quaternary age intrude the country rock.

A Carnian (early Late Triassic) age is firmly established for the limestone at Taylor Creek by a series of conodont samples collected by Kennecott Exploration and identified by Anita Harris (chap. 11). Sampling sites are identified on the recent geologic map of the Duncan Canal–Zarembo Island area (Karl and others, 1999a). Carnian conodonts were recovered from a sample of limestone located on strike about 2.5 kilometers northwest of the creek occurrences; collections from the immediate vicinity of the open cut were barren. Two samples containing latest Early Permian conodonts, located on the ridge a mile to the southwest, and south of the mouth of Taylor Creek along strike a mile to the southeast, respectively, support the younging-to-the-northeast stratigraphic interpretation of early workers (Kerns, 1950). These conodont samples also bracket the permissive age of the pillowed basaltic volcanics and phyllitic greenstone located on the ridge southwest of the occurrence and in the footwall of the Taylor Creek occurrence, respectively, between late Early Permian and early Late Triassic time.

Mineralized rock in the creek bank exposures of Taylor Creek has two distinct styles. The first and most prevalent consists of irregularly distributed veins, patches, and pods of disseminated to locally abundant pyrite, sphalerite, and galena in a matrix of opaque, light gray to white dolomite gangue (fig. 21*C*). Marcasite has been reported at Taylor Creek (Kerns, 1950); however, X-ray diffraction analysis of suspected marcasite identified only pyrite in a dolomite and ankerite gangue (S.J. Sutley, U.S. Geological Survey, written commun., 1999). Pyrite forms millimeter- to centimeter-sized clots and rounded aggregates in white dolomite or in a fine crystalline groundmass of a dark gray sulfide and yellow-orange sphalerite. Galena occurs as fine crystalline blebs and streaks, and less commonly as coarse crystalline remobilized clots. Although not visually identified, the strong silver-antimony enrichment of this assemblage described below suggests the presence of antimonian tetrahedrite, a common mineral in Late Triassic mineral deposits throughout the ATMB. This style appears to be a replacement of the host limestone. However, the presence of rounded grains of pyrite is not a typical texture of epigenetic replacement deposits in carbonate strata and raises the possibility that the present textural form is a result of remobilization. The best example of this style of mineralization is in the south bank of Taylor Creek in a 1.6-meter-thick subhorizontal band over the top of the discovery trench (Taylor, 2003).

The second style of mineralization has only recently been recognized (Taylor, 2003) and may provide critical evidence of genetic process at Taylor Creek. This style consists of matrix- to grain-supported, rounded nodules of pyrite up to several centimeters in diameter in a dolomite matrix, and irregular botryoidal crusts of pyrite growing in and on dolomitic limestone. Locally, orange sphalerite and galena are present as a fine-grained crystalline matrix and as sparse, coarse crystalline clots. The best example of this textural style is in the north creek bank about 200 meters upstream from the open cut. A stratiform(?) horizon about 12 meters long and roughly parallel to the creek consists predominantly of this nodular pyrite "pudding stone" (fig. 21*D*). Conspicuously absent are common indicators of epigenetic styles of mineralization such as discrete quartz-dolomite-sulfide veins or mineralized breccias. The nodular and botryoidal pyrite textures are likely a result of early diagenetic replacement of limestone during carbonate sedimentation. The nodular pyrite textures and intercalations of dolomitic limestone with sulfidic limy phyllite are similar to those observed at the Wetboot occurrence in Towers Creek (Taylor, 2003) except the former are on a larger scale. Significantly, identical nodular

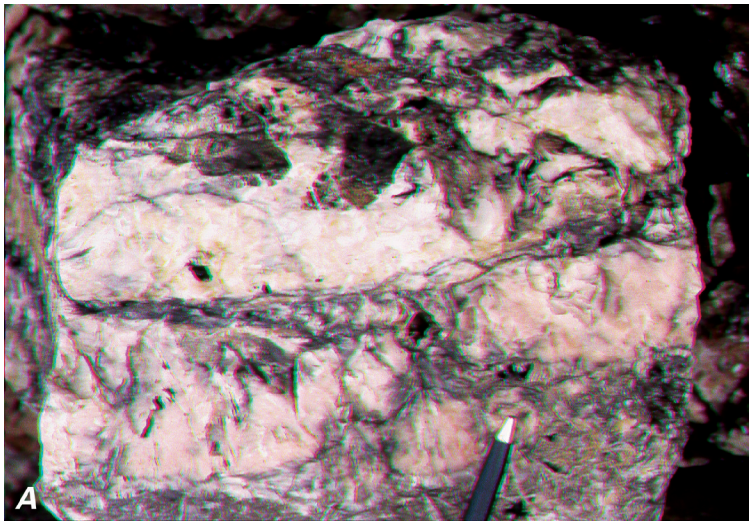

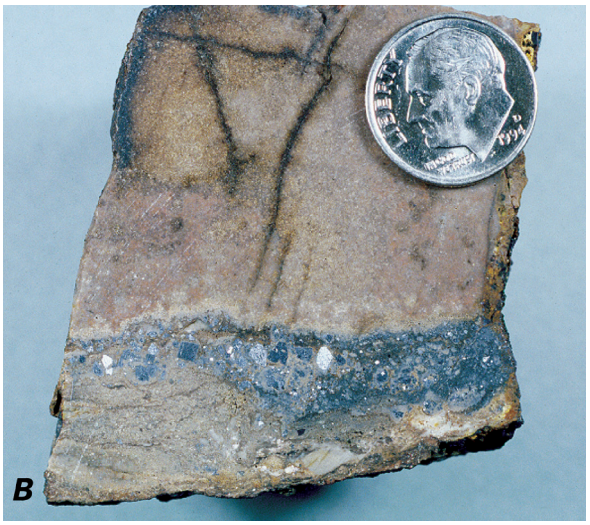

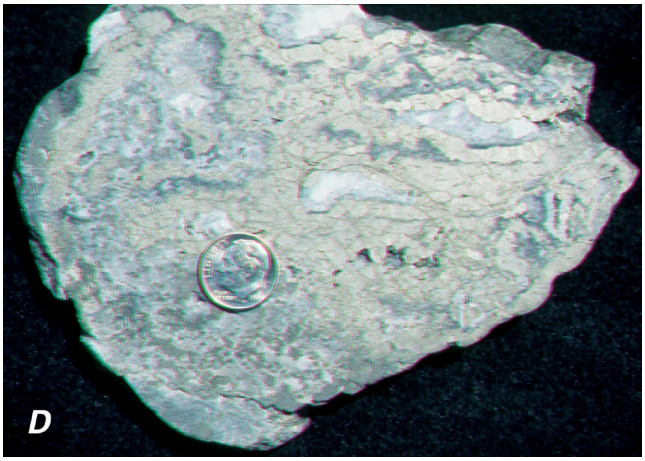

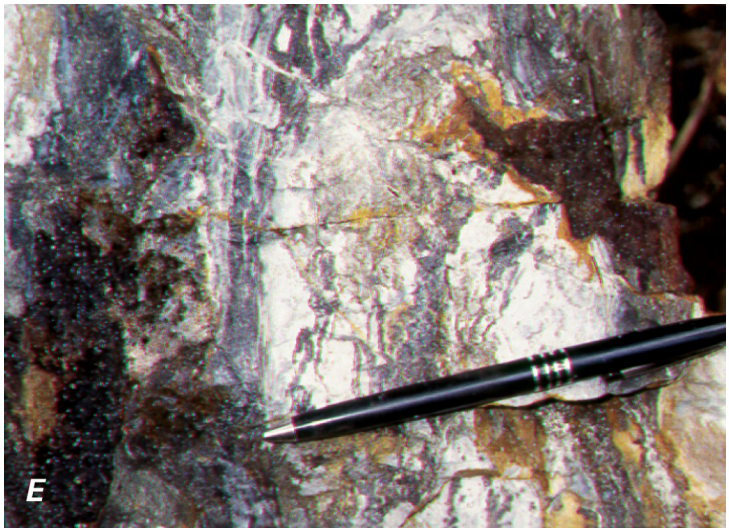

Figure 21 *A*–*E*. Photographs of outcrops and polished rock slabs from mineral occurrences in the central portion of the ATMB. (*A*) Massive vein of pink and white barite cutting clastic sedimentary rocks and limestone at the top of the Keku Volcanics rhyolite. Note botryoidal banding defined by fine-scale galena. Northeastern shoreline of the Cornwallis Peninsula on Kuiu Island, Keku Strait area, central southeastern Alaska. (*B*) Mineralized Cornwallis Limestone breccia from the Kuiu zinc deposit on the Cornwallis Peninsula. Matrix to the clast is composed of sphalerite, galena, and carbonate. (*C*) Mineralized limestone from top of the open cut at the Taylor Creek occurrence, Duncan Canal, central southeastern Alaska. Sample contains pyrite, sphalerite, galena, and tetrahedrite in irregular veins and as replacements of limestone, with a white dolomite gangue. (*D*) Nodular pyrite in limestone from outcrop in creek bank, upstream from the Taylor Creek open cut. This texture is interpreted to be the result of early diagenetic replacement of carbonate mud. (*E*) Semimassive sulfide in a quartz-carbonate-chlorite-altered greenstone at the Lost Show occurrence, near the northwest shore of Woewodski Island in Duncan Canal, central southeastern Alaska. Dark reddish-brown streaks of sphalerite are prevalent, and sulfides fill vuggy open cavities.

pyrite textures are present in footwall carbonate units and in massive pyritic ore at the Greens Creek mine (chap. 9; see also figs. 4C and D in chap. 11). The Taylor Creek occurrences have a geochemical signature consisting of Fe, Zn, Pb, Ag, Sb, Hg, Cd, Mn (Au, As, Cu, and Mo) (Taylor, 2003).

An additional style of structurally hosted, discontinuous, and vein or stockwork-like occurrences are also present in the central portion of the ATMB. These are typified by Lost Show and Brushy Creek on Woewodski Island and by the North Gambier occurrence in Gambier Bay of Admiralty Island. The Lost Show occurrence is located in the northeast quadrant of Section 22 of the Petersburg C–4 15-minute quadrangle, less than a kilometer from the northwest point of Woewodski Island. The occurrence consists of an east-west-trending low ridge of rock on the north side of a small lake. Two trenches have been cleared over the occurrence, exposing its width at the center and at the west end of the low ridge.

The Lost Show occurrence consists of a single, near vertically dipping, 3–4-m-wide stratiform lens of silicified greenstone. The silicified horizon contains as many as six bands (1–30 cm in thickness) of pyrite- and sphalerite-rich, semimassive to massive sulfide in the center trench, which coalesce into thicker bands in the west trench. The lens is continuous along strike for at least 40 meters between the two trenches. Continuity of the lens to the east and west is unknown but likely, based on its consistent thickness over 40 meters. The thickest and best-mineralized massive sulfide is in the western trench and appears to be zoned somewhat across the width of the lens. Massive sulfide against the north side of the lens is sphalerite rich and grades into more silica-pyrite-rich massive sulfide toward the southern edge of the lens. Where massive, the sulfides comprise a fine-grained mixture of pyrite, dark red sphalerite, and minor amounts of a dark gray mineral, possibly galena or tetrahedrite. Semimassive sulfides are texturally similar, with a gangue of gray to white silica. Breccia fragments of quartz, minor vug-fillings of euhedral pyrite, and pyrite veinlets cutting silicified breccia fragments suggest tectonic disruption of the lens and redistribution of sulfides (fig. 21*E*). The occurrence is characterized by a geochemical signature containing Zn, Fe, Cd, Hg, Ag, Sb (Pb, Au, Cu, and Mn) (Taylor, 2003).

The Brushy Creek occurrence is in the southwestern quadrant of section 1 of the Petersburg C–4 15-minute quadrangle, on the southern end of Woewodski Island. Two mineralized open cuts in the southeast bank of the creek are located approximately 50 meters apart, and evidence of weak mineralization is present intermittently for at least 250 meters downstream. Country rock exposed in the creek bank is entirely composed of a brecciated, heavily altered, and weakly foliated mafic metavolcanic or volcaniclastic rock. A small side drainage flowing into Brushy Creek from the southeast contains exposures of thin-bedded, calcareous, quartz-sericite schist with bands of semimassive sulfide. Precursor of the schist is uncertain but could have been a felsic tuff (Taylor, 2003).

The mineral occurrences at Brushy Creek consist of irregularly distributed stockwork calcite-quartz-sulfide veins within brecciated mafic volcanic rock. Two shallow pits in the creek bank each expose 2–3-meter-wide areas crisscrossed by veins. Similar areas of stockwork veining are intermittently exposed in the creek bank downstream for approximately 200 meters. Texturally, all of the sulfides are fine to medium crystalline aggregates of pyrite, dark-reddish sphalerite, and lesser galena. Gangue consists of white quartz and calcite. In slightly more foliated rocks, the clasts are stretched and flattened and the sulfides appear as irregular bands and wisps millimeters to one centimeter in width. In more competent volcaniclastic rocks, sulfides are clearly paragenetically earlier than brecciation of the host rock as the clasts are mineralized and are rotated within the unmineralized matrix and are cut by late quartz-calcite veinlets. In addition to rotation of mineralized clasts, individual bands or stockwork veins are folded. The geochemical signature of the Brushy Creek occurrence consists of Fe, Zn, Ag, Hg, Pb, Sb, Cd, Mn (Au, As, Cu, Co, Ni, and V) (Taylor, 2003).

The barite-quartz-carbonate polymetallic veins and semimassive sulfides at the North Gambier occurrence described in detail by Taylor and others (1992) compose perhaps the northernmost structurally controlled, clearly epigenetic mineral occurrence within the ATMB. The occurrence predominantly consists of sulfide-rich quartz-carbonate-barite veins at the transition between sedimentary rocks and spilitized mafic volcanics. Mineralization occurs primarily within sheared and brecciated zones. Chalcopyrite and barite are the major constituents with lesser bornite, pyrite, sphalerite, galena, covellite, and silver-rich tetrahedrite. Chalcopyrite occurs as clots up to several centimeters in diameter with associated coarsely crystalline bladed, white barite, as millimeter-sized grains disseminated in the greenstone, and as massive, flow-banded material that is intimately intergrown with bornite, covellite, tetrahedrite, and fine-grained pyrite and quartz. Covellite occurs as fine, hairlike needles and laths within the bornite. Tetrahedrite forms small blebs and fracture fillings within the chalcopyrite-bornite assemblage. The dominance of chalcopyrite at the North Gambier occurrence is unusual for the ATMB as is the relatively major proportion of bornite. However, mineralized samples contain 0.1–1 percent copper, 0.1 percent zinc, several parts per million silver, and highly anomalous concentrations of Mn, As, Cd, Mo, Pb, Sb, and Hg, similar to the Greens Creek geochemical signature that occurs consistently throughout the ATMB.

Mineral occurrences that typify the progression to larger, more stratiform morphologies with mineralogical and geochemical features like Greens Creek are also present in the central area of the ATMB and persist northward to the latitude of Mt. Henry Clay. The Butterworth Island occurrence is located just south of the southeastern corner of section 34, in the Petersburg C–4 15-minute quadrangle, just west of Woewodski Island. The occurrence is located below the high tide line in the small spit of land that separates the southeastern

end of Butterworth Island from the small islet to the south. Rocks exposed at low tide between the islands consist of foliated, reddish, highly altered siliceous schist. Immediately to the north, and forming the southern shoreline of Butterworth Island, the siliceous schist is in sharp contact with massive, fractured, unfoliated Cretaceous(?) diorite. Southward the schist grades into a sequence of rocks mapped as Mesozoic volcanics (Brew, 1997). The altered schist hosting the mineral occurrence grades southward into greenschist and moderately foliated mafic metavolcanic rocks that have been intruded by sills of Cretaceous(?) diorite. The diorite contains xenoliths of gabbro probably incorporated from the Mesozoic gabbroic intrusive body that crops out on the northern one-third of Butterworth Island (Brew, 1997).

The Butterworth Island occurrence consists of several subparallel 1–10-cm-thick, semimassive to massive sulfide bands that are conformable with foliation and occur over a width of approximately 4 meters. The mineralized bands are traceable along foliation across the entire width of the low-tide land bridge. The better, more massive sulfide bands are located at low tide on the east side. The best single band is a 10-cm-thick layer of massive pyrite, dark red sphalerite, galena, and probable tetrahedrite. Texturally, the sulfides are fine crystalline and equigranular and appear to form a matrix to clasts of white quartz or chert pebbles and very elongate fragments of thoroughly altered rock. The geochemical signature of the massive sulfide is characterized by very high values of Zn, Fe, Pb, Ag, Hg, Cd, Sb, Co, Mn, (Cu, Au, Mo, and V).

The Castle Island barite deposit is, or was, located in a group of small islands in the middle of Duncan Canal, several kilometers east of the mouth of Castle River. The deposit consisted of a small island almost entirely composed of barite just east of, and connected by a small spit of land to, "Little" Castle Island, the small islet immediately south of Big Castle Island. Little Castle Island is composed from west to east of massive, volcaniclastic, and pillowed mafic volcanic rocks that grade into phyllitic greenstone, which in turn grade into a thin layer of phyllitic pebble conglomerate. Orange-weathering iron-carbonate-altered rock marks a distinctive sheared fault zone running the length of the island that is exposed along the east shoreline. The eastern shore south of the former ore-loading pad consists of a sequence of phyllitic calcareous mudstone, silty limestone, and possibly interbedded graywacke; this sequence is approximately 100 meters southeast of the loading pad along strike and likely represents the footwall rocks to the deposit that are now covered. A small knob in the tide zone south of the loading pad and east of the Little Castle Island shoreline is composed of the calcareous phyllite and is cut by poddy and discontinuous, sulfide-bearing, quartz-carbonate veins, centimeters to 0.7 meter thick. Sulfides are disseminated euhedral grains of coarse crystalline pyrite, green (low iron) sphalerite, and minor galena. Geochemical analyses of the veins indicate that the carbonate is iron and manganese rich, as are carbonate alteration minerals associated with mineral occurrences throughout the ATMB (C.D. Taylor, this study and unpublished data). These veins are probably the metamorphosed feeders to the Castle Island barite deposit.

Previously published records indicate that the Castle Island barite deposit was approximately 95 meters long, 63 meters wide, and extended below sea level to a depth of 47 meters (Grybeck and others, 1984). Maximum elevation of the barite outcrop was between 11 and 18.5 meters above sea level. Enclosing rocks strike northwesterly and dip 50 to 60 degrees to the northeast. A premining estimate based on drilling of the size of the deposit down to 12.5 meters below sea level was 218,000 metric tonnes with a true thickness of the main barite body of 25 to 31 meters (Burchard, 1914; Williams and Decker, 1932). These reports also suggest that the footwall to the deposit consisted of 3–6 meters of "baritic grayschist and limestone" above black slaty argillite, all of which rested on "dark volcanic rocks" that are probably equivalent to the basalt exposed on the islet to the west. Such a stratigraphy is consistent with exposures of presumed footwall sediments to the southeast of the deposit, as previously described. Cross sections based on drilling data suggest that the deposit was essentially a single massive lens dipping eastward, conformably with the enclosing sediments, into Duncan Canal. A horse composed of impure barite, calcite, and schist is indicated at depth near the hanging wall. Sparse exposures of hanging-wall lithologies suggest phyllitic schist and volcanic tuff. The northern limit of the deposit was defined by drilling; the southern boundary was not determined. The barite body was thought to "rake somewhat to the southeast and extend southerly beyond the southern tip of the island" (Williams and Decker, 1932, p. 3), consistent with the general southeast plunge direction of fold axes in Triassic rocks of the area (P.J. Haeussler, written commun., 2000).

Grybeck and others (1984) reported a total production for the Castle Island barite deposit of approximately 0.68 million metric tonnes of barite based upon undocumented sources. Their reinterpretation of unpublished drilling data and cross sections led them to suggest that the deposit "occurred along the trough of a symmetrical open syncline trending about N. 70° W. and centered on the now mined-out island, with limbs dipping 30 to 45 degrees." Grybeck and others (1984) also reported that drilling "indicated a considerable tonnage of lower grade barite interbedded with 'gray schist' (metafelsite?), 'chert,' and 'graphitic schist,' and indications of at least one more high-grade barite lens offshore." Texturally, samples of the barite are massive, sugary, and white to light gray, with millimeter-scale bands and discontinuous wisps of fine crystalline sulfides (fig. 22A). Examination of thin sections indicates the presence of disseminated sphalerite, galena, pyrite, pyrrhotite, bornite, tetrahedrite-tennantite, and chalcopyrite occurring as equant grains 5–300 micrometers in size (Berg and Grybeck, 1980; Grybeck and others, 1984).

Numerous assays of composite drill-core samples and surface chip samples established an average grade of 89

percent barite and 4.5 percent silica, with 0.5–2.5 percent zinc, 0.5–1 percent lead, 1–2 percent iron, 0.5–2.0 troy ounces per ton silver, and traces of gold (Williams and Decker, 1932; Race, 1963; Grybeck and others, 1984). The geochemical signature of the massive barite consists of Ba, Zn, Pb, Ag, Fe, Cd, Sb, Sr (Cu, Au, and Mo). Quartz-carbonate-sulfide veins in the footwall have a similar signature with the notable addition of manganese, arsenic, mercury, and a mafic-ultramafic suite consisting of cobalt, chromium, nickel, and vanadium (Taylor, 2003).

The Pyrola deposit is located in the north-central part of Admiralty Island within a sequence of greenschist-facies rocks correlated with the Retreat Group schists and unconformably overlying limestone, argillite, and mafic volcanic rocks. This sequence of lithologies bears a strong resemblance to the sequence that characterizes the Hyd Group and, although the age of the Pyrola host rocks are not known with certainty, Van Nieuwenhuyse (1984) suggested that they are either Permian or Triassic. The deposit consists of stratiform layers of interbedded barite and massive sulfide hosted in graphitic sediments. A siliceous disseminated pyritic stockwork zone is also present and contains precious metals. The deposit is underlain by a large, semiconformable chlorite-carbonate alteration halo, which is overprinted in the immediate footwall by intense sericite-quartz-pyrite altered rock. The ore mineralogy consists of pyrite, sphalerite, galena, minor chalcopyrite, jamesonite, and boulangerite (Van Nieuwenhuyse, 1984). In addition to the many geological similarities to Greens Creek and other barite-rich polymetallic deposits in the central portion of the ATMB, at Pyrola both sulfur and lead isotopic values of galena are very similar to values at Greens Creek (chap.10).

The Glacier Creek (Main) deposit and the nearby Upper Cap occurrence are on the U.S. side of the border in the Mt. Henry Clay area. They are both stratiform, barite-rich, polymetallic deposits of Late Triassic age that represent the northernmost examples characteristic of the central, transitional portion of the ATMB. The Glacier Creek deposit consists of a 20–30-m-thick, 600-m-long layer of highly altered quartz-sericite schist that contains lenses of massive barite accompanied by bands of sphalerite, galena, and chalcopyrite (MacIntyre and Schroeter, 1985). The deposit is underlain by mafic flows and sedimentary rocks and is overlain by massive pillow lavas (fig. 22B). The Upper Cap occurrence, located several kilometers up Glacier Creek, displays similar features to the Glacier Creek deposit. The occurrence consists predominantly of a 3-m-thick, silica-barite lens with minor amounts of pyrite, sphalerite, galena, and tetrahedrite (fig. 22C; MacIntyre and Schroeter, 1985). The footwall is largely covered by ice; the hanging wall consists of massive basalt flows. Reports of ruby silver (Ag-sulfosalt) at Upper Cap (Merrill Palmer, oral commun., 1994) suggest mineralogical similarities to Greens Creek. X-ray diffraction analysis of reddish-black crystals in silica-barite identified the lead-antimony sulfide mineral geocronite, which also occurs at Greens Creek (chap. 9).

Discussion

We propose, based on the transitional features of the ATMB just described, that the Late Triassic rift in southeastern Alaska formed by oblique propagation into the Alexander terrane resulting in a metallogenic environment setting common both to VMS and to SEDEX environments. Recent work relating the specific nature of both ancient (Barrett and MacLean, 1999) and modern (Hannington and others, 1986; Halbach and others, 1993; Binns and others, 1993; Fouquet and others, 1993; Stoffers and others, 1999) VMS deposits to the location (continental margin, oceanic) and maturity level of the hosting rift basins helps to explain the variations in the mineral occurrences of the ATMB in southeastern Alaska. For example, deposits that form at the tip of rifts propagating into mature arcs (the western Woodlark basin propagating into Papua New Guinea [Binns and others, 1993]; the southern Lau Basin propagating into the North Island of New Zealand from the Valu Fa Ridge to the Taupo volcanic zone [Fouquet and others, 1993]) or where nascent intracontinental rifts split arcs (Japan [Barrett and MacLean, 1999]) are generally of the Kuroko type and are associated with arc-type or heavily calc-alkaline contaminated transitional lavas such as E-MORB (Barrett and MacLean, 1999; cf. the bimodal-mafic division of Barrie and Hannington, 1999). Deposits landward of the propagating rift, or deposits that form on land in the early stages of rifting, display an epithermal or hot-springs style of mineralization (for example, Stoffers and others, 1999; cf. deposits of the Taupo volcanic zone, White, 1981; Hedenquist and Henley, 1985). Deposits that form in the deeper, seaward portion of propagating rifts or in mature rifts are more likely to have a dominantly copper-zinc rich metal assemblage and may be associated with distal clastic sediments (for example, Windy Craggy [Peter and Scott, 1999]; and the Besshi deposits [Slack, 1993]). The deposits occurring in the mature rift settings are usually generally associated with primitive mafic melts that are forming segments of new oceanic crust and may or may not show contamination by melting and incorporation of the rifted crust (Barrett and MacLean, 1999; cf. the mafic-siliciclastic division of Barrie and Hannington, 1999). That such a variation of deposit styles, associated with predictably varying suites of igneous rocks, can be found in a single rift propagating into a mature arc or continental margin provides confirmation for the lithogeochemical and deposit variability of the mineral occurrences in southeastern Alaska. Figure 23 depicts a cross-sectional view through such a tectonic setting showing the various subaerial to deepwater settings of the southeastern Alaska Late Triassic mineral occurrences in the ATMB.

The segment of a propagating oceanic rift that we believe is analogous to the Greens Creek tectonic setting is that portion seaward of the propagating tip of a rift basin and landward of the point at which new oceanic crust begins to form. Within this segment, bimodal volcanism is characterized by peralkaline rhyolites and variably enriched basalts that exhibit chemistry similar to intraplate rocks and varying degrees of crustal contamination (for example, Smith and others, 1977; Smith and Johnson, 1981). Moving seaward, rhyolites disappear from

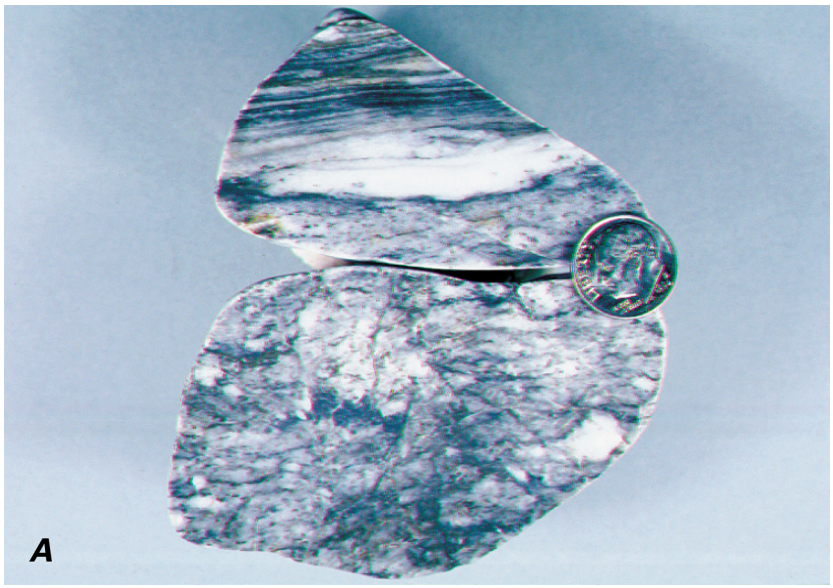

Figure 22 *A*–*C*. Photographs of outcrops and polished rock slabs from mineral occurrences in the central and northern portion of the ATMB. (*A*) Barite-galena-rich float collected on the loading pad at the Castle Island barite mine in the Duncan Canal area, central southeastern Alaska. (*B*) Glacier Creek (Main) deposit in the Mt. Henry Clay area, northern southeastern Alaska. The central, orange-white stripe consists of quartz-sericite-carbonate schist with lenses of massive barite and lesser sulfides. Outcrop above and below consists of massive and pillowed basalt flows. (*C*) Barite-sulfide lens at the Upper Cap occurrence in the Mt. Henry Clay area, northern southeastern Alaska. Rocks overlying the lens are massive basalt flows.

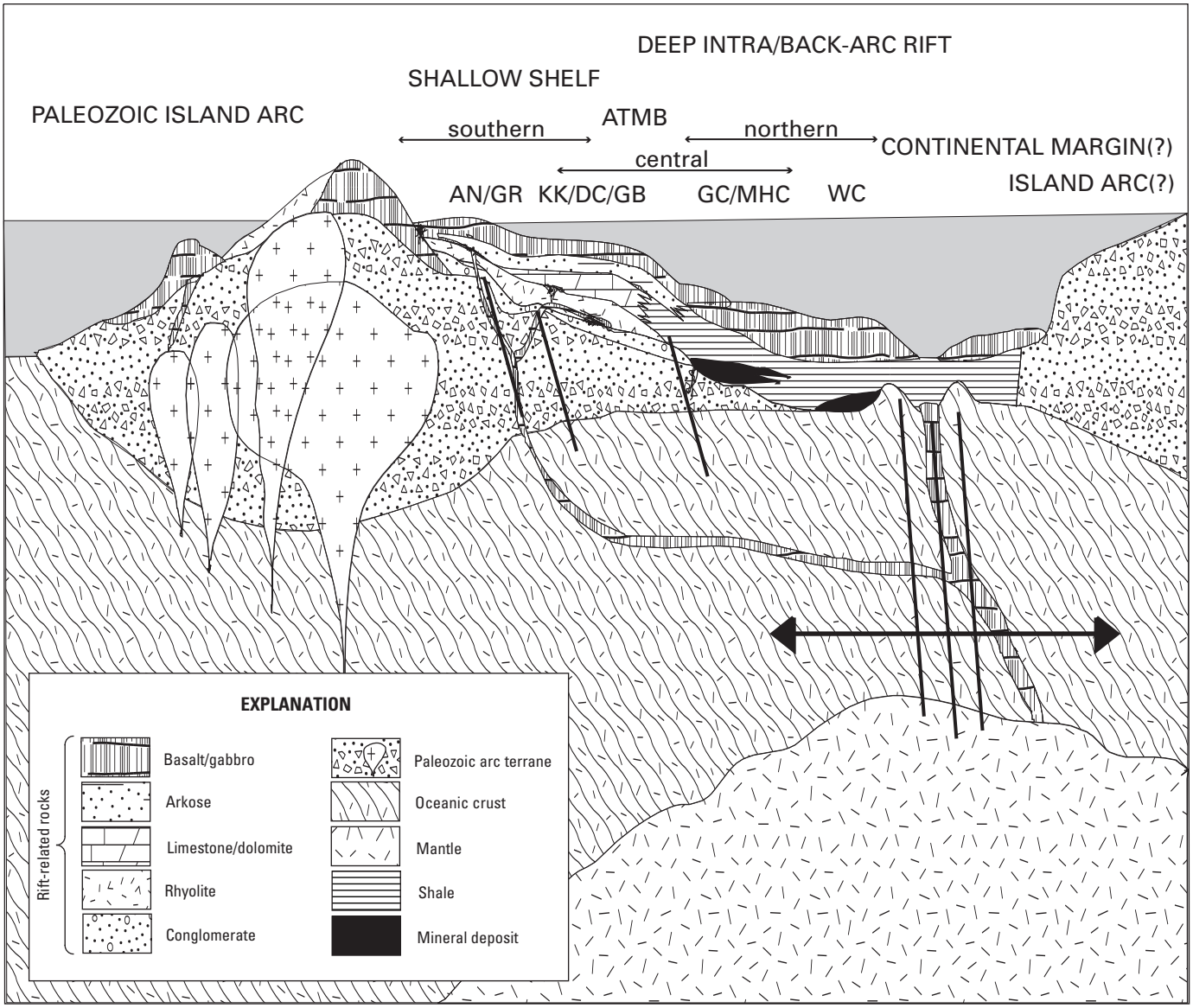

Figure 23. Schematic drawing showing a cross-sectional view of the Upper Triassic metallogenic setting of mineral deposits and occurrences in southeastern Alaska. Diagram shows a series of mineral deposits at progressively deeper water positions within an evolving intra- or back-arc rift. AN/GR, Annette and Gravina Islands; KK/DC/GB, Keku Strait, Duncan Canal, and Gambier Bay on southern Admiralty Island; GC/MHC, Greens Creek on northern Admiralty Island and Mt. Henry Clay; WC, Windy Craggy.

the section and mafic melts become less arc-contaminated and compositionally more similar to ocean ridge basalts, commonly E-MORB or "transitional" basalts (for example, modern examples include Gill and Whelan, 1989, and Stern and others, 1990; and ancient examples include Aitchison and Flood, 1995, and Dadd, 1998). The seaward transition may or may not evolve into a sediment-covered ridge; however, the transition is nevertheless significant in representing the change from a bimodal-mafic to a mafic-siliciclastic metallogenic environment. This transition is exactly like the observed changes in the tectonostratigraphic settings between the Keku Strait, where mineral occurrences of the ATMB are hosted in dolomitic limestone overlying peralkaline rhyolites, and the Greens Creek deposit, where rhyolites are absent. The rift has become sediment-covered, and coeval mafic-ultramafic melts are still heavily contaminated by the Alexander terrane basement that they rise through.

We suggest that the portion of an evolving rift where host lithologies include footwall mafic-ultramafic rocks contaminated by a mature arc and distal clastic sedimentation is strikingly similar to the failed epicontinental rift tectonic setting common to most SEDEX deposits. At the time of Late Triassic rifting, the Alexander terrane was an inactive, continent-sized

landmass of wholly oceanic affinities, cored by sialic Proterozoic and lower Paleozoic crust. At the latitude of Greens Creek, rifting resulted in the formation of a small (second order?), restricted, anoxic, and very organic-rich sedimentary basin, which was intruded by rift-related mafic-ultramafic intrusive rocks. This SEDEX-like metallogenic setting occurred within a propagating rift, which on a larger scale is more similar to the metallogenic setting common to many VMS deposits.

References Cited

Aitchison, J.C., and Flood, P.G., 1995, Gamilaroi Terrane—A Devonian rifted intra-oceanic island-arc assemblage, NSW, Australia, *in* Smellie, J.L., ed., Volcanism associated with extension at consuming plate margins: Geological Society Special Publication no. 81, p. 155–168.

Arculus, R.J., 1987, The significance of source versus process in the tectonic controls of magma genesis: Journal of Volcanology and Geothermal Research, v. 32, p. 1–12.

Barker, Fred, 1994, Some accreted volcanic rocks of Alaska and their elemental abundances, *in* Plafker, G., and Berg, H.C., eds., The geology of Alaska: Boulder, Colorado, Geological Society of America, Decade of North American Geology, v. G–1, p. 555–587.

Barker, Fred, Sutherland-Brown, A., Budahn, J.R., and Plafker, G., 1989, Back-arc with frontal-arc component origin of Triassic Karmutsen basalt, British Columbia, Canada: Chemical Geology, v. 75, p. 81–102.

Barrett, T.J., and MacLean, W.H., 1999, Volcanic sequences, lithogeochemistry, and hydrothermal alteration in some bimodal volcanic-associated massive sulfide systems, *in* Barrie, C.T., and Hannington, M.D., eds., Volcanic-associated massive sulfide deposits—Processes and examples in modern and ancient settings: Society of Economic Geologists Reviews in Economic Geology, v. 8, p. 101–127.

Barrie, C.T., and Hannington, M.D., 1999, Classification of volcanic-associated massive sulfide deposits based on host-rock composition, *in* Barrie, C.T., and Hannington, M.D., eds., Volcanic-associated massive sulfide deposits—Processes and examples in modern and ancient settings: Society of Economic Geologists Reviews in Economic Geology, v. 8, p. 1–11.

Bazard, D.R., Butler, R., Gehrels, G., and Soja, C.M., 1994, New constraints for Late Silurian-Devonian paleogeography of the Alexander terrane, southeastern Alaska: Geological Society of America Abstracts with Programs, v. 26, p. A384.

Berg, H.C., 1972, Geologic map of Annette Island, Alaska: U.S. Geological Survey Miscellaneous Investigations Series Map I–684, scale 1:63,360.

Berg, H.C., 1973, The geology of Gravina Island, Alaska: U.S. Geological Survey Bulletin 1373, 41 p.

Berg, H.C., and Grybeck, D., 1980, Upper Triassic volcanogenic Zn-Pb-Ag-(Cu-Au)-barite mineral deposits near Petersburg, Alaska: U.S. Geological Survey Open-File Report 80–527, 9 p.

Berg, H.C., Jones, D.L., and Coney, P.J., 1978, Map showing pre-Cenozoic tectono-stratigraphic terranes of southeastern Alaska and adjacent areas: U.S. Geological Survey Open-File Report 78–1085, 2 sheets, scale 1:1,000,000.

Berg, H.C., Jones, D.L., and Richter, D.H., 1972, Gravina-Nutzotin belt—Tectonic significance of an upper Mesozoic sedimentary and volcanic sequence in southern and southeastern Alaska: U.S. Geological Survey Professional Paper 800–D, p. D1–D24.

Binns, R.A., Scott, S.D., Bogdanov, Y.A., Lisitzin, A.P., Gordeev, V.V., Gurvich, E.G., Finlayson, E.J., Boyd, T., Dotter, L.E., Wheller, G.E., and Muravyev, K.G., 1993, Hydrothermal oxide and gold-rich sulfate deposits of Franklin Seamount, western Woodlark basin, Papua New Guinea: Economic Geology, v. 88, p. 2122–2153.

Boynton, W.V., 1984, Cosmochemistry of the rare earth elements—Meteorite studies, *in* Henderson, P., ed., Rare earth element geochemistry: Amsterdam, Elsevier, p. 63–114.

Brew, D.A., 1997, Reconnaissance geologic map of the Petersburg C–4 quadrangle, southeastern Alaska: U.S. Geological Survey Open-File Report 97–156–J, 21 p., 1 sheet, scale 1:63,360.

Buddington, A.F., 1923, Mineral deposits of the Wrangell district: U.S. Geological Survey Bulletin 739, p. 51–75.

Burchard, E.F., 1914, A barite deposit near Wrangell: U.S. Geological Survey Bulletin 592, p. 109–117.

Churkin, Michael, Jr., and Eberlein, G.D., 1977, Ancient borderland terranes of the North American Cordillera—Correlation and microplate tectonics: Geological Society of America Bulletin, v. 88, p. 769–786.

Civetta, Lucia, Cornette, Y., Crisci, G., Gillot, P.Y., Orsi, G., and Requejos, C.S., 1984, Geology, geochronology and chemical evolution of the island of Pantelleria: Geological Magazine, v. 121, no. 6, p. 541–562.

Cobb, E.H., 1972, Metallic mineral resources map of the Petersburg quadrangle, Alaska: U.S. Geological Survey Miscellaneous Field Studies Map MF–415, 1 sheet, scale 1:250,000.

Cobb, E.H., 1978, Summary of references to mineral occurrences (other than mineral fuels and construction materials) in the Petersburg quadrangle, Alaska: U.S. Geological Survey Open-File Report 78–870, 52 p.

Cole, J.W., 1978, Tectonic setting of Mayor Island volcano: New Zealand Journal of Geology and Geophysics, v. 21, p. 645–647.

Dadd, K.A., 1998, Incipient backarc magmatism in the Silurian Tumut Trough, new South Wales—An ancient analogue of the early Lau Basin: Australian Journal of Earth Science, v. 45, p. 109–121.

Dudas, F.O., 1992, Petrogenetic evaluation of trace element discrimination diagrams, *in* Bartholomew, M.J., Hyndman, D.W., Mogk, D.W., and Mason, R., Basement tectonics 8—Characterization and comparison of ancient and Mesozoic continental margins—Proceedings of the 8th International Conference on Basement Tectonics (Butte, Montana, 1988): Dordrecht, The Netherlands, Kluwer Academic Publishers, p. 93–127.

Dusel-Bacon, Cynthia, 1994, Metamorphic history of Alaska, *in* Plafker, G., and Berg, H.C., eds., The geology of Alaska: Boulder, Colorado, Geological Society of America, Decade of North American Geology, v. G1, p. 495–533.

Forbes, R.B., Gilbert, W., and Redman, E., 1989, Geologic setting and petrology of the metavolcanic rocks in the northwestern part of the Skagway B-4 quadrangle, southeastern Alaska: Alaska Division of Geological and Geophysical Surveys, Public-Data File 89–14, 43 p.

Ford, A.B., and Brew, D.A., 1993, Geochemical character of upper Paleozoic and Triassic greenstone and related metavolcanic rocks of the Wrangellia terrane in northern southeastern Alaska, *in* Dusel-Bacon, Cynthia, and Till, A.B., eds., Geologic studies in Alaska by the U.S. Geological Survey, 1992: U.S. Geological Survey Bulletin 2068, p. 197–217.

Fouquet, Yves, Von Stackelberg, U., Charlou, J.L., Erzinger, J., Herzig, P.M., Muhe, R., and Wiedicke, M., 1993, Metallogenesis in back-arc environments—The Lau basin example: Economic Geology, v. 88, p. 2154–2181.

Franklin, J.M., 1986, Volcanic-associated massive sulphide deposits—An update, *in* Andrew, C.J., Crowe, R.W.A., Finlay, S., Pennel, W.M., and Pyne, J.F., eds., Geology and genesis of mineral deposits in Ireland: Irish Association for Economic Geology, p. 49–69.

Franklin, J.M., 1993, Volcanic-associated massive sulphide deposits, *in* Kirkham, R.V., Sinclair, W.D., Thorpe, R.I., and Duke, J.M., eds., Mineral deposit modeling: Geological Association of Canada, Special Paper 40, p. 315–334.

Franklin, J.M., Lydon, J.W., and Sangster, D.F., 1981, Volcanic-associated massive sulfide deposits, *in* Skinner, B.J., ed., Economic geology—Seventy-fifth anniversary volume, 1905–1980: El Paso, Texas, The Economic Geology Publishing Company, p. 485–627.

Gardner, M.C., Bergman, S.C., Cushing, G.W., MacKevett, E.M., Jr., Plafker, G., Campbell, R.B., Dodds, C.J., McClelland, W.C., and Mueller, P.A., 1988, Pennsylvanian pluton stitching of Wrangellia and the Alexander terrane, Wrangell Mountains, Alaska: Geology, v. 16, p. 967–971.

Gehrels, G.E., and Barker, G., 1993, Reconnaissance geochemistry of Permian and Triassic basalts of the Taku and Wrangellia terranes, southeastern Alaska, *in* Dusel-Bacon, Cynthia, and Till, A.B., eds., Geologic studies in Alaska by the U.S. Geological Survey, 1992: U.S. Geological Survey Bulletin 2068, p. 218–227.

Gehrels, G.E., and Berg, H.C., 1992, Geologic map of southeastern Alaska: U.S. Geological Survey Miscellaneous Investigations Series Map I–1867, scale 1:600,000.

Gehrels, G.E., and Berg, H.C., 1994, Geology of southeastern Alaska, *in* Plafker, George, and Berg, H.C., eds., The geology of Alaska: Boulder, Colorado, Geological Society of America, Decade of North American Geology, v. G1, p. 451–468.

Gehrels, G.E., Dickinson, W.R., Ross, G.M., Stewart, J.H., and Howell, D.G., 1994, Provenance of detrital zircons in strata of the Cordilleran miogeocline and selected outboard terranes: Geological Society of America Abstracts with Programs, v. 26, p. A384.

Gehrels, G.E., Dodds, C.J., and Campbell, R.B., 1986, Upper Triassic rocks of the Alexander terrane, SE Alaska, and the Saint Elias Mountains of B.C. and Yukon: Geological Society of America Abstracts with Programs, v. 18, p. 109.

Gehrels, G.E., and Saleeby, J.B., 1987, Geologic framework, tectonic evolution, and displacement history of the Alexander terrane: Tectonics, v. 6, p. 151–173.

Gehrels, G.E., Saleeby, J.B., and Berg, H.C., 1987, Geology of Annette, Gravina, and Duke Islands, southeastern Alaska: Canadian Journal of Earth Sciences, v. 24, p. 866–881.

Gill, James, and Whelan, P., 1989, Early rifting of an oceanic island arc (Fiji) produced shoshonitic to tholeiitic basalts: Journal of Geophysical Research, v. 94, no. B4, p. 4561–4578.

Goldfarb, R.J., Nelson, S.W., Berg, H.C., and Light, T.D., 1987, Distribution of mineral deposits in the Pacific Border Ranges and Coast Mountains of the Alaska Cordillera, *in* Elliot, I.L., and Smee, B.W., eds., Geoexpo/86—Exploration in the North American Cordillera: Vancouver, B.C., Association of Exploration Geochemists, p. 19–41.

Goldfarb, R.J., Snee, L.W., Miller, L.D., and Newberry, R.J., 1991, Rapid dewatering of the crust deduced from ages of mesothermal gold deposits: Nature, v. 354, p. 296–298.

Goodfellow, W.D., Lydon, J.W., and Turner, R.J.W., 1993, Geology and genesis of stratiform sediment-hosted (SEDEX) zinc-lead-silver sulphide deposits, *in* Kirkham, R.V., Sinclair, W.D., Thorpe, R.I., and Duke, J.M., eds., Mineral deposit modelling: Geological Association of Canada, Special Paper 40, p. 201–251.

Green, Darwin, MacVeigh, J.G., Palmer, M., Watkinson, D.H., and Orchard, M.J., 2003, Stratigraphy and geochemistry of the RW Zone, a new discovery at the Glacier Creek VMS prospect, Palmer Property, Porcupine mining district, southeastern Alaska, *in* Clautice, K.H., and Davis, P.K., eds., Short notes on Alaska geology 2003: Alaska Division of Geological and Geophysical Surveys, Professional Report 120, p. 35–51.

Grybeck, D.J., Berg, H.C., and Karl, S.M., 1984, Map and description of the mineral deposits in the Petersburg and eastern Port Alexander quadrangles, southeastern Alaska: U.S. Geological Survey Open-File Report 84–837, 87 p., 1 sheet, scale 1:250,000.

Haeussler, P.J., Coe, R.S., and Onstott, T.C., 1992, Paleomagnetism of the Late Triassic Hound Island Volcanics—Revisited: Journal of Geophysical Research, v. 97, p. 19617–19639.

Haeussler, P.J., Karl, S.M., Mortensen, J.K., Layer, P., and Himmelberg, G.R., 1999, Permian and mid-Cretaceous deformation of the Alexander terrane on Admiralty and Kupreanof Islands, southeastern Alaska: Geological Society of America Abstracts with Programs, v. 31, no. 6, p. A–60.

Halbach, Peter, Pracejus, B., and Marten, A., 1993, Geology and mineralogy of massive sulfide ores from the central Okinawa trough, Japan: Economic Geology, v. 88, p. 2210–2225.

Hannington, M.D., Peter, J.M., and Scott, S.D., 1986, Gold in sea-floor polymetallic sulfide deposits: Economic Geology, v. 81, p. 1867–1883.

Hedenquist, J.W., and Henley, R.W., 1985, Hydrothermal eruptions in the Waiotapu geothermal system, New Zealand—Their origin, associated breccias, and relation to precious metal mineralization: Economic Geology, v. 80, p.1640–1668.

Hillhouse, J.W., 1987, Accretion of southern Alaska, *in* Kent, D.V., and Krs, M., eds., Laurasian paleomagnetism and tectonics: Tectonophysics, v. 139, p. 107–122.

Hillhouse, J.W., and Gromme, C.S., 1984, Northward displacement and accretion of Wrangellia—New paleomagnetic evidence from Alaska: Journal of Geophysical Research, v. 89, p. 4461–4477.

Jenner, G.A., 1996, Trace element geochemistry of igneous rocks—Geochemical nomenclature and analytical geochemistry, *in* Wyman, D.A., ed., Trace element geochemistry of volcanic rocks—Applications for massive sulfide exploration: Geological Association of Canada, Short Course Notes, v. 12, p. 51–77.

Jenner, G.A., Longerich, H.P., Jackson, S.E., and Fryer, B.J., 1990, ICP–MS—A powerful tool for high-precision trace-element analysis in earth sciences—Evidence from analysis of selected U.S.G.S. reference samples: Chemical Geology, v. 83, p. 133–148.

Jones, D.L., Silberling, N.J., and Hillhouse, J., 1977, Wrangellia—A displaced terrane in northwestern North America: Canadian Journal of Earth Sciences, v. 14, p. 2565–2577.

Karl, S.M., 1992, Map and table of mineral deposits on Annette Island, Alaska: U.S. Geological Survey Open-File Report 92–690, scale 1:63,360, 57 p.

Karl, S.M., Haeussler, P.J., and McCafferty, A., 1999a, Reconnaissance geologic map of the Duncan Canal/Zarembo Island area, southeastern Alaska: U.S. Geological Survey Open-File Report 99–168, 23 p.

Karl, S.M., Haeussler, P.J., Mortenson, J.K., Layer, P., Savage, N., Wardlaw, B., Harris, A., Murchey, B., and Blome, C., 1999b, New stratigraphic and isotopic constraints on the depositional and deformational history of the Alexander terrane, southeastern Alaska: Geological Society of America Abstracts with Programs v. 31, no. 6, p. A–68.

Kerns, W.H., 1950, Investigation of Taylor Creek lead-zinc deposit, Kupreanof Island, Petersburg, Alaska: U.S. Bureau of Mines Report of Investigations 4669, 13 p.

Large, R.R., 1992, Australian VHMS deposits—Features, styles, models: Economic Geology, v. 87, p. 471–510.

Lathram, E.H., Pomeroy, J.S., Berg, H.C., and Loney, R.A., 1965, Reconnaissance geology of Admiralty Island, Alaska: U.S. Geological Survey Bulletin 1181–R, 48 p.

Leach, D.L., and Sangster, D.F., 1993, Mississippi Valley-type lead-zinc deposits, *in* Kirkham, R.V., Sinclair, W.D., Thorpe, R.I., and Duke, J.M., eds., Mineral deposit modeling: Geological Association of Canada, Special Paper 40, p. 289–314.

Lentz, D.R., 1998, Petrogenetic evolution of felsic volcanic sequences associated with Phanerozoic volcanic-hosted massive sulphide systems—The role of extensional geodynamics: Ore Geology Reviews, v. 12, p. 289–327.

Loney, R.A., 1964, Stratigraphy and petrography of the Pybus-Gambier area, Admiralty Island, Alaska: U.S. Geological Survey Bulletin 1178, 103 p.

Longerich, H.P., Jenner, G.A., Fryer, B.J., and Jackson, S.E., 1990, Inductively coupled plasma-mass spectrometric analysis of geological samples—A critical evaluation based on case studies: Chemical Geology, v. 83, p. 105–118.

MacIntyre, D.G., 1986, The geochemistry of basalts hosting massive sulfide deposits, Alexander terrane northwest British Columbia: British Columbia Ministry of Energy, Mines, and Petroleum Resources, Geological Fieldwork, 1985, Paper 1986–1, p. 197–210.

MacIntyre, D.G., and Schroeter, T.G., 1985, Mineral occurrences in the Mt. Henry Clay area: British Columbia Ministry of Energy, Mines and Petroleum Resources, Geological Fieldwork, 1984, Paper 1985–1, p. 365–379.

Mahood, G.A., and Baker, D.R., 1986, Experimental constraints on depths of fractionation of mildly alkalic basalts and associated felsic rocks—Pantelleria, Strait of Sicily: Contributions to Mineralogy and Petrology, v. 93, p. 251–264.

McClelland, W.C., and Gehrels, G.E., 1990, Geology of the Duncan Canal shear zone—Evidence for Early to Middle Jurassic deformation of the Alexander terrane, southeastern Alaska: Geological Society of America Bulletin, v. 102, p. 1378–1392.

Meier, A.L., and Slowik, T., 2002, Chapter K, Rare earth elements by inductively coupled plasma-mass spectrometry, *in* Taggart, J.E., Jr., ed., Analytical methods for chemical analysis of geologic and other materials: U.S. Geological Survey Open-File Report 2002–223, 10 p.

Meschede, Martin, 1986, A method of discriminating between different types of mid-ocean ridge basalts and continental tholeiites with the Nb-Zr-Y diagram: Chemical Geology, v. 56, p. 207–218.

Mihalynuk, M.G., Smith, M.T., MacIntyre, D.G., and Deschenes, M., 1993, Tatshenshini project, northwestern British Columbia—Part B, Stratigraphic and magmatic setting of mineral occurrences: British Columbia Ministry of Energy, Mines and Petroleum Resources, Geological Fieldwork 1992, Paper 1993–1, p. 189–202.

Miller, L.D., Goldfarb, R.J., Gehrels, G.E., and Snee, L.W., 1994, Genetic links among fluid cycling, vein formation, regional deformation, and plutonism in the Juneau gold belt, southeastern Alaska: Geology, v. 22, p. 203–206.

Muffler, L.J.P., 1967, Stratigraphy of the Keku Islets and neighbouring parts of Kuiu and Kupreanof Islands, southeastern Alaska: U.S. Geological Survey Bulletin 1241–C, 52 p.

Newberry, R.J., and Brew, D.A., 1997, The Upper Triassic Greens Creek VMS (volcanogenic massive sulfide) deposit and Woewodski Island VMS prospects, southeastern Alaska—Chemical and isotopic data for rocks and ores demonstrate similarity of these deposits and their host rocks: U.S. Geological Survey Open-File Report 97–539, 49 p.

Newberry, R.J., and Brew, D.A., 1999, Chemical and isotopic data for rocks and ores from the Upper Triassic Greens Creek and Woewodski Island volcanogenic massive sulfide deposits, southeastern Alaska, *in* Kelley, K.D., ed., Geologic studies in Alaska by the U.S. Geological Survey, 1997: U.S. Geological Survey Professional Paper 1614, p. 35–55.

Newberry, R.J., Crafford, T.C., Newkirk, S.R., Young, L.E., Nelson, S.W., and Duke, N.A., 1997, Volcanogenic massive sulfide deposits of Alaska, *in* Goldfarb, R.J., and Miller, L.E., eds., Mineral deposits of Alaska: Economic Geology Monograph 9, p. 120–150.

Panuska, B.C., 1990, An overlooked world class Triassic flood basalt event: Geological Society of America Abstracts with Programs, v. 22, p. A168.

Pearce, J.A., 1996, A user's guide to basalt discrimination diagrams, *in* Wyman, D.A., ed., Trace element geochemistry of volcanic rocks—Applications for massive sulfide exploration: Geological Association of Canada, Short Course Notes, v. 12, p. 79–113.

Pearce, J.A., and Cann, J.R., 1973, Tectonic setting of basic volcanic rocks determined using trace element analyses: Earth and Planetary Science Letters, v. 19, p. 290–300.

Peter, J.M., and Scott, S.D., 1999, Windy Craggy, northwestern British Columbia—The world's largest Besshi-type deposit, *in* Barrie, C.T., and Hannington, M.D., eds., Volcanic-associated massive sulfide deposits—Processes and examples in modern and ancient settings: Society of Economic Geologists Reviews in Economic Geology, v. 8, p. 261–295.

Pin, Christian, and Paquette, J.-L., 1997, A mantle-derived bimodal suite in the Hercynian Belt—Nd isotope and trace element evidence for a subduction-related rift origin of the Late Devonian Brevenne metavolcanics, Massif Central (France): Contributions to Mineralogy and Petrology, v. 129, p. 222–238.

Race, W.H., 1963, Property examination report, Castle Island barite deposit, Duncan Canal, Alaska, Petersburg quadrangle: State of Alaska Division of Mines and Minerals, 13 p.

Richards, M.A., Jones, D.L., Duncan, R.A., and DePaolo, D.J., 1991, A mantle plume initiation model for the Wrangellia flood basalt and other oceanic plateaus: Science, v. 254, p. 263–267.

Rollison, Hugh, 1993, Using geochemical data—Evaluation, presentation, interpretation: New York, Longman Scientific and Technical, 352 p.

Saleeby, J.B., 1994, Tectonic history of the Insular Suture Zone, southeastern Alaska: Geological Society of America Abstracts with Programs, v. 26, p. A384.

Sampson, S.D., McClelland, W.C., Patchett, P.J., Gehrels, G.E., and Anderson, R.G., 1989, Evidence from neodymium isotopes for mantle contributions to Phanerozoic crustal genesis in the Canadian Cordillera: Nature, v. 337, p. 705–709.

Sampson, S.D., Patchett, P.J., Gehrels, G.E., and Anderson, R.G., 1990, Nd and Sr isotopic characterization of the Wrangellia terrane and implications for crustal growth of the Canadian Cordillera: Journal of Geology, v. 98, p. 749–762.

Sampson, S.D., Patchett, P.J., McClelland, W.C., and Gehrels, G.E., 1991, Nd and Sr isotopic constraints on the petrogenesis of the west side of the northern Coast Mountains batholith, Alaska and Canadian Cordillera: Canadian Journal of Earth Science, v. 28, p. 939–946.

Savage, N.M., 1994, Terrane affinities of Middle and Late Devonian conodonts from the Wadleigh limestone, southeastern Alaska: Geological Society of America Abstracts with Programs, v. 26, p. A158.

Slack, J.F., 1993, Descriptive and grade-tonnage models for Besshi-type massive sulphide deposits, *in* Kirkham, R.V., Sinclair, W.D., Thorpe, R.I., and Duke, J.M., eds., Mineral deposit modeling: Geological Association of Canada, Special Paper 40, p. 343–371.

Smith, I.E.M., Chappell, B.W., Ward, G.K., and Freeman, R.S., 1977, Peralkaline rhyolites associated with andesitic arcs of the southwest Pacific: Earth and Planetary Science Letters, v. 37, p. 230–236.

Smith, I.E.M., and Johnson, R.W., 1981, Contrasting rhyolite suites in the Late Cenozoic of Papua New Guinea: Journal of Geophysical Research, v. 86, no. B11, p. 10257–10272.

Stern, R.J., Lin, P.-N., Morris, J.D., Jackson, M.C., Fryer, P., Bloomer, S.H., and Ito, E., 1990, Enriched back-arc basin basalts from the northern Mariana Trough—Implications for the magmatic evolution of back-arc basins: Earth and Planetary Science Letters, v. 100, p. 210–225.

Stoffers, Peter, Hannington, M., Wright, I., Herzig, P., de Ronde, C., and Shipboard Scientific Party, 1999, Elemental mercury at submarine hydrothermal vents in the Bay of Plenty, Taupo volcanic zone, New Zealand: Geology, v. 27, p. 931–934.

Taggart, J.E., Jr., ed., 2002, Analytical methods for chemical analysis of geologic and other materials, U.S. Geological Survey Open-File Report 2002–223, variously paginated.

Taylor, C.D., 1993, Summary of geochemical data—Annette Islands Reserve, southeast Alaska, *in* Godwin, L.H., and Smith, B.D., eds.: Northwest Mining Association special symposium 1993 on economic mineral resources of the Annette Islands Reserve, Alaska, p. 77–82.

Taylor, C.D., 2003, Descriptions of mineral occurrences and interpretation of mineralized rock geochemical data in the Stikine geophysical survey area, southeastern Alaska: U.S. Geological Survey Open-File Report 2003–154, 51 p.

Taylor, C.D., Cieutat, B.A., and Miller, L.D., 1992, A follow-up geochemical survey of base metal anomalies in the Ward Creek/Windfall Harbor and Gambier Bay areas, Admiralty Island, S.E. Alaska, *in* Bradley, D.C., and Dusel-Bacon, C., eds., 1991 Geologic Studies in Alaska: U.S. Geological Survey Bulletin 2041, p. 70–85.

Taylor, C.D., Newkirk, S.R., Hall, T.E., Lear, K.G., Premo, W.R., Leventhal, J.S., Meier, A.L., Johnson, C.A., and Harris, A.G., 1999, The Greens Creek deposit, southeastern Alaska—A VMS-SEDEX hybrid, *in* Stanley, C.J., and others, eds., Mineral deposits—Processes to processing: Rotterdam, Balkema, p. 597–600.

Taylor, C.D., Premo, W.R., Meier, A.L., and Taggart, J.E., Jr., 2008, The metallogeny of Late Triassic rifting of the Alexander Terrane in southeastern Alaska and northwestern British Columbia: Economic Geology, v. 103, p. 89–115.

Van Nieuwenhuyse, R.E., 1984, Geology and geochemistry of the Pyrola massive sulfide deposit, Admiralty Island, Alaska: Tucson, University of Arizona, unpublished Master's thesis, 170 p.

Warme, J.E., and Kuehner, H-C., 1998, Anatomy of an anomaly—The Devonian catastrophic Alamo impact breccia of southern Nevada, *in* Ernst, W.G., and Nelson, C.A., eds., Integrated earth and environmental evolution of the southwestern United States: Boulder, Colo., Geological Society of America, p. 80–110.

White, D.E., 1981, Active geothermal systems and hydrothermal ore deposits, *in* Skinner, B.J., ed., Economic geology—Seventy-fifth anniversary volume, 1905–1980: El Paso, The Economic Geology Publishing Company, p. 392–423.

Williams, J.A., and Decker, P.A., 1932, Exploring Castle Island barite deposit by diamond drilling, a compilation—Unpublished report available from the Juneau office of the U.S. Bureau of Land Management, listing # MR 117–1, 46 p.

Wilson, Marjorie, 1989, Igneous petrogenesis—A global tectonic approach: London, Unwin Hyman, 466 p.

Winchester, J.A., and Floyd, P.A., 1977, Geochemical discrimination of different magma series and their differentiation products using immobile elements: Chemical Geology, v. 20, p. 325–343.

Wood, D.A., 1980, The application of a Th-Hf-Ta diagram to problems of tectonomagmatic classification and to establishing the nature of crustal contamination of basaltic lavas of the British Tertiary Volcanic Province: Earth and Planetary Science Letters, v. 50, p. 11–30.